The Dissertation Committee for Fernando Almada-Calvo Certifies that this is the approved version of the following dissertation:

Effect of temperature, dissolved inorganic carbon and light intensity on the growth rates of two microalgae species in monocultures and co-cultures

Committee:

Kerry A. Kinney, Supervisor

Lynn E. Katz, Co-Supervisor

Gerald E. Speitel Jr.

Mary Jo Kirisits

Halil Berberoglu

Effect of temperature, dissolved inorganic carbon and light intensity on the growth rates of two microalgae species in monocultures and co-cultures

by

Fernando Almada-Calvo, B.S., M.S.E.

Dissertation

Presented to the Faculty of the Graduate School of

The University of Texas at Austin

in Partial Fulfillment

of the Requirements

for the Degree of

Doctor of Philosophy

The University of Texas at Austin

May 2014

Dedication

For my wife and sons.

Acknowledgements

First and foremost, I want to thank my advisors, Dr. Katz and Dr. Kinney, for providing the best guidance during these last six years that I have been in graduate school. They certainly helped me enormously to improve this work. They provided a good balance between freedom to pursue my interests and giving precise guidance and push towards achieving goals. I have the upmost respect for them.

Also, I want to thank all of EWRE students, faculty and staff. Everybody helped to shape this work. Especially, JP and Felipe who helped me solve practical problems in the lab. Dr. Kirisits provided me with excellent feedback on some of the work I was planning on doing and Charlie saved my experiments by re-building from scratch the water circulator's temperature controller when it failed. This work would have never been accomplished without all of you.

Special thanks go to Dr. Berberoglu and his students. I received great advice from Dr. Berberoglu, particularly on a key parameter for this study: Light penetration. His students, especially Tom and Altan helped me perform some of the light measurements and lent me a couple of key instruments to do so.

Also, I want to thank my sponsor, the Mexican Council of Science and Technology (CONACYT). This scholarship program is an excellent platform that gives Mexican students the opportunity to pursue graduate degrees overseas and I hope they continue the program for years to come.

I want to thank my parents and sisters for their constant encouragement. They certainly made this process more enjoyable.

Last but not least, I want to thank my wife Natalia for her total support these last four years. Especially these last two years and a half after Mateo was born. Spending her

weekends alone with a two year old (terrible twos are real) while I worked in the lab was very tough. I could never have achieved this if it had not been for her. Of course, I want to thank Mateo for just being there. His smile when I get home is the best gift anyone could hope for. And thanks to Agustín for being the best post-graduation gift.

Effect of temperature, dissolved inorganic carbon and light intensity on the growth rates of two microalgae species in monocultures and co-cultures

Fernando Almada-Calvo, Ph.D.

The University of Texas at Austin, 2014

Supervisors: Kerry A. Kinney and Lynn E. Katz

The enormous biodiversity of microalgae as well as their high photosynthetic rates can be exploited for a wide variety of applications including the production of high value chemicals, nutraceuticals, aquaculture feed, and most recently, biofuels. Regardless of the application, the productivity of the microalgae culture must be optimized in order to make the systems economically feasible. One environmental factor that greatly affects the productivity of mass cultivation systems is temperature since it can be prohibitively expensive to control in outdoor systems. Temperature affects microalgae growth rates both directly by its effect on metabolic rates, and indirectly, by changing the bioavailability of the inorganic carbon present in solution. In the first part of this research, the effects of dissolved inorganic carbon (DIC) concentration (varied by sparging CO_2-enriched air) and temperature on the growth of a model microalga species (*Nannochloris* sp., UTEX LB1999) were investigated in a turbidostat bioreactor. The results indicate that increasing DIC concentration yields higher microalgae growth rates up to an optimum value (around 3 mM for *Nannochloris* sp.) but higher concentrations actually inhibited growth. Since increasing the temperature decreases the DIC

concentration for a given gas pCO_2, it is necessary to adjust the pCO_2 to maintain the target DIC concentration in the optimal range for growth.

In the next phase of the research, the effect of average light intensity (Gav) and temperature on the growth rate of two microalgae species (*Nannochloris* sp., UTEX1999. and *Phaeodactylum tricornutum*, UTEX646) was investigated. Growth rates were measured over a range of average light intensities and temperatures using a turbidostat bioreactor. A multiplicative model was developed to describe growth as a function of both average light intensity and temperature.

In the third phase of this research, both microalgae species were grown together to explore the effects of temperature fluctuations on the population dynamics of the co-culture. It was observed that *Nannochloris* was inhibited by the presence of *P. tricornutum* in the medium, probably due to the excretion of secondary metabolites into the medium that affected *Nannochloris* growth (allelopathic effects). The temperature and average light intensity model developed under monoculture conditions was modified to incorporate the allelopathic effects observed. The resulting model provided a reasonable fit to the dynamic behavior of a *Nannochloris/P. tricornutum* co-culture subjected to temperature variations in chemostat experiments.

Table of Contents

List of Tables

List of Figures

Chapter 1: Introduction

MOTIVATION

The capacity of microalgae to fix carbon dioxide, produce oxygen, consume nutrients (nitrogen and phosphorus) and store energy in the form of biochemical compounds have made them the subject of a number of research projects since the 1950s (Goldman, 1979a). Various commercial applications of microalgae already exist, including the production of food for human or animal consumption (mainly aquaculture feed), production of high value chemicals such as beta-carotene (Borowitzka 1999), astaxanthin and DHA, as well as nutrient removal in waste water treatment (Pulz and Gross 2004; Day, Benson, and Fleck 2010; Hoffmann 1998; Oswald 2003). The potential for microalgae to provide a means of transforming solar energy into biofuels is a promising area of research, due to microalgae's relatively high photosynthetic efficiency and their ability to grow in salt and brackish water on non-arable land (Talbot et al., 1991; Chisti, 2008; Stephens et al., 2010).

CHALLENGES

An economically attractive approach to grow microalgae in mass quantities is through the use of open outdoor systems such as shallow raceway ponds. High algae productivity is essential in these systems for economic feasibility and to yield a positive energy balance. However, the high yields observed in laboratory studies, which have made them so attractive for possible uses in solar energy capture, have failed to translate to open mass cultivation systems.

Temperature, light intensity and nutrient concentrations are the main factors that affect an algal species' productivity and dominance in natural systems (Reynolds 2006). Thus, it is not surprising that one of the reasons for underperformance in open mass

cultivation systems is the fact that open ponds lack temperature control (Goldman, 1979 b) and are often not optimized with respect to availability of the key nutrient, dissolved inorganic carbon (DIC). This issue is especially significant in shallow ponds installed in dry climates where it is common to have high solar radiation during the day that leads to temperature fluctuations (Benemann and Tillet, 1987). Not only does temperature have a direct impact on growth rates, it also affects the solubility of carbon dioxide in water leading to variations in the bioavailability of DIC for microalgae growth. Thus, the effects of temperature on growth should be evaluated independently of the effects of DIC on growth. Moreover, temperatures swings may occur outside of the optimum range for growth of a particular microalgae species. The use of multispecies cultures can promote increased productivity across a broader temperature range. However, competition, allelopathy (the production of a toxic metabolite that inhibits growth of another species) and co-shading (attenuation of light due to absorption of light by the other species) may affect microalgae productivity in multispecies systems. These effects must be understood in order to develop large scale microalgae cultivation systems.

APPROACH

Ecological theory and experimental data suggest that the higher the biodiversity of primary producers (i.e. microalgae), the higher the productivity and stability of the ecosystem (Lehman and Tilman 2000; David Tilman, Reich, and Knops 2006). Understanding the effects of temperature, DIC concentration, and light attenuation on the specific growth rates of microalgae is an important step toward optimizing productivity of any microalgae system, but understanding and predicting these effects is even more important in multispecies systems.

The objective of this study was to examine the key factors affecting microalgae growth (temperature, light attenuation, and DIC concentration) in monocultures and develop a model that predicts algae growth in a multispecies system. These effects were examined using two representative marine microalgae species, *Nannochloris sp* (UTEX LB1999 and UTEX 1999.) and *Phaeodactylum tricornutum* (UTEX 646). The research was divided into three phases (presented in Chapters 3, 4 and 5)

The goal of the first phase of research was to independently examine the effects of DIC and temperature on *Nannochloris* sp. While previous research has identified the optimum temperature range for *Nannochloris* sp. growth and the positive effect of DIC on growth rate, these studies failed to account for the inherent temperature effects on carbon dioxide solubility. Thus, it has not been possible to determine whether the optimal DIC value for growth varies with temperature.

Phase two studies focused on independent examination of the effects of temperature and average light intensity (self-shading effects) on the growth rate of two microalgae species at ambient DIC concentrations. The goal of this phase of research was to develop a model for the specific growth rate, μ, that incorporates both of these factors. Two microalgae species that varied with respect to optimal temperature growth range, size and pigmentation were selected as representative species to achieve this goal. These two species exhibit very different growth vs temperature profiles: *Nannochloris* sp. (UTEX 1999.) has small spherical cells (2μm diameter), contains chlorophyll *a* and *b* and grows optimally at 25-28 °C. *Phaeodactylum tricornutum* (UTEX 646) cells are rod shaped (10μm long), grow optimally between 22-25°C and contain chlorophyll *a*, and *c* (green) along with xanthophyll (yellow) and other pigments that give it a distinctive brown color (Lepetit et al., 2013).

The final phase of this work focused specifically on co-cultures. The goal of the research was to develop a model that describes growth as a function of temperature and average light intensity, and incorporates allelopathic inhibition to describe the population dynamics of the cultures over a series of cyclical temperature variations.

Chapter 2: Literature Review

MICROALGAE AND ITS USES

Algae are a large and heterogeneous group of (mostly) photosynthetic organisms that produce oxygen, live in aquatic habitats and lack the body and reproductive features of land plants. According to this definition, algae include organisms that range from unicellular highly specialized bacteria to giant kelp. This group of organisms can be classified in at least 12 different phyla, each having enormously different physical, chemical and genetic differences. It is estimated that about 30-40 thousand species of algae exist (Graham et al., 2009). Within the photosynthetic, free floating (planktonic), single cells organisms, also called microalgae approximately 5,000 species have been described for the marine environment only (Reynolds, 2006 a). In addition to their huge biodiversity and potential to be used in a wide variety of applications, their importance for the functioning of life on earth is immense. At least half of the primary productivity of the planet is performed by oceanic microalgae and they constitute the base of the aquatic food chain (Falkowski, 2012).

Mass cultivation of microalgae has gained considerable attention from the research and industrial sectors, mainly due to their potential for producing high value products such as pharmaceuticals, nutritional supplements and pigments (Pulz and Gross, 2004), their ability to remove nutrients and other contaminants from municipal and industrial waste water (Oswald, 2003) and their photosynthetic capacity. The first record of algae used for human consumption dates back to the sixth century A.C. when Nori (*Porphyra*), the alga used for sushi, was collected from the sea. Today, this alga is cultivated in special farms in shallow sea water and the industry has a yearly turnover of nearly one billion dollars. More recently, other photosynthetic microorganisms such as *Chlorella* and *Spirulina* (cyanobacteria) have been cultivated to produce nutritional

supplements, where the biomass is produced, harvested, dried and sold in the form of powder or in pills. Approximately 3,000 tons of *Spirulina* and 2,000 tons of *Chlorella* biomass are produced every year. *Dunaliella* is also grown to produce carotenoids, which are used either for human consumption or for animal feed (Pulz and Gross, 2004).

In the past few decades, with the instability in oil prices and concerns over climate change, the idea of using microalgae to produce liquid fuels has gained renewed consideration (Chisti, 2008; Scott et al., 2010; Smith et al., 2010). Certain microalgae species are highly efficient in converting solar energy into chemical energy and a few of these are capable of storing significant quantities of lipids, up to 50% of their dry weight. These lipids are suitable for the production of energy dense liquid fuels, such as diesel or jet fuel (Schenk et al., 2008). However, much more research and development is needed to make this technology viable.

Another application that has received attention over the last fifty years has been the use of microalgae for nutrient removal in wastewater treatment. Dr. William Oswald from The University of California at Berkeley investigated the engineering aspects of using algae as a means to remove nutrients from wastewater and provide oxygen for aerobic bacteria to remove organic compounds in stabilization ponds (Oswald et al., 1957). Also, the possibility of using microalgae for the dual purpose of removing nutrients and producing valuable products from biomass has been reviewed by several authors (Benemann et al., 1977; Goldman, 1979 b; Noüe et al., 1992; Olguın, 2003; Oswald, 2003; Pulz and Gross, 2004). This process is especially attractive because valuable products could potentially be obtained with recycled nutrients and minimal energy inputs.

CHALLENGES FOR OUTDOOR MASS CULTIVATION OF ALGAE

Although microalgae biomass has been used to produce high value chemicals, food and nutritional supplements, outdoor mass cultivation for lower value, commodity products, such as biodiesel has been limited. One of the reasons for this is the energetic burden that the production of nutrients needed for algal growth has on the total energy balance of the process (Lardon et al., 2009; Clarens et al., 2010). In addition, the productivity of outdoor cultures has failed to match the yields observed in tightly-controlled laboratory culture experiments. Frequent biological contamination and uncontrolled temperature variations play an important role in reducing the productivity and stability of outdoor mass culture systems.

Biological Contamination

The cultivation of algae in outdoor open ponds is the most cost effective technology for mass producing large quantities of algae. However, these systems are prone to biological contamination which makes it difficult to maintain a stable and productive mono-algal culture for long periods of time. The high nutrient concentrations (nitrogen and phosphorus) as well as high dissolved and particulate organic carbon concentrations, usually present in algal cultures, make it very attractive for colonization by small herbivores, bacteria, fungi and other microalgae species. The growth of other organisms may alter algae growth by competing for nutrients and light and/or, in the worst case scenario, actively inhibit, lyse or ingest algae cells. Invasion of herbivorous protozoa or small crustaceans such as *Daphnia* may very rapidly end the productivity of a pond system (Goldman and Ryther, 1976; Goldman, 1979 a; Fishman et al., 2010). Invasion of native microalgae may also displace the desired algae species, making the production of a desired product very difficult.

The mass production of *Spirulina* and *Dunaliella* in outdoor ponds is possible mainly because the growth medium used is highly selective for these species. *Spirulina* grows in very alkaline medium whereas *Dunaliella* grows in high salinity waters. *Chlorella*, however, is a very robust, fast growing and a widespread algae genus, and mass production in outdoor ponds is possible, although frequent culture failures are common. Japanese and Taiwanese factories use organic substrates, such as acetate (mixotrophic growth) and closed systems to maintain highly productive cultures of *Chlorella*. The high value of the Chlorella product makes it economically feasible to employ closed, heterotrophic culture systems (Hase et al., 2000) but such a system likely would not be economically or energetically feasible for mass production for biofuels or other high volume, low cost commodity products.

Lack of Temperature Control

Another problem for outdoor ponds is the lack of temperature control, as it makes optimizing the growth of a particular algae strain a challenge. During the 1970s, the Department of Energy (DOE) carried out a program to investigate the possibility of using microalgae to mass produce oil for the subsequent production of biodiesel. Several algae species were screened for their ability to grow in salt or brackish water and accumulate lipids. Approximately 300 species were identified as having good biofuel producing potential. During the program, pilot outdoor production units were tested in New Mexico where they demonstrated that it is possible to cultivate oil producing algae in outdoor open ponds with productivities as high as 50 g m^{-2} day^{-1} for short periods. However, longer term stability and productivity of the cultures were limited by diurnal and seasonal temperature fluctuations. Maximum temperature fluctuations from 15˚C at night to 35˚C

during the day were observed during the pilot tests and these temperature variations were sufficient to decrease the productivities to 7 g m^{-2} day^{-1} (Sheehan, 1998).

Seasonal temperature fluctuations can also affect algal productivity. In climates where seasons bring marked temperature changes, it is common to observe fluctuations in the natural phytoplankton composition. It is normal to observe peaks of algae growth during different seasons, and these seasonal variations are more closely associated with temperature changes rather than hours of light or light intensity (Goldman and Ryther, 1976). In these geographical regions, it is almost impossible to keep a mono-algal culture stable all year long.

TEMPERATURE EFFECTS ON ALGAL GROWTH

Temperature, a measure of the average kinetic energy of molecules, affects a wide variety of biochemical processes in the cells of living organisms. In general terms, temperature affects cellular processes in two ways:

i) It increases or decreases the biochemical reaction rates happening inside and outside the cells.

ii) It affects the structure and therefore the functionality of many molecules crucial for the performance of the cell's machinery.

While at higher temperatures, chemical reactions tend to go faster, certain enzymes may denature and lose their reaction specificity or given a high enough temperature, lose functionality completely. Other structural components of the cells, such as the lipid bilayer or structural proteins may start to disassemble. At low temperatures, the reaction rates slow down, and proteins may also change structure. Given a low enough temperature, cells will stop dividing.

It is important to recognize that cells are very complex systems, where a huge number of reactions are taking place at the same time. Any model that attempts to describe cell division rates as a function of temperature has to somehow capture the sum of these reactions, or at least the reaction that limits the growth, which can change depending on the conditions and in most cases is unknown.

General approach to describe growth as a function of Temperature

In very broad terms, microbial growth as a function of temperature can be described by three cardinal temperatures:

1) T_{inf} : Minimum temperature under which growth cannot occur
2) T_{sup} : Maximum temperature above which growth cannot occur
3) T_{opt} : Optimum temperature, where growth is at its maximum

These three temperatures shapes the general profile of the temperature-growth curve. The nature of this curve is highly species dependent.

A common approach to describe microbial growth within T_{inf} and T_{opt} is to use an exponential term in the form of an Arrhenius equation (Goldman, 1974):

$$\mu = Ae^{\left(-\frac{Ea}{RT}\right)}$$

Where A is a constant (1/time), Ea is the growth activation energy (J mol^{-1}), R is the universal gas constant (J K^{-1} mol^{-1}) and T is temperature (K).

This approach works reasonably well when dealing with temperatures that are well within the T_{inf}-T_{opt} range. However, at temperatures above T_{opt}, the model overestimates the observed growth rates. An alternative approach to describe growth that takes into account the decrease in growth rate after T_{opt} is by the use of the following expression (James and Boriah, 2010):

$$\mu = Ae^{-K(T-Topt)^2}$$

Where K (T^{-2}) and A (1/time) are constants that determine the width and height of the curve respectively. In this case, the model describes a symmetrical curve.

Another approach to deal with the decrease in growth rates at temperatures higher than T_{opt} with an asymmetrical curve is by the use of a second exponential term (Bitaubé Pérez et al., 2008):

$$\mu(T) = A_0 e^{\left(\frac{E_a}{RT}\frac{T-To}{To}\right)} - B_0 e^{\left(\frac{E_b}{RT}\frac{T-To}{To}\right)}$$

Where A_0 and B_0 are specific rates of growth and deactivation (1/time) at the reference temperature T_o(K). E_a and E_b are activation energies of growth and deactivation respectively (J mol^{-1}) and R is the gas constant (J mol^{-1} K^{-1}). The values of A_0, B_0, E_a and E_b will determine the skewedness and height of the curve. It is common for microbial growth to show a steeper decline in growth after T_{opt}, which makes the curves skewed to the right. For some microbial species, the decline at higher than optimal temperatures is very abrupt.

Another approach to capture the behavior of the growth curve as a function of temperature is the use of discontinuous models such as the following one:

$$\mu = \begin{cases} \mu_{max} e^{\left(-K_T\left(\frac{T-T_{opt}}{T_{sup}-T_{opt}}\right)^2\right)} \; at\; T > T_{opt} \\ \mu_{max} e^{\left(-K_T\left(\frac{T-T_{opt}}{T_{inf}-T_{opt}}\right)^2\right)} \; at\; T < T_{opt} \end{cases}$$

Where T is incubation temperature (°C), μ_{max} is the maximum growth rate (1/time), K_T is an empirical constant, T_{opt} , T_{sup} and T_{inf} are the cardinal temperatures mentioned above (°C).

The appropriate model to describe the growth of microalgae will depend mainly on the specific microalgae species and the range of temperatures the model intends to describe.

Overall, there is a general trend seen in phytoplankton growth as a function of temperature. Eppley (1972) gathered data from several microalgae laboratory experiments performed for different species at a range of temperatures and developed an equation that puts a limit, or a line of maximum expectation, to the growth rate of microalgae at temperatures from 0 to 40°C. The shape of the graph follows an exponential curve described by the following equation:

$$\mu_{max} = 0.851(1.066)^t$$

Where μ_{max} has units of doublings per day and t is temperature in °C.

In any given ecosystem, microalgae growth rates will tend to be below this curve and the different species will be distributed on different sides under the curve, depending on their temperature adaptation. Overall, diatoms tend to grow best at the lower end of this range, green algae tend to grow best in the mid-range and cyanobacteria usually have a higher temperature tolerance. Most species used for mass cultivation grow best between 20 and 30°C. Although Eppley's approach is useful to understand the limitations of microalgae growth in general terms and the limits of primary productivity in natural environments, it does not explain how individual microalgae species will behave in a given situation. For instance, in the case of mass culturing operations, where a particular species is responsible for the production of the desired product, the most useful model will be the one calibrated specifically for that species.

Temperature, apart from directly affecting the growth rate of microalgae by increasing or decreasing the biochemical reaction rates in the cell, it can also affect it indirectly, by changing the bioavailability of some substrates. For example, the dissolved

inorganic carbon concentration decreases with increased temperature. Understanding the effects of temperature on the bioavailability of DIC and on the growth of microalgae is crucial to predict their behavior in outdoor cultures.

DISSOLVED INORGANIC CARBON (DIC) EFFECTS ON ALGAL GROWTH

A common practice to enhance microalgae growth rates is to bubble CO_2-enriched air into the growth medium in order to increase the bioavailability of carbon in the culture media (Chisti, 2008; Eriksen, 2008; Li et al., 2008; Schenk et al., 2008). CO_2-enriched air has a higher CO_2 partial pressure (P_{CO_2}) than ambient air which drives the dissolution of more CO_2 into the medium, yielding an increase in the total dissolved inorganic carbon (DIC) concentration. When the culture conditions are appropriate (temperature, salinity, light) microalgae cells respond to this additional carbon with higher growth rates in a manner similar to heterotrophic microorganisms when more organic substrate, such as glucose or lactate, is added to the growth medium.

A common approach to study the effects of DIC concentration on the growth rates of microalgae is to vary the CO_2 concentration in the gas phase in contact with the culture. It is clear from the published data that increasing the CO_2 concentration in the gas phase results in higher algae productivity up to a threshold level, where inhibition is observed. This level varies from species to species. For example, Chiu et al. found that for *Nannochloropsis oculata*, the optimal gas phase CO_2 concentration at 26ºC and 300 μmol m^2s^{-1} was 2% (Chiu et al., 2009), while Jacob-Lopes found that for *Aphanotece microscopic* Nägeli, the optimal CO_2 concentration was 15% at 35ºC and ll klux (Jacob-Lopes et al., 2008). In contrast, other species like *Chloroccocum littorale*, are able to tolerate very high CO_2 concentrations, up to 50% (Ota et al., 2009).

Microalgae, when performing photosynthesis, take up DIC from the culture medium to store biochemical energy, build biomass and reproduce. However, DIC exists as four different molecules: Dissolved carbon dioxide ($CO_{2(aq)}$), carbonic acid (H_2CO_3), bicarbonate (HCO_3^-), and carbonate (CO_3^{2-}). The relative quantity of each depends on the pH of the solution. The mechanism for DIC uptake varies among microalgae species. Some, have a greater affinity for specific forms of dissolved inorganic carbon, either CO_2^* (sum of $CO_{2(aq)}$ and H_2CO_3), HCO_3^- or $CO_3^=$. For example, *Nannochloris maculata* and *Nannochloris atomus* have been reported to have a greater affinity for CO_2* (Huertas et al., 2000). Other species such as *Nannochloropsis oculata* and *Monallantus* sp. have a higher affinity for HCO_3^- (Munoz and Merrett, 1989). These differences are due to the different affinities of the active transport enzymes for either CO_2^* or HCO_3^-. These enzymes can be present either on the plasma membrane or on the chloroplast. Although some microalgae species have certain affinities to one or the other DIC species, most algae possess active transport mechanisms for both CO_2* and HCO_3^- (Colman et al., 2002; Giordano et al., 2005). At the pH levels present in most continuous CO_2-enriched cultures (6.5-8.5), the majority (more than 85%) of the DIC is in the form of these two species. Furthermore, as DIC is the sum of all inorganic carbon species and acid base reactions are fast compared with algae growth, the cell division rate is dependent on DIC, independently of which inorganic carbon species the algae prefers (Goldman et al., 1974; Carvalho et al., 2006). Therefore, it makes sense to use DIC concentration as the independent variable to estimate the growth rate of microalgae, in systems sparged with CO_2-enriched air.

Also, as stated above, temperature affects the solubility of inorganic carbon. This effect must be taken into consideration when estimating the amount of dissolved inorganic carbon in solution. However, the studies that have investigated the combined

effects of temperature and gas-phase CO_2 concentration on the specific growth rates of selected microalgae species (Hanagata et al., 1992; Jacob-Lopes et al., 2008; Chinnasamy et al., 2009), did not consider the changes in the solubility of DIC due to temperature. One study did take into consideration the effects of temperature on the solubility of inorganic carbon. Fu et al. (2007) investigated the impact of higher atmospheric CO_2 concentration and temperature in the growth of two microalgae species. However, the ranges of concentrations tested were relevant to ambient CO_2 conditions, and not to mass culturing operations.

LIGHT INTENSITY EFFECTS ON ALGAL GROWTH

The conversion of light energy into chemical energy is performed by the photosynthetic apparatus inside the chloroplasts, in the case of eukaryotic cells, or on the thylakoid membrane, in the case of photosynthetic bacteria. This apparatus has a very complex structure on molecular to membrane scales and it varies dramatically across phylogenetic groups. In general, it consists of two photosystem reaction centers (PSI and PSII) surrounded by proteins bound to light absorbing pigments called Light Harvesting Complexes (LHC) that help absorb light energy and transfer it to the reaction centers in PSI and II, where the main photosynthetic reactions take place. PSII is the center where the energy captured by the LHCs is used to oxidize a chlorophyll *a* molecule. The excited electrons, product of the oxidation, are then channeled through an electron transport chain linked to a proton transfer mechanism across the thylakoid, which creates a proton gradient that is used to create ATPs. The electrons eventually reach PSI, where more light energy is used to excite them even further to reduce NADP to NADPH. The oxidized Chlorophyll *a* in PSII is reduced by a water molecule, essentially splitting the H_2O molecule into H^+ (which is also used in an H^+ gradient to produce ATP) and O_2. In

summary, the photosynthetic process is powered by photons that excite the electrons in Chlorophyll *a* to produce ATPs, NADPH and oxygen. Carbon reduction into organic molecules is independent of light, as the reducing power to carry out the process is provided by the NADPH produced in PSI.

For photosynthesis, the range of wavelengths used by plants is between 400 and 700 nm. The light at these wavelengths, also called the photosynthetically active radiation (PAR) range, is considered useful for bioenergetic purposes. Outside of this range, little is captured for growth. However, even though it may not be captured for growth, it does not mean it will not have an effect on growth. Ultraviolet light has the capacity to alter the growth behavior, by causing damage to certain cell components.

In photoautotrophic cultivation systems, the only energy source for microalgae growth comes from the photons provided by light and therefore algae growth is totally dependent on the amount of light available to them. Therefore, under nutrient replete conditions, growth is understandably dependent on the rate at which the light reactions of photosynthesis produce ATP and NADPH. Therefore it is expected that the more light available for PSI and PSII to absorb, the faster the microalgae will fix inorganic carbon and build biomass. However, as any enzyme catalyzed reaction, there is a point where an increase in substrate concentration (in this case photons), does not translate into a higher reaction rate. In general, the more light intensity the higher the growth rate, until it reaches a point of saturation, following a rectangular hyperbolic curve. However, at high light intensity, the photosynthetic apparatus may become damaged due to excessive energy. In particular, the reaction center within PSII is where the most damage occurs (Adir et al., 2003). When the rate of PSII regeneration is lower than the rate at which it is damaged, photosynthetic inhibition is observed. The light intensity at which photo-inhibition is observed is highly variable among species (Sorokin and Krauss, 1958).

Some, like *Synechocystis minima* can be inhibited at light intensities as low as 100 μmol/m^2-s at 20°C (Dauta et al., 1990) whereas *Coelastrum microporum* will not start to be inhibited until it is subjected to about 500 μmol/m^2-s at 25°C (Bouterfas et al., 2002).

Several models have been developed in the last 100 years to describe algae photosynthetic rate and growth rate as a function of light intensity (G). Although photosynthetic rate is not the same as growth rate, since growth is the sum of many reactions, some that take place in the light and others that are independent of it such as respiration; it is still true that the behavior of models that describe photosynthetic rates vs light are similar as the ones that describe growth rate vs light. These models can be divided into two classes: 1) Saturation models, that describes growth as a function of light intensity as a rectangular hyperbolic curve where a light saturation level is reached and 2) Inhibitory models, that take into account photo-inhibition, where a maximum growth rate is reached at an optimal light intensity, above which growth rate starts to decline.

Within the light saturation models one of the most used because of its simplicity is the Monod equation shown below (Huisman et al., 2002; Berberoglu et al., 2008):

$$\mu = \frac{\mu_{max} G}{K_G + G}$$

where μ is the specific growth rate (1/time), μ_{max} is the maximum specific growth rate (1/time), G is the light intensity (μmol m^{-2} s^{-1}) and K_G is the light half saturation constant (μmol m^{-2} s^{-1}). This model treats light intensity as if it was a substrate concentration and assumes that the enzymes of the photosynthesis apparatus gets saturated by light (G) at a certain level, which is dependent on the value of K_G; where the higher the value of K_G the higher the light saturation point.

Another model, developed by Falkowski et al. (1985), that uses an exponential term is written bellow:

$$\mu = \mu_{max}\left(1 - e^{-\left(\frac{a\,G}{\mu_{max}}\right)}\right)$$

Where a is an empirical constant (day^{-1} m^2 s μmol^{-1}), μ_{max} is the maximum growth rate (1/day) and G is light intensity (μmol m^{-2} s^{-1}). The behavior of this model is similar to the Monod equation; however it tends to have a steeper slope at lower light intensities and therefore reaches a maximum growth rate at lower light intensities. The level of light intensity at which the microalgae reaches light saturation is judged by the initial slope: a/μ_{max}, where a lower slope means a higher light saturation point.

Within the inhibitory models, the model developed by Steele has been used extensively (Steele, 1962):

$$\mu = \mu_{max}\left(\frac{G}{G_{opt}}\right)e^{\left(1-\frac{G}{G_{opt}}\right)}$$

Here, G_{opt} is the light intensity where growth is observed to be optimal and G is the incubation light intensity.

Another model that can be used to describe growth with inhibition as a function of light intensity is the one developed by Eilers and Peeters:

$$\mu = \frac{\mu_{max}2(1+\beta)G_r}{{G_r}^2 + 2\beta G_r + 1}$$

Where Gr is G/G_{opt} and β is an empirical constant that determines how steep the curve declines at higher than optimal light intensities. This model describes a growth decline with a lower slope than the model developed by Steele and the β parameter makes the model more adaptable to empirical data.

It is important to note that microalgae have the capacity to acclimate to different light intensities and qualities (photoacclimation). The photosynthetic apparatus is quite flexible at increasing or decreasing the ratio of reaction centers PSI:PSII as well as the

amount of LHCs, and their associated pigments. For example, it is common for microalgae cells to increase their light harvesting pigments such as Chlorophyll *b* and *c* when subject to low light intensities. This is thought to be an adaptation to increase photosynthetic efficiency when light is limiting. On the other hand, some microalgae when subject to high light intensities will lower the amount of light harvesting pigments and decrease the amount of energy that is transferred to the PSII to decrease photodamage (Raven and Geider, 2003). For example, at low light intensities *Dunaliella salina* and *Chlamydomonas reinhardtii* have been shown to up-regulate the chlorophyll *a* oxygenase (CAO) and the LHCb genes, which code for the enzyme that transforms chlorophyll *a* into chlorophyll *b* and the LHCb protein respectively. The LHCb complexes with chlorophyll *b* to help harvest light and transfer its energy to PSI and II (Tanaka et al., 1998; Masuda et al., 2003; Nakagawara et al., 2007). Measurements of the expression of these genes could be used to assess the light limitation status of dense microalgae cultures. Understanding the mechanisms involved in light harvesting adaptation may lead to the future development of highly efficient microalgae strains.

Influence of temperature on photosynthesis

Since temperature affects all reactions occurring in the cells, it is reasonable to expect that photosynthesis rates will also be affected by it. Indeed, it has been observed that temperature induces changes to the light intensity at which photosynthesis gets light saturated or the point at which light inhibition is observed; the lower the temperature, the lower the point where light saturation and/or light inhibition occurs. This is because at low temperatures, the reaction rates of the photosynthetic apparatus slow down while the energy coming from light remains the same. The energy that can't be processed through chemical reactions is then scattered through the cells or radiated back to the medium and

not utilized to any useful process in the cell. When the excess energy becomes too high it can damage the photosynthetic apparatus, causing inhibition.

The extent of the effects that temperature has on the light saturation or inhibition point is dependent on various factors, such as the amount and type of pigments present in the cells and the adaptability of the species to specific conditions. For example Talbot found that in the case of *Oscillatoria agardhii*, the observed optimum light intensity at 20°C was 82 μmol $m^{-2}s^{-1}$ and at 30°C was 87 μmol $m^{-2}s^{-1}$ only a 6% increase. However, for *Phormidium bohneri,* at the same temperatures, I_{opt} was observed to be 239 and 499 μmol $m^{-2}s^{-1}$ a more than a 100% increase (Talbot et al., 1991).

Light self-shading effects

When photons penetrate into a water body, they will either get absorbed, scattered by particles or pass through. The amount of light and the wavelengths that gets selectively absorbed depends on the type and concentration of chemicals dissolved in the water body as well as on the amount of particles suspended on the water column. In clear waters, the wavelengths that get more readily absorbed are in the red and infrared range and blue-green light can penetrate to considerable depths. However, when there are particles, light will get scattered and absorbed and will not penetrate much into the water column. The effects on light intensity and quality as a function of water depth are important to estimate the productivity of photosynthetic organisms in oceans and lakes. In a mass culturing systems, where high cell densities are achieved, it is important to study how light changes as a function of depth and biomass concentration. The more algae cells present in the culture, the less light will penetrate the medium and the culture may become light limited. Therefore, in a batch culture system, light availability is a dynamic parameter which decreases as more biomass is produced.

For estimating the amount of light available in a given culture, it is common to assume that the algae cells act as an absorptive substance that follows a Beer-Lambert type behavior. For a microalgae suspension, illuminated from the top only, light intensity will decrease exponentially as a function of depth:

$$G_D = G_{in} e^{-E_{ext} X D}$$

Where G_D is the light intensity (μmol m^{-2} s^{-1}) at a depth D (cm), G_{in} is the incident light (μmol m^{-2} s^{-1}), E_{ext} is the extinction coefficient (cm^2 $cells^{-1}$), and X is the concentration of microalgae (cells cm^{-3}). The value of the extinction coefficient depends on the microalgae's pigments and size and therefore is species dependent. It is important to note that this approach is just an approximation of the behavior of light inside the culture as it assumes that all wavelengths are absorbed equally and neglects scattering. In practice, it is possible to measure light on the PAR range across the depth of the culture at various biomass concentrations (X) and obtain an extinction coefficient that fits the behavior of the system.

As seen above, the average light inside a given culture system will be a function of the amount (X) and the type (E_{ext}) of microalgae in suspension, but also of the geometry of the reactor. Recirculating an algae suspension through a 5cm diameter clear tubular reactor will have a different average light intensity than a 30cm deep recirculating pond.

In order to estimate the effects of light penetration on the growth rate of a well-mixed microalgae culture, three different approaches have been tested:

1) Light intensity is averaged across the reactor and used to estimate growth rate of the microalgae at that average light. The reasoning is that microalgae suspended in a well-mixed reactor will randomly move in all directions inside the reactor and

experience all light levels. And therefore, the energy that the cells will ultimately use for growth will be an average of the energy that penetrates the reactor (Grima Molina et al., 1994; Berberoglu et al., 2008). This may be a reasonable approach for suspensions subject to incident light that is below the light inhibition level.

2) Light at every point in the reactor is used to estimate growth at distinct positions in the reactor and then averaged across the reactor. Mathematically this assumes that the cells are either static inside the reactor and always receive the same amount of light depending on their position relative to the light source, or that the growth rate instantly responds to the light level (Huisman et al., 2002).

3) Cells are "followed" across their path throughout the reactor. As cells moves back and forth through the light attenuation profile, they are subjected to high frequency light intensity fluctuations. The growth is then estimated according to the response to fluctuating light:

   a. Growth is calculated by using an average of the light intensity received by the cells throughout the exposure time.

   b. The dynamics of light adaptation of the cells are taken into account. This approach requires a basic knowledge on how the cells respond to high frequency fluctuating light.

It has been observed that when microalgae are exposed to high frequency light pulses, their growth rate depends on the average of the light intensity pulses, without taking into account the dark periods. However, at lower frequencies, the dark periods become more important and needs to be taken into account when averaging light intensities. This is explained by the fact that growth is a multistep process and light energy capture is only the first of many. There is some kind of "growth inertia" after the light is turned off that can last a few seconds (Grima Molina et al., 1996). However, in

order to apply this approach, it is necessary to know the photosynthetic dynamic responses to fluctuating light of the microalgae in question which is not always possible to estimate.

BIODIVERSITY AND PRIMARY PRODUCTIVITY

Outdoor open microalgae culture systems will be subject to the same environmental conditions that microalgae in nature face, including the presence of competing algae species, predators and pathogenic organisms. The dynamic nature of environmental parameters such as temperature and light also play an important role in determining the stability and productivity of outdoor microalgae open systems. Of these parameters, temperature is probably the most important parameter determining the succession of algal species in the culture.

Algae-Algae nutrient competition

In a continuous culture with nutrient limitation, algae competition based purely on nutrient consumption, will lead to the dominance of the species that grows more rapidly at the substrate concentration present (Reynolds, 2006 b). If two limiting substrates exist, (for example, phosphorus and silicon in the case of diatom microalgae) and the algae have similar resource saturated growth rates (similar μ_{max}), then two different species are expected to coexist within the culture if one has a higher affinity to one limiting nutrient and the other has a higher affinity to the other limiting nutrient. This coexistence has been shown to occur with *Astrionella formosa* and *Cyclotella meneghiniana*, where *A. formosa* has a half saturation constant for phosphorus (K_P) of 0.03µmol/L and a silicon half saturation constant (K_{Si}) of 3.9µmol/L, whereas *C. meneghiniana* have a K_P of 0.25 µmol/L and a K_{Si} of 1.4 µmol/L. When high Si:P ratios were present in the growth medium, *Cyclotella* dominated, whereas at low Si:P ratios, *Astrionella* dominated and at

intermediate values both coexisted. If we extrapolate this behavior to other nutrients such as iron, vitamins and other trace metals, this theory suggests that the maximum number of species present in a continuous culture at steady state is equal to the number of limiting nutrients in the system (Reynolds, 2006 b).

Paradox of the Plankton

Although continuous culture experiments predict the dominance of a limited number of algae species, the paradox lies in the fact that in nature we observe hundreds if not thousands of different species coexisting together (Benemann and Tillet, 1987). Part of the explanation for this phenomenon is that natural systems are very rarely homogeneous or operating under steady state conditions. Light, temperature and nutrients are unevenly distributed and always fluctuating. These dynamic conditions make it possible for different species to coexist and/or to be dominant for a certain length of time and decline afterwards. In high nutrient waters, like a mass culturing pond, mono-algal cultures are more common, but usually only for a limited period of time, as temperature induced community changes often occur (Goldman and Ryther, 1976). This suggests that under dynamic conditions, a multispecies algae culture is desired to maintain stability. In the case of temperature based algae competition, the temperature fluctuations need to be within the range and frequency tolerated by the algal species present.

Biodiversity effects on productivity and stability

Biodiversity or ecological diversity is a measure of how many species of organisms coexist in a limited space and time. Although the hypothesis that a more diverse ecosystem tends to be more stable and productive has been debated over the last few decades (Tilman, 2000), recent experiments in the field and at laboratory scale, have shown that this hypothesis is true at least for primary producers in natural environments.

In this case, productivity refers to the carbon fixation or biomass production and stability refers to the variation through time of that production. Experiments with land plants and sea weed where the number of species was controlled and the stability and biodiversity monitored over time showed clearly how increasing the number of species (even randomly chosen from a larger pool) increased biomass production and the stability of the system (Tilman et al., 2006; Stachowicz et al., 2008).

One explanation for this behavior is the fact that organisms are usually adapted to grow in a defined range of conditions (range of temperature or nutrient concentration) and if that condition changes, their growth rate will decrease. In land plants or sea weed, the chemistry of the soil or attachment surface (for seaweed), their location with respect to sunlight, temperature and nutrient concentration, each play a role in determining which species will be more suitable to grow at a determined place. Therefore, it follows that having more species adapted to grow in the different niches associated with a particular growth environment, will result in a higher colonization of the area.

Recent experiments (Stockenreiter et al., 2011; Corcoran and Boeing, 2012) performed with microalgae assemblages, compared the productivity and lipid production of multispecies cultures of varying diversity with the ones obtained with monocultures. They found that on average, multispecies cultures outperformed the monocultures in terms of productivity and lipid production and that the particular combination of species in a given community dictated the productivity. They observed that the most productive microalgae species had to be present for the community as a whole to be more productive.

These experiments also tested the capacity of the communities to recover after the addition of a herbivore to the culture. They observed that the more diverse the culture, the faster it recovered from the addition of a herbivore. The impact of a predator or pathogen

invasion can be contained by having multiple species in the culture system since it is common for predators or pathogens (bacteria, fungi or viruses) to be somewhat specific on which species they affect. Therefore it is expected that having several species within the culture will contain the effects on productivity since the pathogen will attack some species but not all, limiting the decrease in productivity.

Allelopathic interactions

Every organism on earth is subject to competition either within its own species or with other species that compete for space, nutrients and energy. Several mechanisms for competition among species have evolved, including the production of growth inhibiting substances. These types of interactions between microalgae species is called allelopathy. Some authors (International Allelopathy Society, 1996) have defined allelopathy in very broad terms as the effects that one species (plant, algae, microalgae, fungi or bacteria), called the donor, has on the growth of another, called receptor, via the secretion of secondary metabolites. The effects can either be of growth enhancement or growth inhibition caused by a direct or indirect chemical interaction. Other authors narrow the definition to refer only to chemical interactions among algae species where the donor excrete a chemical that inhibits the growth of the receptor (Legrand et al., 2003). Within this work, the former definition will be used.

The most common method to determine if an allelopathic interaction exist between two species is by cross-culturing: growing the suspected allelochemical producer in pure culture, then filtering the spent medium and growing the other species in the cell-free spent medium, amended with nutrients. The growth rate of the species grown in the spent medium is compared to the growth rate obtained in a blank medium (no allelochemical). If the growth rate is slower in the spent medium, an allelopathic

interaction may be present among the species. This technique has been used to investigate several microalgae species including cyanobacteria, diatoms, dinoflagellates and green microalgae (Arzul and Gentien, 2006).

Allelopathic agents, the secondary metabolites that inhibit the growth of competing microalgae, can vary widely in nature and in their mechanism of action. Within the allelochemicals produced by microalgae, peptides, alkaloids, organic acids and long chain fatty acids have been isolated (Legrand et al., 2003).

One group of allelochemicals, mainly polyunsaturated fatty acids and their derivatives are named APONINs or AParent Oceanic Naturally occurrINg cytolins (Arzul and Gentien, 2006). These allelochemicals are produced by the marine *Gomphosphaeria aponina* (cyanobacteria) and some species of the *Nannochloris* genus (chlorophyta). These substances have been shown to have cytolitic activity towards *Karenia brevis* (dinoflagelate) and *Chatonella subsala* (Macías et al., 2007).

Another group of allelochemicals are glycolipid derivatives (Arzul and Gentien, 2006). The major glycolipids found in microalgae consist of one or two galactose units linked to a glycerol residue. The most important classes are monogalactosyldiacylglycerol (MGDG) and digalactosyldiacylglycerol (DGDG). Glycolipids display an allelopathic effect when the fatty acids are polyunsaturated. These allelochemicals have been observed to cause allelopathic effects in several phytoplankton species and are produced by *Synechococcus* sp., *Gyordinium*cf. *aureolum*, *Chryschromulina polylepis*, and *Phaeodactylum tricornutum* (Chan et al., 1980).

Aminoacid based allelochemicals have been isolated from cyanobacteria. These chemicals have antibiotic and cytotoxic activities. Some of these are cyclic peptides, where Fischerellin A is the most known, which is produced by *Fischerella musciola*. It inhibits PSII activity and therefore affects any photosynthetic organism (Srivastava et al.,

1998). Other cyclic peptides have been shown to deter herbivore feeding, such as Laxaphycin A produced by *Hormothamnion enteromorphoides* (Pennings et al., 1997).

The majority of allelochemicals have been described only by their activity spectra, molecular weights or other gross chemical characteristics such as polarity. Allelopathic interactions have been observed or suspected within several microalgae species, however the precise description of the interaction is lacking. In a review by Legrand et al. (2002) they found 38 species of microalgae that have been observed to have allelopathic interactions with other microalgae species or bacteria. Of these, 20 had a known allelochemical and the rest were unknown.

As seen above, many allelochemicals are not specific to a particular species, but rather may inhibit many species in various degrees, including predators. This is why it has been theorized that having species that exude allelochemicals into the growth medium may deter the presence of predators in the culture, making them more stable through time (Shurin et al., 2013).

Chapter 3: Effects of DIC and Temperature on the growth rate of a model microalgae species.

INTRODUCTION

Microalgae can be used to make a wide variety of products including platform chemicals, nutraceuticals, aquaculture feed, fertilizers and even triglycerides for biodiesel production. The interest in microalgae for biodiesel production has increased recently as concerns over climate change grow. Microalgae are an attractive option for many applications due to their relatively high photosynthetic efficiency as well as the fact that algae can be cultivated on land unsuitable for food crops and with alternative sources of water such as sea water and waste water (Sheehan, 1998; Chisti, 2008; Dismukes et al., 2008; Li et al., 2008; Schenk et al., 2008; Costa and de Morais, 2010). However, for sustainable and economically feasible microalgae production, the productivity of microalgae systems must be optimized to minimize their physical and carbon footprints, water demand and nutrient requirements (N and P) (Lardon et al., 2009; Stephenson et al., 2010; Davis et al., 2011; Pate et al., 2011; Wigmosta et al., 2011).

One of the most economically feasible methods for microalgae cultivation is through the use of outdoor open ponds, where CO_2 enriched air is sparged through the medium to increase the dissolved inorganic carbon (DIC) concentration to enhance microalgae growth rates. However, these systems usually lack temperature control and, therefore, are subject to daily and seasonal temperature fluctuations.

Temperature affects the productivity of microalgae cultures in two ways: 1) it affects the microalgae growth rate by regulating the biochemical reaction rates within the cells and 2) it dictates the bioavailability of carbon to the cells, as it controls the solubility of CO_2 in the growth medium. For instance, a moderate increase in temperature will increase microalgae growth rates but will also decrease the solubility of CO_2; the

resulting decrease in available inorganic carbon for the algae potentially limits the growth rate. Therefore, understanding the combined effect that temperature has on growth rate and the bioavailability of carbon is essential for optimizing microalgae productivity in open outdoor ponds.

The effects of temperature (T) and DIC on microalgae specific growth rate (μ) has been studied extensively, but generally only one variable (either DIC or T) has been investigated at a time without taking into account how T affects DIC. Studies that have examined the effects of inorganic carbon on specific growth rate have either varied the amount of dissolved inorganic carbon (DIC) present or varied the CO_2 concentration in the gas phase. In all of these studies, the effects of temperature were not taken into account (Caperon and Smith, 1978; Chen and Durbin, 1994; Clark et al., 1999; Huertas et al., 2000; Nakamura et al., 2005). Other studies have investigated the combined effects of temperature and gas-phase CO_2 concentration on the specific growth rates of selected algae species (Hanagata et al., 1992; Jacob-Lopes et al., 2008; Chinnasamy et al., 2009), but none of these considered how changes in temperature affect the solubility of inorganic carbon. Fu investigated the combined impact of elevated gas phase CO_2 and temperature due to climate change on DIC solubility in the oceans and the growth rate of two cyanobacteria species (Fu et al., 2007). However, the range of concentrations investigated (2.03 – 2.15 mM DIC) are more relevant to ambient CO_2 conditions but not the CO_2-enriched gases used to yield highly productive microalgae cultures.

The main objective of this study was to independently examine the effect of DIC and temperature on the specific growth rate of a representative microalgae species in seawater (*Nannochloris* sp. UTEX LB1999) and to develop a mathematical model to link DIC (estimated by measuring alkalinity and pH) and temperature to growth rates. The resulting model describes the combined effects of temperature and DIC on biomass

production. A turbidostat reactor was used to maintain DIC, temperature and biomass concentration constant while measuring growth rates at each experimental condition.

THEORETICAL CONSIDERATIONS

The total amount of inorganic carbon in solution is the sum of dissolved carbon dioxide, carbonic acid, bicarbonate and carbonate ($DIC = [CO_2{}^*] + [HCO_3^-] + [CO_3^{2-}]$, $CO_2{}^*$ is the sum of dissolved carbon dioxide and carbonic acid). In an open system, the concentration of DIC is a function of the carbon dioxide partial pressure (P_{CO_2}), pH, alkalinity, and temperature, but the relative amount of each DIC species in the medium is primarily a function of pH (at a given ionic strength).

Alkalinity is defined as the hypothetical amount of acid needed to attain the pH of a solution containing $CO_2{}^*$ and water. In waters where the carbonate system is the most important acid-base system present, alkalinity is typically only a function of the bicarbonate and carbonate concentrations. In sea water, however, where borate, phosphates and other bases are present, alkalinity is also a function of the concentration of these weak bases. In this study, the synthetic sea water used for the net specific growth rate determination contained several weak bases such that the alkalinity equation becomes:

$$Alk = [HCO_3^-] + 2[CO_3^{2-}] - [H^+] + [OH^-] + [Tris^-] + [B(OH)_4^-] + [HPO_4^{2-}] + 2[PO_4^{3-}]$$

Equation 1

Rearranging

Equation 1 to make DIC a function of $[H^+]$ and total component concentrations (C_i), we obtain:

$$DIC = \frac{Alk + [H^+] - \frac{K_W}{[H^+]} - \alpha_T C_T - \alpha_B C_B - \alpha_{P_3} C_P - 2\alpha_{P_2} C_P}{\alpha_{C_1} + 2\alpha_{C_2}}$$

Equation 2

Where:

$$\alpha_{C1} = \frac{[HCO_3^-]}{DIC} = \frac{K_{aC1}[H^+]}{K_{aC1}K_{aC2}+K_{aC1}[H^+]+[H^+]^2} \quad \text{Equation 3}$$

$$\alpha_{C2} = \frac{[CO_3^{2-}]}{DIC} = \frac{K_{aC1}K_{aC2}}{K_{aC1}K_{aC2}+K_{aC1}[H^+]+[H^+]^2} \quad \text{Equation 4}$$

$$\alpha_T = \frac{[Tris]}{C_T} = \frac{K_{aT}}{K_{aT}+[H^+]} \quad \text{Equation 5}$$

$$\alpha_B = \frac{[B(OH)_4^-]}{C_B} = \frac{K_{aB}}{K_{aB}+[H^+]} \quad \text{Equation 6}$$

$$\alpha_{P2} = \frac{[HPO_4^{2-}]}{C_P} = \frac{K_{aP1}K_{aP2}[H^+]}{K_{aP1}K_{aP2}K_{aP3}+K_{aP1}K_{aP2}[H^+]+K_{aP1}[H^+]^2+[H^+]^3} \quad \text{Equation 7}$$

$$\alpha_{P3} = \frac{[PO_4^{3-}]}{C_P} = \frac{K_{aP1}K_{aP2}K_{aP3}}{K_{aP1}K_{aP2}K_{aP3}+K_{aP1}K_{aP2}[H^+]+K_{aP1}[H^+]^2+[H^+]^3} \quad \text{Equation 8}$$

Acid dissociation constants (K_{ai}) can be calculated using empirical equations where the effects of temperature and ionic strength or salinity are taken into account. Table 1 shows the equations used in this study to calculate the acid dissociation constants.

Table 1: Main acid-base components of the medium along with the corresponding empirical equations used to calculate the equilibrium constants for the system used in this study as a function of salinity (S), ionic strength (I), and temperature (T).

Component	Acid-Base reactions	Equations for equilibrium constants [S (g/kg), T(K)]	Reference
Carbonate	$CO_{2(gas)} \leftrightarrow H_2CO_3^*$	$lnK_H\left(\frac{mol}{l \cdot atm}\right) = -58.0931 + 90.5069 * \left(\frac{100}{T}\right) + 22.2940 * \ln\left(\frac{T}{100}\right) + S * (0.027766 - 0.025888 * \left(\frac{T}{100}\right) + 0.0050578 * \left(\frac{T}{100}\right)^2)$	(Weiss, 1974)
	$H_2CO_3^* \leftrightarrow H^+ + HCO_3^-$	$pK_{aC1} = A_1 + \frac{B_1}{T} + C_1 lnT + pK^0_{aC1}$ $A_1 = 13.4191S^{0.5} + 0.0331S - 5.33 * 10^{-5}S^2$ $B_1 = -530.123S^{0.5} - 6.103S$ $C_1 = -2.0695S^{0.5}$ $pK^0_{aC1} = -126.34048 + \frac{6320.813}{T} + 19.56822 lnT$	(Millero et al., 2006)
	$HCO_3^- \leftrightarrow H^+ + CO_3^{2-}$	$pK_{aC2} = A_2 + \frac{B_2}{T} + C_2 lnT + pK^0_{aC2}$ $A_2 = 21.0894S^{0.5} + 0.1248S - 3.687 * 10^{-4}S^2$ $B_2 = -772.483S^{0.5} - 20.051S$ $C_2 = -3.3336S^{0.5}$ $pK^0_{aC2} = -90.18333 + \frac{5143.692}{T} + 14.613358 lnT$	(Millero et al., 2006)
Tris buffer	$TrisH^+ \leftrightarrow Tris + H^+$	$pK_{aT} = 6.165 * 10^{-5} * S^2 - 0.023755 * S + 6.313 * \frac{S}{T} - 22.5575 + \frac{3477.5496}{T} + 3.32867 * \ln(T)$	(Millero, 1986)

Table 1 continued: Main acid-base components of the medium along with the corresponding empirical equations used to calculate the equilibrium constants for the system used in this study as a function of salinity (S), ionic strength (I), and temperature (T).

Boric acid	$B(OH)_3 + H_2O \leftrightarrow B(OH)_4^- + H^+$	$lnK_{aB} = 148.025 + 137.194S^{0.5} + 1.6214S + (-8966.9 - 2890.5S^{0.5} - 77.94S + 1.728S^{1.5} - 0.0996S^2)/T + (-24.4344 - 25.085S^{0.5} - 0.2474S)lnT + 0.053105S^{0.5}T$	(Dickson, 1990)
Phosphate	$H_3PO_4 \leftrightarrow H^+ + H_2PO_4^-$	$K_{aP1} = -\frac{75}{T} + 2.16 - 0.35I^{0.5}$	(Dickson and Riley, 1979)
	$H_2PO_4^- \leftrightarrow H^+ + HPO_4^{2-}$	$K_{aP2} = \frac{737.6}{T} + 4.176 - 0.851I^{0.5}$	
	$HPO_4^{2-} \leftrightarrow H^+ + PO_4^{3-}$	$K_{aP3} = \frac{2404}{T} + 1.31 - 0.87I^{0.5}$	
Water	$H_2O \leftrightarrow H^+ + OH^-$	$K_w = 1.1825 * 10^{-4}T^2 - 0.1034T + 34.313 - \left(\frac{I^{0.5}}{1 + I^{0.5}} - 0.2I\right)\left(\frac{298}{T}\right)^{2/3}$	(Butler, 1982)

In an open system where the base concentrations are known and changes in pH are only due to changes in P_{CO2} (not due to other acid or base additions), it is possible to calculate any of the three interdependent variables: Alkalinity, DIC or pH, by knowing two of the others (Equation 2). In practice, it is easy to measure pH with a potentiometer and alkalinity by means of a titration. It is also possible to calculate the theoretical CO_2 partial pressure in equilibrium with a particular DIC concentration and pH.

$$P_{CO_2} = \frac{DIC\ \alpha_{C0}}{K_H} \qquad \text{Equation 9}$$

To illustrate the dependence of DIC on pH, P_{CO2}, and temperature the model described above was used to plot DIC and pH versus CO_2 concentration in the gas phase at equilibrium in Figure 1. At higher CO_2 gas phase concentration, the pH decreases and the DIC concentration increases. The dependence of DIC concentration on temperature is also shown; for a given CO_2 gas phase concentration, the DIC concentration is lower at 35°C than at 15°C.

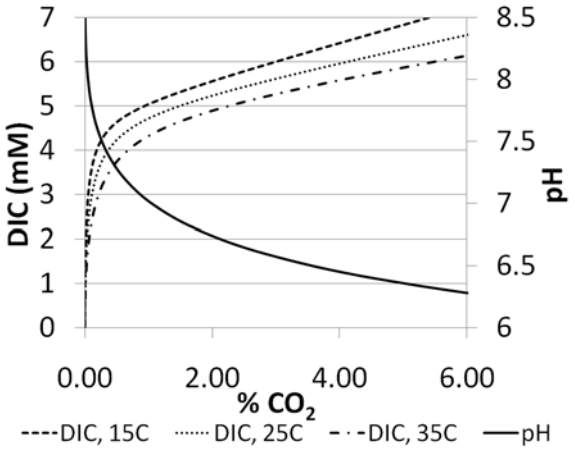

Figure 1: DIC concentration and pH as a function of CO_2 gas phase concentration at 15, 25 and 35°C for a synthetic sea water medium with a total alkalinity of 5mM.

MATERIALS AND METHODS

Experimental Approach

Since alkalinity, pH and average light intensity inside the reactor are a function of biomass concentration, a turbidostat bioreactor was used to maintain the same biomass concentration during all experiments. Net specific growth rates were determined during continuous culture at 15, 25 and 35°C and DIC concentrations between 0.8 and 5.9mM (See Table 2).

Experimental Conditions

At the beginning of each experiment, 2.25 L of sterile medium was placed in the reactor and seeded with a 250 mL inoculum (optical density between 0.5 and 1 at 680 nm) of *Nannochloris* sp. (UTEX LB1999). The culture was allowed to grow in batch mode until the turbidity of the culture medium in the reactor reached 150 Formazin Turbidity Units (FTU). During the batch growth phase of all experiments, the temperature of the reactor was maintained at 25ºC and ambient gas-phase carbon dioxide concentration (approximately 390 ppm) was provided to the reactor. In only one experiment, a 3% CO_2 air mix was injected during the batch growth phase.

Once the reactor reached the turbidity set point, the pump injected fresh medium in order to keep the biomass concentration constant. Temperature was modified depending on the condition to be tested, the alkalinity was measured and the desired DIC concentration was obtained by adjusting the pH (calculated to reach the desired DIC) by increasing or decreasing the CO_2 concentration in the gas phase. It is important to note that during continuous culture, the DIC concentration, pH, temperature and biomass concentration were kept constant for at least 15 hours of operation, to assure steady state conditions and then changed to a different T and DIC combination. Depending on the

experiment, two or three T and DIC combinations were tested. A total of 9 experiments were conducted and 23 conditions tested (see Table 2). Two experiments were performed independently at the same exact conditions: 25˚C and 5.8 mM DIC to assess reproducibility. The media injection rate for both were very similar to each other (72.9 and 72.7 g/h), which demonstrates the reproducibility of the experiments.

Table 2: Summary of experimental conditions

Temperature (°C)	Alkalinity (meq/L)	pH	DIC (mM)
15	4.4	8.4	1.4
	4.6	6.9	4.8
	4.7	6.5	5.8
	5.2	7.0	5.3
	4.9	8.2	2.5
	5.2	7.9	3.7
25 (Nitrogen limited)	3.1	7.9	0.9
	4.7	6.8	4.8
	4.2	8.1	1.3
25	5.2	8.4	1.3
	4.2	8.1	1.3
	5.2	6.8	5.3
	5.2	6.6	5.8
	5.2	6.6	5.8
	4.8	7.9	2.5
	5.2	7.7	3.4
	4.9	8.4	1.1
35	5.0	8.1	1.2
	5.0	6.6	5.2
	5.1	6.4	5.9
	5.1	8.0	1.6
	5.2	7.6	2.9
	5.3	7.3	3.9

Nitrogen limitation during continuous culture was assessed by spiking the culture with nitrate from an initial nitrate concentration of 0.2 mM to a final concentration of 2 mM and measuring the net specific growth rate before and after the spike. A change in growth rate was observed from 0.3 to 0.38 day^{-1}, which meant that the culture was not nitrogen saturated. The experiments performed with 1mM nitrate concentration at 25°C had a growth rate of 0.35 and 0.34 day^{-1}, which are within the experimental error of the observed growth rate at 2mM (within 10%); therefore, a 1 mM concentration was assumed to be nitrogen replete. Also, assuming that the nitrogen content of the cell (dry weight) was 6.3%, the amount of nitrogen needed to reach 0.28g/L (maximum biomass concentration reached) would be 1.8 mg/L or 0.126 mM of Nitrate, which represents only a 12.6% decrease in total nitrogen concentration.

Culture conditions

Nannochloris sp. (UTEX LB1999) was used as a model marine microalgae species. It was grown in a modified ASP medium (Andersen, 2005) with the following composition (per liter): NaCl, 23.38g; KCl, 0.75g; $CaCl_2$, 1.12g; $NaHCO_3$, 0.168g; $MgCl_2 \cdot 6H_2O$, 4.06g; $MgSO_4 \cdot H_2O$, 4.93g; Tris(hydroxymethyl)aminomethane base, 0.58g; $NaNO_3$, 0.085g; Na_2HPO_4, 0.032g; Fe-EDTA, 0.842mg; EDTA, 14 mg; $ZnSO_4 \cdot 7H_2O$, 10.064mg; H_3BO_3, 24.732mg; $CoCl_2 \cdot 6H_2O$, 0.071mg; $CuSO_4 \cdot 5H_2O$, 0.075mg; $MnCl_2 \cdot 4H_2O$, 1.979mg; $NaMoO_4 \cdot 2H_2O$, 1.21mg; Vitamin B_{12}, 0.5µg, Vitamin B_1, 100 µg; Biotin, 0.5µg. The medium was prepared with ACS grade reagents and adjusted to pH 7.5. For the experiments performed under nitrogen limitation, the medium contained a $NaNO_3$ concentration of 0.017g/L (0.2mM).

DIC determination

To determine DIC concentration, the pH and alkalinity of the medium were measured every 24 hours to confirm that they stayed within 10% of the set level for each experiment. The average of the measured pH and alkalinity values were used to calculate the DIC concentration for each experiment. The pH was measured using a VWR sympHony pH probe (14002-780, West Chester, Pennsylvania) connected to a Coulter Beckman pH meter (Phi570, Fullerton, California). Alkalinity was measured by a potentiometric titration to end-point pH according to method 2320B of Standard Methods for the Examination of Water and Wastewater (APHA, 1998).

Nitrate

Nitrate was measured potentiometrically using an ion selective nitrate electrode (Cole-Parmer® EW-27502-31, Vernon Hills, Illinois) connected to a Beckman Coulter potentiometer (Phi570, Fullerton, California). A calibration curve was obtained over the range of concentrations used in the experiments.

Suspended Solids Determination

Suspended solids were determined following Standard Method SM2540D30. Twenty five milliliter samples were filtered through a preconditioned filter (Millipore® RW03) which was weighed in advance. The filter was then dried in an aluminum pan at 104ºC for 24 hours and weighed after letting it cool in a desiccator for fifteen minutes (APHA, 1998).

Optical density

Optical density measurements were used to corroborate turbidity readings made from the meter inside the reactor during each experiment. Absorbance was measured using a 1 cm quartz cuvette at 680 nm with an Agilent 8453 spectrophotometer.

Reactor Configuration

The experiments were carried out in a transparent, rectangular (10 x 24 x 10.5 cm) reactor, submerged in a water bath (Fisher Scientific constant water circulator, 1013P, Pittsburgh, Pennsylvania). Each side received 160 µmol $m^{-2}s^{-1}$ in the PAR range provided by two 32 watts Phillips bulbs (F32T8/Cool White Plus) on each side. Light was measured with a LI-192 Underwater Quantum Sensor (Li-Cor, Lincoln, Nebraska). The reactor was equipped with a turbidimeter (Hach Solitax®, Düsseldorf, Germany) coupled with a controller (Hach sc100, Loveland, Colorado) programmed to pump fresh medium when the culture reached a predetermined turbidity value (150 FTU). The liquid volume within the bioreactor (2.5L) was held constant by withdrawing excess medium from the top of the bioreactor via a vertical, stainless steel tube connected to a vacuum flask. All the equipment in contact with the culture medium was either autoclaved (silicon tubing, glassware) or sanitized with bleach and subsequently rinsed with autoclaved deionized water (turbidimeter, reactor) prior to the start of each experiment.

CO_2 gas was added to the system by blending 99.999% pure CO_2 (Matheson TRI-GAS UN 1013, Parsippany, New Jersey) with laboratory compressed air. Two volumetric gas flow meters were used to regulate the individual volumetric flow rates. The mixed gas was filtered (Whatman, 3µm Hepa-VentTM gas line filter) and humidified before being injected into the culture medium at a constant rate (3000±150 cm^3/min) via an aquarium aerator located at the bottom of the reactor.

Growth Rate

During continuous culture conditions, the weight of the fresh medium was continuously measured (Ohaus Scout® SP4001, Pine Brook, New Jersey) and a graph of the mass of medium injected into the reactor versus time was constructed. The slope of the graph was taken as a valid measurement of the influent flow rate (Qin), only when the

data remained linear (linear trend line's $R^2 > 0.98$) for at least 15 hours of operation, to assure that the system was operating at steady state condition. This time frame was determined by experiments where it was observed that the rate of medium injected after 15 hours remained constant for 90 hours of operation. A mass balance was performed to estimate the net specific growth rate at each condition:

$$\frac{dVX}{dt} = \mu XV - Q_{out}X \qquad \text{Equation 10}$$

$$\frac{dV}{dt} = Q_{in} - Q_{out} - Q_{Ev} \qquad \text{Equation 11}$$

where V: Volume of reactor (mL), Q_{in}: Influent volumetric flow (mL/hr), Q_{out}, effluent volumetric flow (mL/hr), Q_{Ev}: rate of evaporation (mL/hr) experimentally determined at each temperature, X: Biomass concentration in the reactor (g/mL), and μ: Net specific growth rate (hr^{-1}). At steady state:

$$Q_{out} = \mu V \qquad \text{Equation 12}$$

$$Q_{out} = Q_{in} - Q_{Ev} \qquad \text{Equation 13}$$

Rearranging equations 12 and 13, μ was calculated with the following equation:

$$\mu = \frac{Q_{out}}{V} = \frac{Q_{in} - Q_{Ev}}{V} \qquad \text{Equation 14}$$

During batch culture, growth rate was calculated for each experiment by fitting the optical density vs time data to an exponential regression curve during the exponential portion of the growth curves.

RESULTS AND DISCUSSION

Net specific growth rates measured in continuous culture

Net specific growth rates were determined in continuous culture at 15, 25 and 35˚C and a DIC concentration range of 0.9-5.9 mM. Figure 2 shows the mass of media injected vs time obtained for Experiments 3, 4, 5 and 6 carried out at a DIC concentration

of 5.8-5.9 mM and the three temperatures tested. As evident in Figure 2, at higher temperature, a higher influent flow rate was observed (slope of each data set), which translates into a higher growth rate (See Eq. 14)). The linear behavior of the four sets of data for Experiments 3, 4, and 5 was maintained for at least 20 hours as confirmed by the R^2 values which were all higher than 0.998.

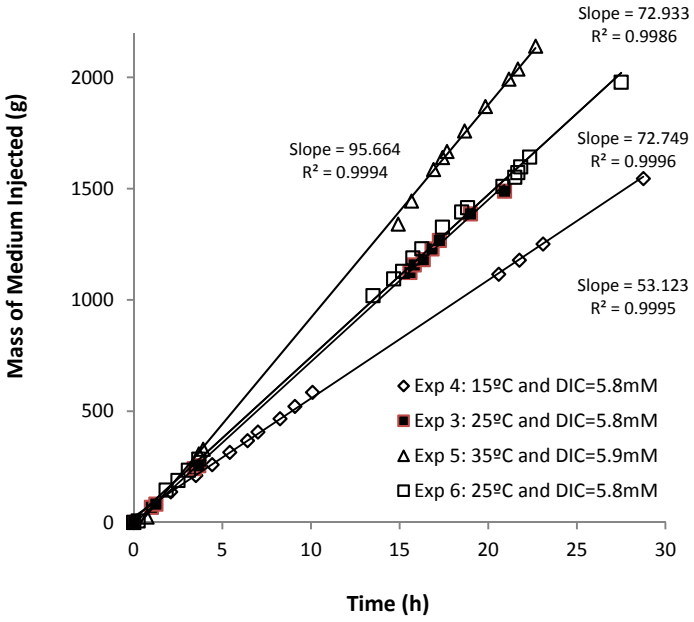

Figure 2: Mass of medium injected vs time at temperatures of 15, 25 and 35^0C and DIC concentrations of 5.8-5.9mM

Effects of DIC and Temperature

Bioreactor data collected at different temperatures and DIC concentrations are plotted in Figure 3. Higher temperatures yielded higher specific growth rates and DIC levels between 1 and 3 mM led to higher specific growth rates. Above a DIC concentration of approximately 3.5 mM inhibition was observed for experiments performed at 25 and 35°C. Although the reason for this inhibition is not well understood, as most research on microalgae has been performed on conditions typically encountered in natural habitats (low DIC concentrations), inhibition at high DIC concentrations have

been observed for several microalgae species (Hanagata et al., 1992; Yue and Chen, 2005; Papazi et al., 2008). Some researchers have linked high CO_2 concentrations in the growth medium to cytoplasmic and chloroplast acidification which results in lower photosynthetic efficiencies (Satoh et al., 2001; Miyachi et al., 2003). An increase in temperature from 15°C to 35°C for algae grown at a DIC concentration of approximately 3 mM resulted in a 2.29 fold growth rate increase. A similar trend was observed for algae grown at DIC concentrations of 5.3 and 5.8 mM where a 1.7 fold increase was observed. However, for algae grown at low DIC (1.3 mM), the increase in specific growth rate with temperature was only a factor of 1.4. These results suggest that at low DIC, temperature has less of an impact on the specific growth rate of this microalgae species. For outdoor algae cultures, these results suggest that it would be a useful strategy to maintain DIC levels at the optimum concentration, even when diurnal changes in temperature take place.

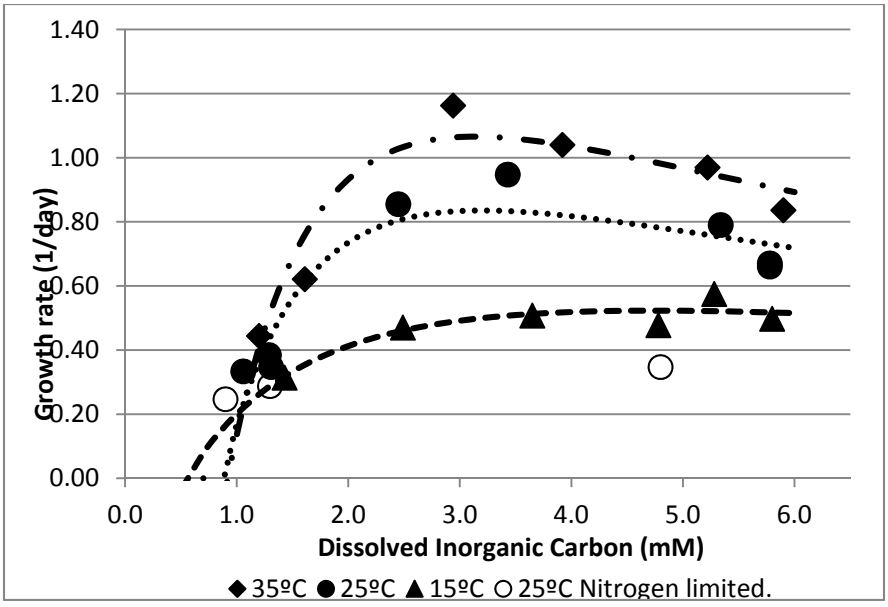

Figure 3: Net specific growth rates (1/day) measured at different DIC concentrations and temperatures. Dotted lines are a Monod with inhibition and critical substrate concentration model fitted with the obtained data.

Data gathered at 15°C and under nitrogen limited conditions, indicate that at these conditions, DIC concentration had less of an impact on growth than that observed at higher temperature and non-limiting conditions. For instance, at 15°C, the growth rate increased 50% when the DIC concentration increased from 1.3 mM to 2.5 mM, while the same increase in DIC at 25°C yielded a 2.2 fold increase and at 35^0C a change in DIC concentration from 1.2 to 2.9 mM yielded a 2.63 fold increase. In the case of nitrogen limitation, even a fivefold increase in DIC concentration resulted in only a 50% rate increase.

Since DIC concentration was changed by varying the CO_2 concentration in the gas phase, the pH of the medium changed between 6.5 and 8.5, depending on the desired DIC concentration. Previous research suggests that pH variations in this range do not significantly affect the cell functioning in other ways besides changing the DIC concentration. Huertas and Lubián (1998) investigated the maximum photosynthetic rate of *Nannochloris oculata*, at constant DIC concentration (10mM) for three different pH conditions. These researchers found that at pH values of 5.5, 7.5 and 8.2 the photosynthetic rate did not vary significantly, 7.32, 7.33 and 7.45 $nmolO_2/10^6$cells-h, respectively. Also, experiments performed with *Chlorella vulgaris* grown with bacteria and glucose as an organic carbon source at 25°C, show that within a pH range of 6.5 and 8.5 the growth rate did not vary more than 7%, between 0.46 and 0.43 day^{-1} (Mayo, 1997). Another study, investigated the effects of pH (between 7 and 9.5) on the growth of two marine species, *Thalassiosira pseudonana* and *T. oceanica*; it was found that growth rate was not affected by pH in the range between 7 and 8.8, above this range, growth was inhibited. This experiment was performed without CO_2 addition. Furthermore, a model developed to account for the effects of pH on *Nannochloropsis salina* growth indicates that growth is not affected between a pH range of 4.5 to 8.5 (James et al., 2013).

Bioreactor data was used to fit a Monod with inhibition model (see Figure 3). This model was chosen, as it has already been used to model microalgae growth as a function of dissolved inorganic carbon concentration (Berberoglu et al., 2008). This model also incorporates a critical DIC concentration below which no microalgae growth occurs (DIC_0). Monod models with a critical substrate concentration term have been used before to describe microbial growth on organic carbon substrates (Law and Button, 1977; Kovárová et al., 1996) as well as microalgae growth on inorganic carbon (Novak and Brune, 1985). The model is described by the following set of equations:

$$\mu = \mu_{max} \frac{S}{K_S + S + \frac{S^2}{K_I}} \quad \text{Equation 15}$$

$$S = (DIC - DIC_0) \quad \text{Equation 16}$$

where μ_{max} is the maximum specific growth rate (1/day), DIC is the dissolved inorganic carbon concentration (mM), DIC_0 is the critical DIC concentration (mM), K_s and K_I are the half saturation and inhibition constants, respectively (mM). The model at 15°C was fit using nonlinear regression in Polymath 6.1 by adjusting the following model parameters: μ_{max}, K_s, K_I and DIC_0. The maximum growth rates (μ_{max}) for 25 and 35°C were estimated by assuming that the ratio between the maximum growth rate obtained by the model and the growth rate observed (μ_{obs}) at 2.7±0.2 mM (near the maximum observed) is constant across all temperatures:

$$\left[\frac{\mu_{max}}{\mu_{obs}(DIC = 2.7 \pm 0.2mM)}\right]_{T=15°C} = \left[\frac{\mu_{max}}{\mu_{obs}(DIC = 2.7 \pm 0.2mM)}\right]_{T=25\ and\ 35°C}$$

Therefore, for the models at 25 and 35°C, three parameters (K_s, K_I and DIC_0) were used to fit the model to the data. Table 3 shows the parameter values obtained for models at 15°C, 25°C and 35°C, together with their respective 95% confidence intervals.

Table 3: Best Fit model parameters for Monod with inhibition kinetics with critical DIC concentration (DIC_0).

Parameter	15°C	95% C.L.	25°C	95% C.L.	35°C	95% C.L.
Ks	1.59	±0.08	1.15	±0.85	1.25	±0.65
K_I	11.10	±8.12	4.72	±2.72	3.92	±1.40
DICo	0.55	±0.01	0.87	±0.24	0.92	±0.18
μ_{max}	0.92	±0.07	1.66	NA	2.27	NA

The inhibition constant (K_I) obtained for the model at 15°C was quite different from the ones obtained at 25 and 35°C. This is probably because at 15°C, temperature becomes the growth limiting factor so that an increase in DIC does not affect the growth rate as much as at higher temperatures, making the curve flatter, without apparent inhibition. The confidence intervals were calculated following the method described by Wahman (2006). Also, it is important to mention that at low DIC concentrations (below 1mM) the fitted models at 25 and 35°C tend to converge and possibly cross over, which would result in a higher predicted growth rate at 25°C than at 35°C.

Batch growth rate

Net specific growth rates during batch operation at 25°C were determined to be 0.98±0.11 day^{-1} for cultures grown at ambient CO_2 levels and 1.3 day^{-1} for the experiment grown with 3% CO_2. Takagi and Yamaberi tested the same algal strain used in this study (*Nannochloris* sp. UTEXLB1999) for lipid content at different nitrogen concentrations (Yamaberi et al., 1998; Takagi et al., 2000). Utilizing data directly from their reported batch growth experiments, it was possible to calculate approximate specific growth rates which varied between 1.2 and 1.8 $days^{-1}$ at 30^0C, 10 klux and 3% CO_2 in NORO medium. The rates measured in this study were lower than those obtained by Takagi which is expected since the present study was conducted at 25°C, instead of 30°C.

Specific growth rates measured during batch operation (0.98±0.11 day^{-1}) were higher than those measured during continuous culture (0.33-0.38 $days^{-1}$) even though the other experimental conditions (temperature and gas phase CO_2 concentration) were identical. This is probably due to a decrease in light penetration into the medium at the higher biomass concentration maintained during continuous operation. The biomass concentration during the continuous operation phase varied between 0.25 g/L and 0.28 g/L. In order to estimate the effect of decreased light penetration on the specific growth rate, the model developed by Berberoglu (2008) for *Anabaena variabilis* (adapted for the biomass concentration and geometry of the reactor used in this study) was used. At incident irradiance (G_{in}) of 8.2klux (the same value as the current study), DIC concentration of 2 mM, and a biomass of 0.1 g/L, the estimated specific growth rate (μ) is 1 day^{-1}. In contrast, for a biomass concentration of 0.26 g/L (the same value as the one observed in the current study), the estimated specific growth rate becomes 0.57 day^{-1} which represents a 43% decrease.

Previous studies have reported a range of microalgae specific growth rates based on batch experiments. Although these calculations are valuable and provide a good estimate of how an algae species will behave under a given set of conditions, algae mass cultivation is expected to operate in continuous or semi-continuous mode, where the media is replaced at a certain rate to maintain a target biomass concentration. Growth measured in batch systems which are not subject to light limitations will yield significantly different specific growth rates than those achievable in continuous mass culturing systems where biomass concentrations are high, and light limitations exist. Furthermore, as alkalinity changes with algae growth, determining the specific growth rate at a specific DIC concentration poses significant challenges. The use of a turbidostat

to measure specific growth rates when DIC is the limiting factor for growth is a better choice to predict algae growth as a function of DIC levels.

Alkalinity and pH

Alkalinity and pH both increased during the batch phase of the experiments (Figure 4); however alkalinity remained constant when the system was operated in continuous feed mode. The pH changes observed during continuous feed operation were due to variations in the CO_2 concentration in the gas phase and the rise in alkalinity is due to nitrate and phosphate uptake by the algae during batch growth. During continuous culture alkalinity remained constant. The data from one experiment is shown in Figure 4 but similar behavior was observed in the other experiments. Depending on the experiment, the alkalinity varied slightly between 4.6 and 5.3 meq/L while the pH ranged from 6.5 to 8.4 (depending on the DIC concentration set point).

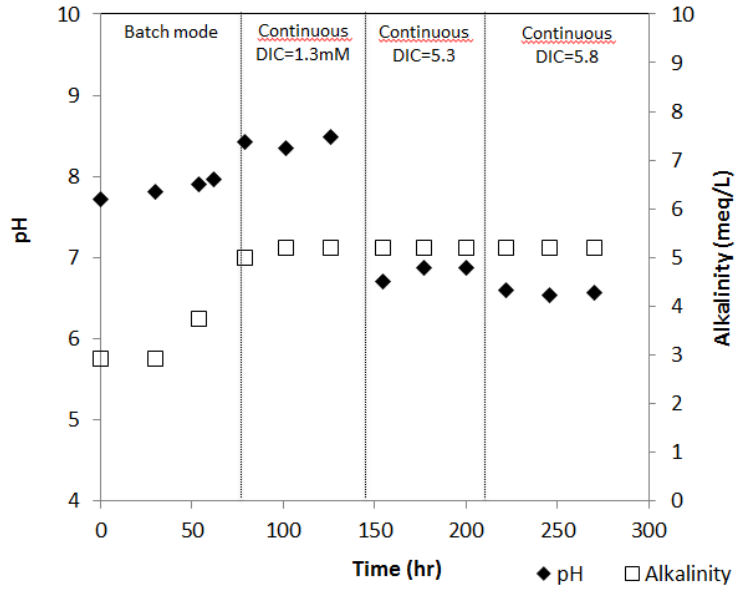

Figure 4: Measured alkalinity and pH throughout a continuous experiment at three different DIC concentrations and 25ºC.

The average change in alkalinity during batch mode for the experiments under nitrogen limitation conditions was 1.7 meq/L, whereas the alkalinity change for the rest of the experiments averaged 2.2 meq/L. Nitrogen uptake has been shown to increase as the nitrogen concentration of the media increases, which could explain the difference between the two different alkalinity changes (Richardson et al., 1969; Rhee, 1978).

Effect of a hypothetical temperature change on net specific growth rate

The model developed can be used to evaluate the effect of a temperature change on the productivity of an algae culture system. For example, if a system is operating at 15˚C with the same medium as investigated in this study and a gas phase CO_2 concentration of 0.1% (see Figure 5, a), assuming gas-liquid equilibrium, the medium would have a DIC concentration of approximately 3.5 mM. If the system temperature increases to 35˚C, the liquid-gas equilibrium would change, bringing the DIC concentration down to about 2.2mM and a growth rate of 0.96 $days^{-1}$ (see Figure 5, b). In contrast, if the CO_2 level of the gas phase was adjusted to keep the DIC at 3.3 mM (see Figure 5, c), the specific growth rate would be 1.14 day^{-1}.

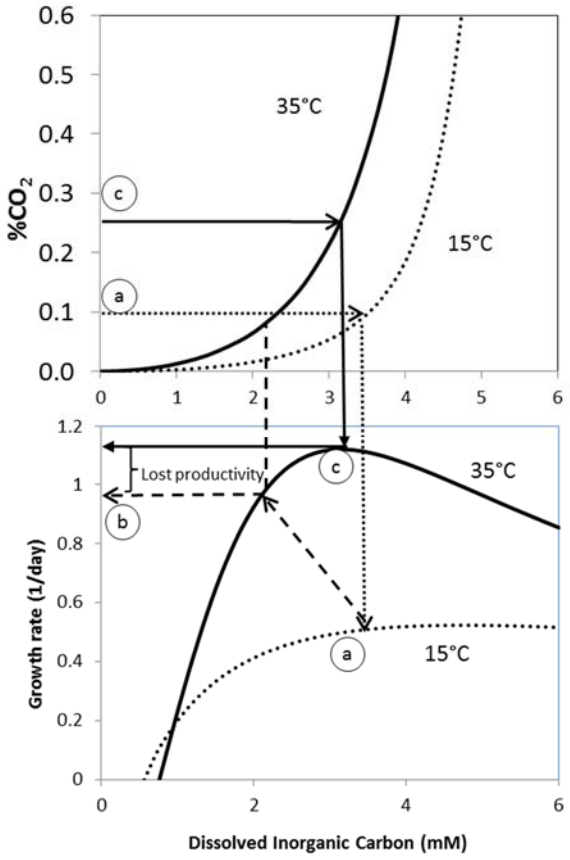

Figure 5: Effect of a hypothetical temperature change from 15 to 35°C on algal net specific growth rate.

Temperature changes of this magnitude during algae cultivation have been documented in New Mexico (Sheehan, 1998) and at UT Austin's outdoor culturing facilities (UT CEM, personal communication). Assuming a biomass concentration of 0.25g/L and a pond of 1,000 m^3 (a 10cm deep pond covering 1 hectare), the lost productivity of operating the culture without DIC control would be 45 kg of algae per day or 16.4 tons/year. Although this estimate is only for a continuous culture grown in constant light with no limiting nutrients, this methodology can be useful to understand the

potential impact of temperature, alkalinity and CO_2 gas phase concentration on the productivity of a given culture system.

CONCLUSIONS

Nannochloris growth was stimulated by the addition of DIC into the medium by means of CO_2 enriched air. However, inhibition was observed at DIC concentrations higher than 3 mM. At 15°C, a temperature considered low for this species, growth is not stimulated as much with increasing DIC concentration. This suggests that metabolic rates are slowed down sufficiently such that the growth controlling factor is temperature and not DIC and higher DIC concentrations do not increase the algae production rate.

It was also observed that growth rate increases with increasing temperature, but the effect is less pronounced at low DIC concentrations. This means that at low DIC concentration, carbon is the limiting factor for growth. Even at high metabolic rates due to a high temperature, there is not enough carbon to grow more cells.

The results obtained in this study showed an optimum DIC concentration where a maximum growth rate of *Nannochloris* is observed. This result has been masked in studies that have failed to isolate the effects of temperature and DIC concentration on the growth rate of microalgae. This suggests that in order to keep the DIC concentration within the optimal range, it is necessary to adjust the pCO_2 to offset the effects of temperature on the solubility of inorganic carbon in the medium.

Chapter 4: Microalgae growth rate as a function of temperature and light penetration.

INTRODUCTION

The high photosynthetic efficiency of microalgae and potential for high lipid and biomass yields have made microalgae a focus of interest within the renewable energy community for decades. Beyond the energy production, their enormous biodiversity makes them suitable for a wide variety of applications including water treatment, aquaculture feed, and the production of high value chemicals such as nutraceuticals and food supplements (Oswald, 2003; Pulz and Gross, 2004). The economic viability of a microalgae production system depends to a great extent on the biomass production rate. Optimizing the productivity of microalgae culture systems requires a clear understanding of the key variables that control their growth rates.

One environmental variable that can significantly impact the productivity of microalgae cultures in outdoor production systems is temperature. In most mass culturing systems, controlling the temperature of the growth medium is not economically feasible, as it requires high energy consumption for heating and a large amount of water for evaporative cooling. Other temperature control strategies, such as the use of greenhouses, infrared radiation reflectors or light dilution systems, pose an extra burden on the economics of these systems (Stephens et al., 2010). This becomes particularly important for systems operated in climates with high diurnal or seasonal temperature variability. Understanding climate variations and the effects of temperature on growth rate is an essential factor in species selection for a particular geographic region.

Light attenuation through a microalgae suspension due to self-shading is also an important factor that influences culture productivity. At low cell densities and short light paths (less than 5cm), it is reasonable to assume that all the cells within the culture

experience the same light intensity. Yet, in reactors with longer light paths and higher microalgae cell densities, more light is absorbed, scattered and/or converted to heat within the bioreactor; as a result, a light attenuation profile emerges that is dependent on the cell density, the size of the microalgae cells, and the type of pigments the cells contain (Thompson, 2006). These effects are usually apparent in mass culturing operations, where high biomass concentrations are maintained to obtain high yields and avoid excessive dewatering costs. In such a system, cells inside the reactor experience varying light intensities, depending on their position relative to the light source and therefore, light may become the growth limiting factor.

Temperature and light intensity effects on growth rates of microalgae have been studied previously for a variety of algae species. However, growth rates have usually been determined in batch cultures, where biomass concentration in the culture is maintained sufficiently low so that the growth rate is not affected significantly by self-shading effects (Mayasich et al., 1987; Dauta et al., 1990; Talbot et al., 1991; Bouterfas et al., 2002; Bitaubé Pérez et al., 2008). The attenuation in light intensity within a culture due to self-shading effects may be unimportant in natural waters where nutrient concentration is the most important factor controlling microalgae growth rates. However, for eutrophic waters or commercial microalgae operations where high nutrient concentrations are expected and high biomass densities are present, the effects of self-shading on biomass growth rates cannot be ignored.

Turbidostat reactors, where microalgae cultures can be maintained at a specified biomass concentration, can be useful for studying (and controlling) the effects of light penetration on microalgae growth rates (Huisman et al., 2002). Indeed, while light limited chemostat experiments have been used to identify the effects of self-shading on microalgae growth rates, these experiments are limited in their ability to isolate effects of

light penetration from other factors that affect growth such as temperature. One study (Mazzuca Sobczuk and Chisti, 2010), used a chemostat to explore the effects of dilution rate and temperature on biomass and lipid productivity of *Choricystis minor*. Although this study explored the effects of dilution rate on biomass and lipid productivity, it did not characterize the light penetration inside the reactor in order to link average light intensity in the reactor to growth rate at different temperatures.

To our knowledge, the effects of temperature and average light intensity on microalgae growth rate have not been studied previously in a systematic manner that isolates the effects of self-shading from other parameters by controlling the biomass concentration as well as temperature.

The objective of this study is to decouple the effects of temperature and light attenuation on the growth rates of two microalgae species: *Nannochloris* sp. (UTEX 1999.) and *Phaeodactylum tricornutum* (UTEX 646). It is important to note that the *Nannochloris* sp. strain used in this research phase was not the same as the one used in the previous chapter, as this one was an axenic culture, kept in agar, instead of in liquid medium. Optimal growth for these two microalgae species occur within two distinct temperature ranges. The diatom *P. tricornutum* thrives at temperatures lower that 25°C (Goldman and Mann, 1980) whereas the green alga *Nannochloris* sp. grows optimally at 26-28°C. A microalgae production system situated in a geographic region that has average summer temperatures that exceed 25°C, and winter temperatures between 10 and 22°C, may be able grow *Nannochloris* during the summer and *P. tricornutum* during the winter.

In order to separate the effects of temperature and light attenuation (self-shading) on growth rates, a turbidostat culture was used. The advantage of a turbidostat is that it makes it possible to fix biomass concentrations so that self-shading by biomass is

constant over time. In this work, no extra CO_2 was added to the culture and DIC was kept constant across the different temperatures tested. Net specific growth rates can be determined by measuring the dilution rate of the system.

MATERIALS AND METHODS

Experimental approach

Two types of reactor systems were employed in this research. A series of batch experiments were performed to determine the net specific growth rate of *Nannochloris* sp. and *P. tricornutum* over a temperature range between 10 and 40°C; these experiments were conducted at low biomass concentrations to avoid self-shading effects. A turbidostat bioreactor was then used to estimate the growth rate of each microalgae species over a broader range of biomass densities for temperatures between 15 and 36°C and average light intensities between 100 and 250 μmol $m^{-2}s^{-1}$.

Batch growth experiments

An aluminum block, 10cm x 60cm x 20cm, containing 2cm diameter wells was constructed to accommodate 20 ml glass culture tubes. The wells contained apertures on the side to allow light exposure to the culture inside the glass tubes. A linear temperature gradient was created by means of two heat exchangers placed at both ends of the aluminum block: one that cools with a chilled water circulator and another that uses a thermocouple controller to heat the reactor. Temperatures were stable for the duration of each experiment. Each glass tube contained 20 mL of growth medium and was inoculated with 1mL of algae culture. The biomass concentration was measured every 24 hours for 5 days by counting cells under a microscope (Nikon Eclipse 80i, Nikon, Melville, NY) using a hemocytometer (Hausser Bright-Line 3100, Hausser Scientific, PA). The specific

growth rate (1/days) was determined by fitting the biomass concentration versus time data to an exponential growth model.

Turbidostat growth experiments

Turbidostat experiments were designed to measure net specific growth rates over a range of temperatures and cell densities. For each growth rate measurement, the cells were grown in a 2L cylindrical glass reactor (turbidistat) maintained at constant biomass concentration and temperature (see Figure 6). The reactor was sealed using a glass cap that had inlets for a pH probe (Cole-Parmer Autoclavable pH Probe, Sealed/DJ/Glass), an air sparger tube and sampling ports. Two lamps, each containing two fluorescent bulbs, 1m in length (Sylvana cool white 4100K, Sylvana, Danvers, MA) were placed on each side of the reactor to illuminate the system. The incident light intensity on the sides closest to the lights was 183.2 $\mu molm^{-2}s^{-1}$ as measured by a Waltz Submersible Spherical Micro Quantum Sensor (US-SQS/L, Effeltrich, Germany). Air bubbled into the medium was pre-humidified by sparging it into a 2L Erlenmeyer flask filled with autoclaved distilled water. Evaporation losses from the culture medium were minimal (less than 1% over a 24 hour period at 33°C). The temperature within the turbidostat culture was controlled using a water bath circulator (Fisher Scientific Isotemp 1013P, Pittsburgh, PA). During each turbidostat run, three to four conditions (that varied with respect to temperature and biomass concentration) were tested.

A continuous recirculation system was employed to measure turbidity in the turbidostat with a Hach Solitax® turbidity probe (Düsseldorf, Germany) that was inserted into a glass flow through cell. Turbidity was maintained at a constant value using a controller (Hach sc100, Loveland, Colorado) programmed to pump fresh medium into the reactor at a set turbidity value. The mass of medium injected into the reactor was

monitored by measuring the weight of the fresh medium reservoir, using a portable electronic balance (Ohaus Scout® SP4001, Pine Brook, New Jersey). The weight of the fresh medium reservoir was recorded every three hours. The dilution rate was calculated by dividing the rate of medium injected (mL/day) by the volume of the reactor (2000mL), to yield the net specific growth rate (1/day) of the microalgae at the conditions (temperature and biomass concentration) tested.

The mass balance on the biomass in the reactor is described by the following equation:

$$\frac{dX}{dt} = \mu X - DX \qquad \text{Equation 17}$$

Where X is biomass concentration (cells/mL), μ is the net specific growth rate (1/day) and D is the dilution rate (1/day).

At steady state, $\frac{dX}{dt} = 0$ and therefore μ is equal to D.

The growth rate at a particular condition was considered to be at steady state, when the rate of medium injected remained constant for more than 15 hours.

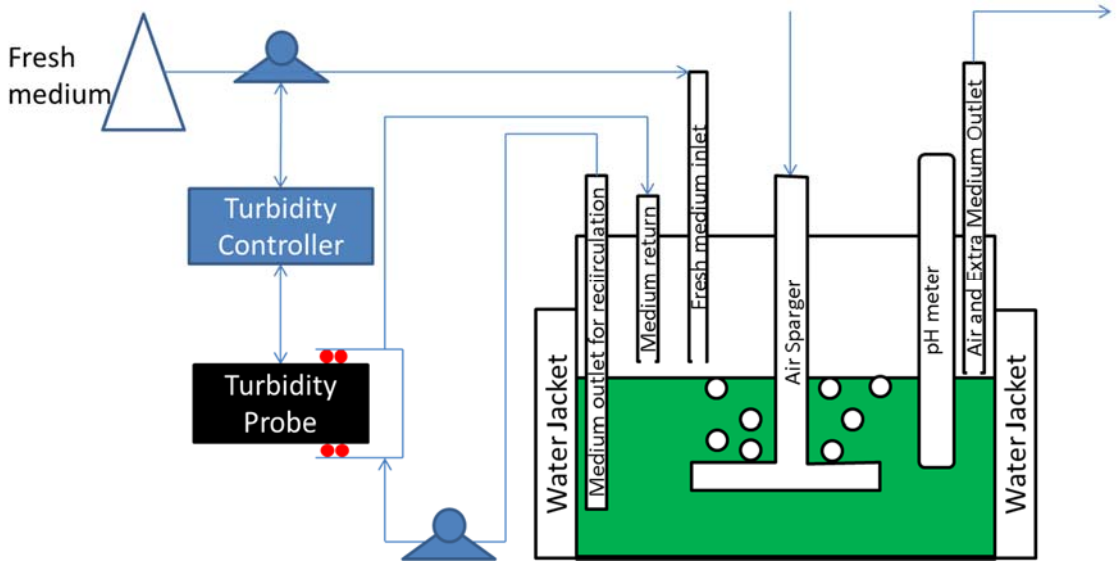

Figure 6: Turbidostat reactor setup

Growth Media

All the experiments were performed using a modified ASP medium (Andersen, 2005) with the following composition (per liter): NaCl, 23.38g; KCl, 0.375g; $CaCl_2$, 0.56g; $NaHCO_3$, 0.168g; $MgCl_2 \cdot 6H_2O$, 4.06g; $MgSO_4 \cdot H_2O$, 4.93g; Tris(hydroxymethyl)aminomethane base, 0.606g; $NaNO_3$, 0.425g; Na_2HPO_4 0.048g; $Na_2SiO_3 \cdot 9H_2O$ 0.057g; Fe-EDTA, 0.842mg; EDTA, 14 mg; $ZnSO_4 \cdot 7H_2O$, 10.064mg; H_3BO_3, 24.732mg; $CoCl_2 \cdot 6H_2O$, 0.071mg; $CuSO_4 \cdot 5H_2O$, 0.075mg; $MnCl_2 \cdot 4H_2O$, 1.979mg; $NaMoO_4 \cdot 2H_2O$, 1.21mg; Vitamin B_{12}, 0.5µg, Vitamin B_1, 100 µg; Biotin, 0.5µg. The medium was prepared with ACS grade reagents, adjusted to pH 7.3 and autoclaved for 45 min at 121°C.

Cell density using a Flow Cytometer

A LSRFortessa cytometer (BD Biosciences, San Jose, CA) was used to determine cell densities during the turbidostat experiments. Samples were taken from the culture, diluted by a factor of ten. One mL of the diluted sample was introduced into a falcon tube (BD Falcon polystyrene test tube, 12 x 75-mm, 352052) where 50 µL of 5-5.9µm Accucount Fluorescent Particles (Spherotech Inc., Lake Forest, IL) were added to a final concentration of $5x10^4$ particles/mL. A laser with a wavelength of 488nm was used to measure fluorescence of both the microalgae cells and the spheres. Cells were counted on the red (670nm Long Pass filter) channel, whereas the fluorescent particles were counted using the green fluorescence (530nm filter) channel. For a more detailed discussion on this method, refer to Appendix B. Data was acquired until 200 fluorescent particles were counted, and then the concentration in cells/mL was calculated using the following equation.

$$\frac{cells}{ml} = Cells\ counted \left(\frac{50{,}000}{200}\right)(10) \qquad \text{Equation 18}$$

Average light intensity

Light intensity inside the reactor was measured in discrete points using a submersible Spherical Micro Quantum Sensor (US-SQS/L, WALZ, Effeltrich, Germany) across two axes of the reactor cylinder (one parallel and the other perpendicular to the light source) at three different depths for a range of biomass concentrations of *Nannochloris* and *P. tricornutum*. The sensor has a reported measurement error of ±5%. Seven data points were taken across each axis. Three in one end of the axis, one in the center and three at the other end. Thus, for each depth, light intensity was measured at four locations in three concentric rings (see Figure 7). For each concentric ring, an average light intensity was obtained, calculated from the four points located within the ring ($G_{av,i,d}$).

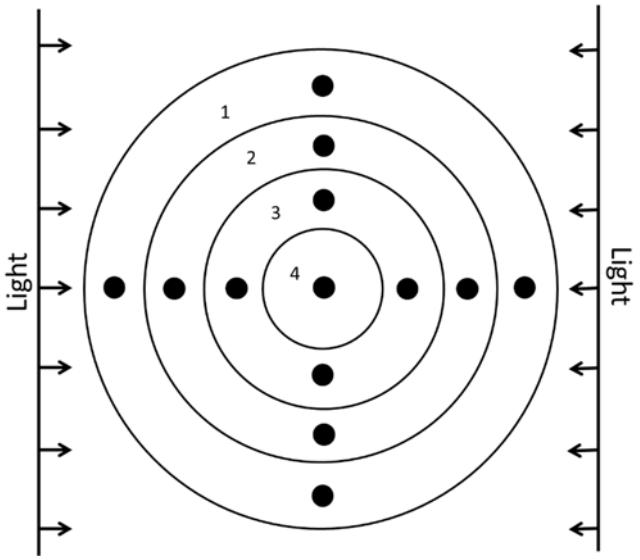

Figure 7: Cross section of reactor from above. Each black dot represents the point where a light measurement was taken. Concentric rings are numbered 1 through 4.

To obtain an estimate of the average light intensity across the reactor cross section area for each depth, a weighted average was obtained by using each of the ring's areas (1, 2, 3, 4), as described by the following formula:

$$G_{av,d} = \frac{A_{r,1}G_{av,1,d}+A_{r,2}G_{av,2,d}+A_{r,3}G_{av,3,d}+A_{r,4}G_{av,4,d}}{A} \quad \text{Equation 19}$$

Where $G_{av,d}$ is the average light intensity at depth "d", $G_{av,i,d}$ is the average light intensity in ring "i" at depth "d", $A_{r,i}$ is the area of ring "i" and A is the cross section area of the reactor (sum of the ring's areas). To calculate the average light intensity across the entire reactor volume, an average was calculated from the averages of the three depths.

RESULTS AND DISCUSSION

Growth rates determined in batch culture

A total of 13 batch culture experiments were conducted. The results from one typical batch culture experiment (Figure 8) indicates that an exponential relationship exists between biomass concentration and time; such a relationship is typical in systems in which nutrient and light limitations are absent. The growth rate can be determined by fitting the data to:

$$X = X_0 e^{\mu t} \quad \text{Equation 20}$$

where X is the biomass concentration (cells/mL) at time t, X_0 is the biomass concentration at t=0 and μ is the specific growth rate (1/days). In the batch experiments conducted in this work, exponential growth was observed only during the first several days of each experiment. Thus, growth rates were determined for each temperature and each species using only the data that was within the exponential growth phase, which was typically within the first six days of the experiments.

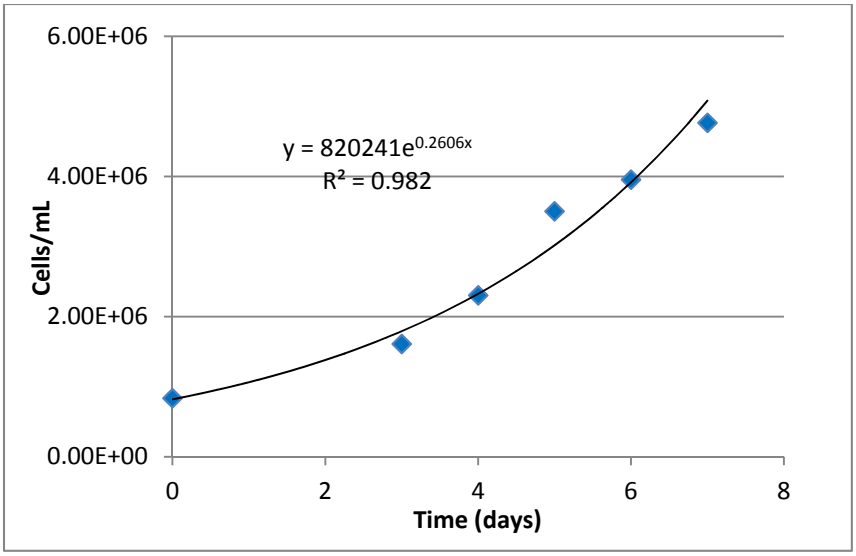

Figure 8: Growth data for *P. tricornutum* at 26.5°C. The continuous line represents the exponential growth model fit to the data.

The impact of temperature on the growth rates of each species is similar; however, the optimum temperature for growth varies between the species. The results shown in Figure 9 indicate that a parabolic relationship exists between growth rate and temperature for each species. The optimum growth rate for *P. tricornutum* occurs between 20 and 25°C whereas the optimum growth rate for *Nannochloris* sp. is between 25 and 30°C. While both curves are parabolic in nature, the growth rate of *P. tricornutum* rapidly declines at temperatures higher than 24°C, skewing the parabolic relationship at higher temperatures. The optimal temperature for growth observed in these experiments and the general shape of the curves are in accord with other studies (Cho et al., 2007; Bitaubé Pérez et al., 2008). These measurements also confirm the findings of Dr. Goldman's group from Woods Hole Oceanographic Institution (Goldman and Ryther, 1976). During their outdoor pond mass culture experiments in the 1970s, they regularly observed that *P. tricornutum* was the dominant algae species between 10 and 23°C

whereas a *Nannochloris* species (together with other assorted species) dominated at temperatures higher than 23°C (Goldman and Mann, 1980).

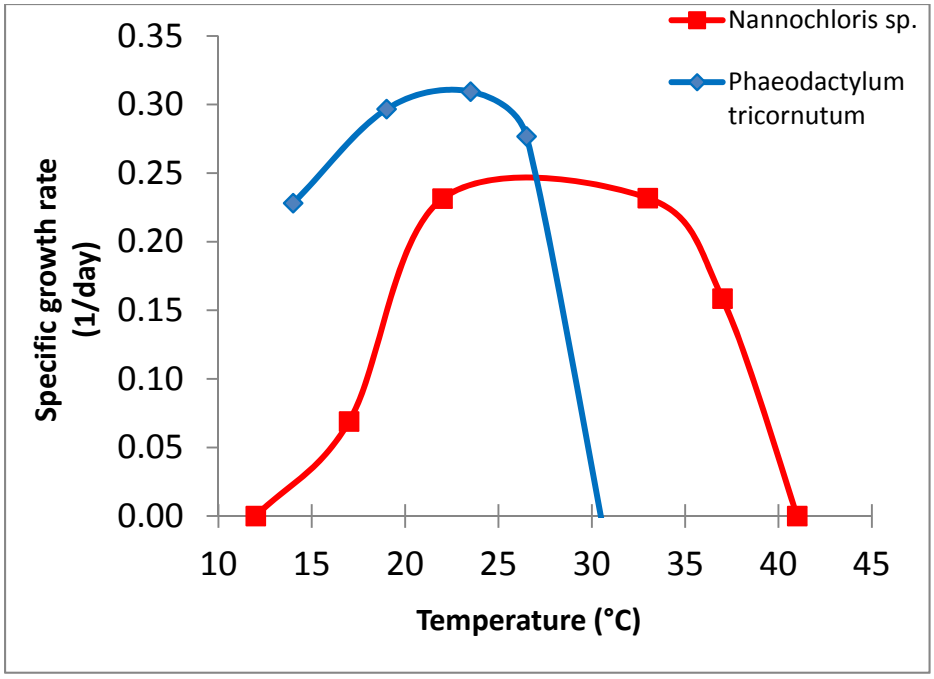

Figure 9: Net specific growth rates of *Nannochloris sp* and *P. tricornutum* as a function of temperature as measured in batch cultures. Decay rates for *P. tricornutum* at temperatures above 30°C are not shown; the table with complete data is provided in Table 13 in the Appendix.

Although measuring growth rates in batch cultures yields useful information for predicting the general behavior of microalgae populations in natural systems and the possible outcomes of phytoplankton competition under different temperature regimes, the model does not describe growth data collected as the cell densities increase. For instance, as shown in Figure 10, as algae growth reached relatively high cell densities (in excess of $5x10^6$cells/mL or approx. 120mg/mL for *P. tricornutum* and $1x10^7$ cells/mL or approx. 60mg/L for *Nannochloris*), deviations from the exponential growth curves are evident.

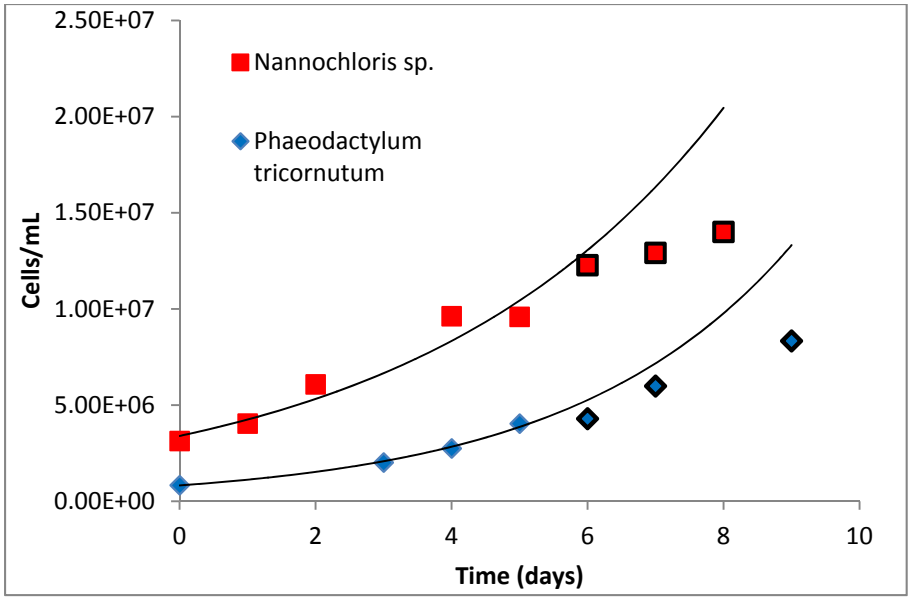

Figure 10: Experimental growth curves (cells/mL vs time) of *Nannochloris* and *P. tricornutum* at 33°C and 23°C respectively, grown to relatively high densities in batch culture. Continuous lines represent an exponential growth model fitted to the first 5 days of data. Data points in black boxes were not used to fit the model.

Since these cultures were nutrient replete (see nutrient limitation experiments in Appendix B), the deviations from exponential growth over time cannot be attributed to nutrient limitations. A more reasonable explanation for the deviation from exponential growth is that light attenuation due to self-shading may limit growth rates at high cell densities. Light limitation was reported to occur in *Isochrysis galbana* cultures when grown to densities higher than approximately 200mg/L in a cylindrical reactor with an incident irradiance of 820 µmol $m^{-2}s^{-1}$ (Grima Molina et al., 1996). Thus, algae growth rates estimated from data collected in batch systems should only rely on data collected at low biomass concentrations as data collected at higher concentrations may overpredict growth rates. Estimates of growth rates at higher cell densities are necessary for

commercial operations and the development of models that predict growth as a function of both temperature and cell density are required to optimize algae production.

Several models exist that incorporate the effect of either temperature or light intensity; however, no single model has been evaluated for estimating growth rates for both of these parameters at concentrations relevant to commercial growth reactors (i.e. greater than biomass concentrations of several hundred mg/L). Thus, models for both temperature and growth rate must be evaluated independently, and a composite model that describes growth rates as a function of temperature and light intensity must be developed.

Models to Describe Growth Rate as a Function of Temperature

To estimate the effects of temperature and self-shading on the net specific growth rates of microalgae, a series of experiments were performed in a continuous flow turbidostat. In the first set of experiments, growth rates were determined at fixed biomass concentrations over a range of temperatures (between 15 and 35°C). The constant biomass concentration maintained in the turbidostat provided constant light intensity, which made it possible to isolate the effects of temperature on growth rate from the effects due to changing light intensity. Figure 11 and Figure 12 summarize the growth rates measured for *P. tricornutum* and *Nannochloris* in the experiments performed at fixed biomass concentrations of $5x10^6$ and $2.3x10^7$ cells/mL respectively. The data were used to calibrate and compare three models that describe growth rate as a function of temperature. These models, developed by Huang et al (2011), Bitaube et al. (2008) and Lehman et al. (1975), were chosen because they are capable of describing skewed curves and have been used previously to describe microalgae growth as a function of temperature.

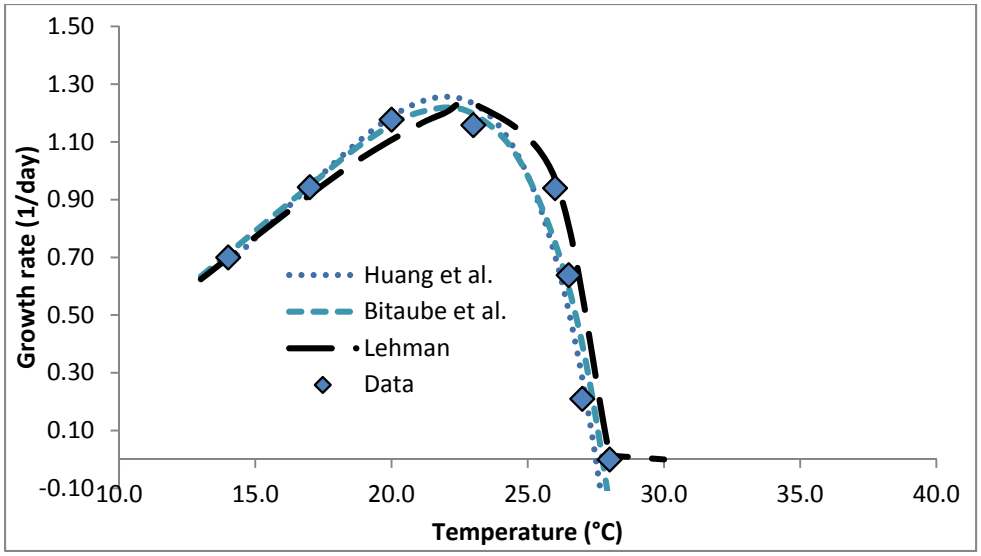

Figure 11: Net specific growth rates of *P. tricornutum* as a function of temperature at a fixed biomass concentration ($5x10^6$ cells/mL). Symbols represent experimental data; dashed lines represent best fits using models developed by Huang et al.(2011), Bitaube et al. (2008) and Lehman et al. (1975).

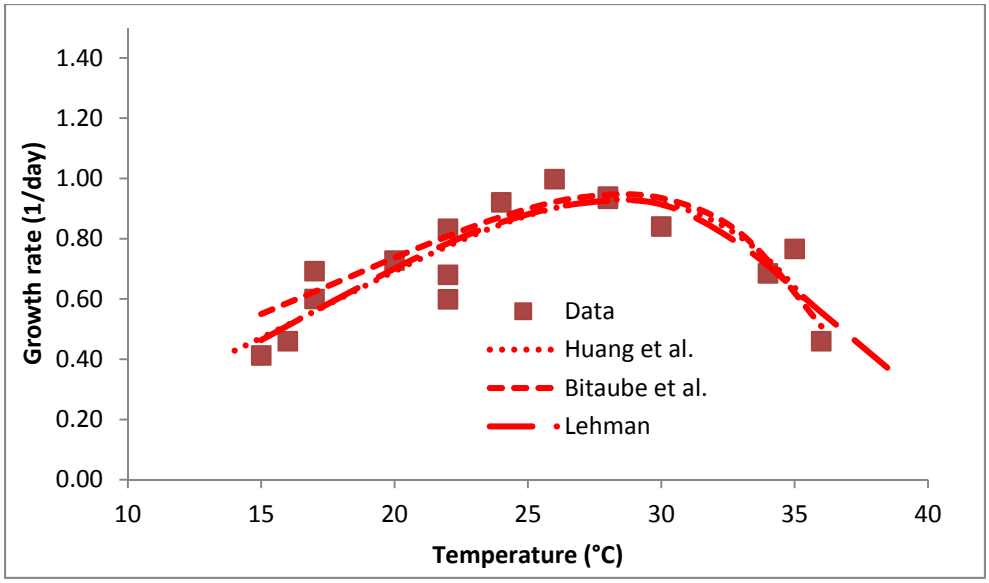

Figure 12: Net specific growth rates of *Nannochloris* as a function of temperature at a fixed biomass concentration ($2.3x10^7$cells/mL). Symbols represent experimental data; dashed lines represent best fits using models developed by Huang et al. (2011), Bitaube et al. (2008) and Lehman et al. (1975).

It is important to recognize that even though the impact of light intensity is constant in these experiments, its impact on growth rates is incorporated into model parameters; it is either embedded in the maximum specific growth rate for each species or in the empirical pre-exponential term of each model where:

$$\mu'_{max}, A', A_o \; and \; B_0 = k * f(G_{av}) \qquad \text{Equation 21}$$

Huang et al. (2011) developed the following model of microbial growth, based on the Arrhenius equation and Eyring-Polanyi transition theory:

$$\mu(T) = A'Te^{-\left(\frac{\Delta G\prime}{RT}\right)^{\alpha}}[1 - e^{B(T-T_{\sup})}] \qquad \text{Equation 22}$$

where μ(T) is the net specific growth rate (1/day), A′ (1/day), B (1/K) and α are empirical constants, ΔG' (J/mol) is equivalent to a Gibbs free energy of activation term, R is the gas constant (J/mol K), T_{sup} is the maximum temperature above which no growth is observed and T is the incubation temperature (K). For this model, it is necessary to calibrate four parameters: A', B, α and ΔG. T_{sup} was estimated directly from the data for *P. tricornutum*, where above 27.5°C no growth is observed and in the case of *Nannochloris* from batch growth experiments where no growth is observed above 41°C (See Appendix A).

Bitaubé Pérez et al. (2008) used the following model to describe *P.tricoruntum*'s specific growth rate as a function of temperature, based on an Arrhenius type model:

$$\mu(T) = A_0 e^{\left(\frac{E_a}{RT}\frac{T-To}{To}\right)} - B_0 e^{\left(\frac{E_b}{RT}\frac{T-To}{To}\right)} \qquad \text{Equation 23}$$

where A_0 and B_0 are specific rates of growth and deactivation (1/day) at the reference temperature To=293 K. Ea and Eb are activation energies for growth and deactivation (kcal/mol), respectively and R is the gas constant (kcal/mol-K). For this model, four model parameters are calibrated using the experimental data: A_0, B_0, E_a and E_b.

Dauta et al., (1990) used the following model to describe the growth of four fresh water microalgae as a function of temperature, based on a model developed by Lehman (1975):

For r T>Topt

$$\mu(T) = \mu_{max}{}' e^{\left(-K_T\left(\frac{T-T_{opt}}{T_{sup}-T_{opt}}\right)^2\right)}$$

For T<Topt

$$\mu(T) = \mu_{max}{}' e^{\left(-K_T\left(\frac{T-T_{opt}}{T_{inf}-T_{opt}}\right)^2\right)} \qquad \text{Equation 24}$$

where K_T is an empirical constant, T_{opt} is optimum temperature for growth, T_{inf} is the lower temperature below which no growth is observed and T_{sup} is the higher temperature where no growth is observed. For this model, four variables are used as fitting parameters: μ_{max}, K_T, T_{opt} and T_{inf}. T_{sup} was obtained directly from the data, as explained above.

Estimates of the mean square error (MSE) between the calibrated model and the experimental data for each algae species are presented in Table 4. The error estimates are relatively close for *Nannochloris* but vary for *P. tricornutum,* where Lehman's model provided the lowest mean square error. Table 5, 6, and 7 summarize the parameters obtained from fitting the data to the models together with the 95% confidence limits for each parameter. The confidence intervals were calculated following the method described by Wahman, (2006).

Table 4: Mean square errors (MSE) for Huang, Betaube and Lehman models for *Nannochloris*'s and *P. tricornutum*'s growth rate curves

Model	**Mean square error (MSE)**	
	P. tricornutum	***Nannochloris***
Huang	0.2	0.11
Bitaube	0.15	0.11
Lehman	0.04	0.12

Table 5: Parameters obtained from fitting data to Huang (2011) et al. model

Model Parameters	*P. tricornutum*	95% C.L	*Nannochloris*	95% C.L
A' (1/day)	0.092	$\pm 2.4 \times 10^{-5}$	0.017	$\pm 9.6 \times 10^{-6}$
$\Delta G'$ (J/mol)	2683.1	±1553.2	2548.2	±16.34
B (1/K)	0.19	±2.68	0.095	±0.023
α	10.94	±0.001	12.88	±0.002

Table 6: Parameters obtained from fitting the data to Bitaubé Pérez et al. (2008) model

Model Parameters	*P. tricornutum*	95% C.L	*Nannochloris* sp.	95% C.L
A_0 (1/day)	5.71	$\pm 1.2 \times 10^{-4}$	7.29	$\pm 5.2 \times 10^{-4}$
Ea (kcal/mol)	27.72	±12.1	17.79	±0.13
B_0 (1/day)	4.56	±2.6	6.56	±0.07
Eb (kcal/mol)	32.65	$\pm 5.96 \times 10^{-5}$	18.80	$\pm 3.2 \times 10^{-5}$

Table 7: Parameters obtained from fitting data to Lehman (1975) model.

Model Parameters	*P. tricornutum*	95% C.L	*Nannochloris* sp.	95% C.L
K_T	2.98	±0.97	1.46	±0.81
T_{inf} (°C)	0.00	±34.76	8.78	±4.94
T_{opt} (°C)	25.36	±0.86	28.75	±2.94
μ_{max}'(1/days)	1.27	±1.05	0.93	±0.13

The Arrhenius type model used by Bitaube Perez has the advantage that it incorporates the activation energy of growth and decay. These parameters carry some information regarding the behavior of the microalgae. A high activation energy for growth means that the organism's growth rate will increase more per unit increase in temperature. Also, a high activation energy of decay translates into a steep decline at

higher than optimal temperatures. Comparing the growth curves for *P. tricornutum* and *Nannochloris*, it can be seen that *P. tricornutum* has a steeper incline at temperatures below the optimum value and a steeper decline at temperatures above the optimum than does *Nannochloris*. This behavior is observed in the values obtained for Ea and Eb for *P. tricornutum* (27.72 and 32.65 kcal/mol) and *Nannochloris* (17.79 and 18.8 kcal/mol). In the case of the Huang model, the activation energy (ΔG') values obtained show the same trend. *P. tricornutum* has a higher ΔG' than Nannochloris (2683 vs 2548 J/mol).

The model developed by Lehman (1975) is a totally empirical model. The fitting parameter K_T has no true physical meaning; however, it is a simple model capable of describing the behavior of the system based on the three cardinal temperatures T_{inf}, T_{opt} and T_{sup}. This model was chosen to represent the growth of both microalgae species as a function of temperature because of its simplicity and because it obtained the lowest MSE for *P. tricornutum'*s curve.

Light penetration as a function of biomass concentration

Since the growth rate of a microalgae culture depends on light availability (Huisman et al., 2002; Reynolds, 2006 c) and self-shading may limit light availability at biomass concentrations required for commercial systems, models developed to describe algae growth rates (as a function of temperature or other parameters) must also incorporate the impact of light limitations to growth. To this end, it was first necessary to develop a model to predict the average light intensity (G_{av}) inside the experimental reactor at any given biomass concentration for both microalgae species. G_{av} was measured for a range of biomass concentrations for *Nannochloris* sp. and *P. tricornutum* as described previously. Figure 13 shows the results of these measurements. As cell density increases, the average light intensity decreases for each species. It can be

observed that, at the same cell density, the *P. tricornutum* suspension absorbs more light than the *Nannochloris* suspension.

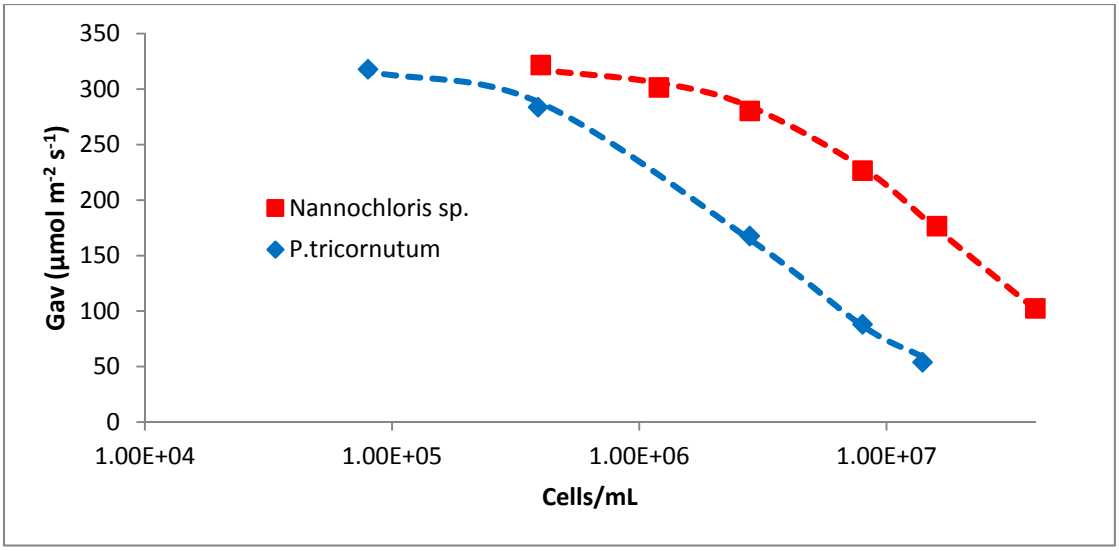

Figure 13: Average light intensity (Gav) for *Nannochloris* sp and *P. tricornutum* as a function of biomass concentration

A mathematical formulation that follows Beer-Lambert law behavior has been previously used to describe light attenuation in the photosynthetically active range (PAR) in microalgae cultures. The PAR range refers to the range of wavelengths that the photosynthetic pigments can absorb and use to carry out the photosynthetic reactions. This model has been used to estimate the average light intensity inside a culture at any given biomass density (Berberoglu et al., 2008). The mathematical expression describes light intensity (G) as a function of incident light (G_{in}), pseudo extinction coefficient (E_s), biomass concentration (X) and depth (d) for an algae suspension that receives light from the top in rectangular coordinates:

$$G = G_{in} e^{-E_s X d} \qquad \text{Equation 25}$$

The same expression can be adapted for a rectangular reactor where light comes from two sides with the same incident light intensity:

$$G_l = G_{in}\left(e^{-E_s X l} + e^{-E_s X (L-l)}\right) \qquad \text{Equation 26}$$

where G_l is the light intensity at depth l in the reactor and L is the total width of the reactor. Adapting this equation to cylindrical coordinates, it is possible to obtain an expression to calculate the average light intensity of the reactor as a function of biomass concentration by shell integration of the function G=f(r) from 0 to radius R and dividing it by the cross sectional circular area of the cylinder:

$$G_{av} = \frac{2\pi \int_0^R r\, f(r)\, dr}{\pi R^2} = \frac{2}{R^2}\int_0^R r G_{in}\left(e^{-E_s X (r+R)} + e^{E_s X (r-R)}\right) dr \qquad \text{Equation 27}$$

where R is the radius of the reactor and G_{av} is the average light intensity inside the reactor. The solution of this integral is:

$$G_{av}(X) = 2\left(\frac{G_{in}\, e^{-2E_s XR}}{E_s^2 X^2 R^2}\right)\left((E_s XR - 1)e^{2E_s XR} + 2e^{E_s XR} - E_s XR - 1\right) \qquad \text{Equation 28}$$

This expression was fit to data presented in Figure 13 by adjusting the pseudo extinction coefficient (E_s) for each species and minimizing the sum of the squares of the difference in $G_{av}(X)$ between the model and the data. The pseudo extinction coefficients for *Nannochloris sp* and *P. tricornutum* obtained from calibration of the model were $6.55 \times 10^{-12} \pm 0.72 \times 10^{-12}$ cm^2/cell and $4.14 \times 10^{-11} \pm 0.42 \times 10^{-11}$ cm^2/cell, respectively. The errors were calculated based on the standard deviation of cell density measurements using the error propagation method. It is not surprising that the pseudo extinction coefficient for *P. tricornutum* is higher because the cells are larger and the pigments (fucoxanthins) absorbs over a broader range of wavelengths (Lepetit et al., 2013). It is important to note

that this model assumes a constant incident light intensity across the reactor, which is not the case for the reactor geometry and light placement used. Nevertheless, the model does provide a reasonable representation of the average light intensity within the reactor as a function of the particular algae species and biomass concentration.

Models for growth as a function of average light intensity (Gav) and temperature

For nutrient replete cultures, net specific growth rate is mainly a function of light availability. This dependence can be modeled as a Monod type light saturation model expressed by the following equation:

$$\mu = \frac{\mu_{max} G_{av}}{K_G + G_{av}} \qquad \text{Equation 29}$$

This model assumes that the average light intensities are within a range where no inhibition occurs. There are several models that describe growth rate as a function of light intensity that take into account light inhibition (Huisman et al., 2002). However, since the incident light intensity and the average light intensity inside the reactor in these experiments did not exceed 300 μmol $m^{-2}s^{-1}$, it was assumed that the operating conditions were below the level of inhibition. Although the light intensity at which growth starts to be inhibited can vary between species, and some can be inhibited at light intensities as low as 100 μmol/m^2-s, others will not start to show signs of inhibition until subjected to 500 μmol/m^2-s (Sorokin and Krauss, 1958; Dauta et al., 1990). For *P. tricornutum*, inhibition is not observed at light intensities lower than 350 μmol $m^{-2}s^{-1}$ (Terry et al., 1985) and for *Nannochloris atomus* inhibition is not observed at light intensities lower than 300 μmol $m^{-2}s^{-1}$(Geider and Osborn, 1986).

The mathematical expression described in Equation 29 above, does not require the specific geometry of the reactor or the light apparatus characteristics as inputs; rather, it uses the average light intensity in the photosynthetically active range (PAR) measured in

a well-mixed microalgae suspension to estimate growth. Therefore, it can potentially be applied to any culture, regardless of geometry and other specific characteristics of each system, as long as no light inhibition exists.

For this work, a multiplicative model was used to describe the effects of both, light penetration and temperature on the growth rate of microalgae:

$$\mu = \mu_{max} f(G_{av}) f(T) \qquad \text{Equation 30}$$

Where:

$$f(T) = \begin{cases} e^{\left(-K_T\left(\frac{T-T_{opt}}{T_{sup}-T_{opt}}\right)^2\right)} \; at\; T > T_{opt} \\ e^{\left(-K_T\left(\frac{T-T_{opt}}{T_{inf}-T_{opt}}\right)^2\right)} \; at\; T < T_{opt} \end{cases} \qquad \text{Equation 24}$$

$$f(G_{av}) = \frac{G_{av}}{K_g + G_{av}} \qquad \text{Equation 29}$$

In this multiplicative model, the Lehman (1975) model is used for temperature and Equation 29 is used for light intensity. The most important assumptions regarding this model is that average light intensity does not affect the general shape of the temperature function f(T), and that temperature does not affect the light saturation profiles, that is, the half saturation constants do not vary significantly within the range of temperatures tested.

The net specific growth rates determined from turbidostat experiments for two temperatures (17 and 22°C for *P. tricornutum* and 17° and 28°C for Nannochloris) and average light intensity ranging from 90 to 280 μmol $m^{-2}s^{-1}$ are shown in Figure 14 and Figure 15. These data were used to calibrate the model above (Equation 30) using μ_{max} and K_g as fitting parameters. The resulting maximum growth rates and light half saturation constant obtained in this study are shown in Table 8. The parameters for the temperature function f(T) (K_T, T_{opt}, T_{sup} and T_{inf}) were determined previously in the

constant biomass experiments conducted at different temperatures (see Table 7). The model (Equation 30) is plotted in Figure 14 b) and 15 b) for *P. tricornutum* and *Nannochloris* sp. respectively, for both of the temperatures tested for each species.

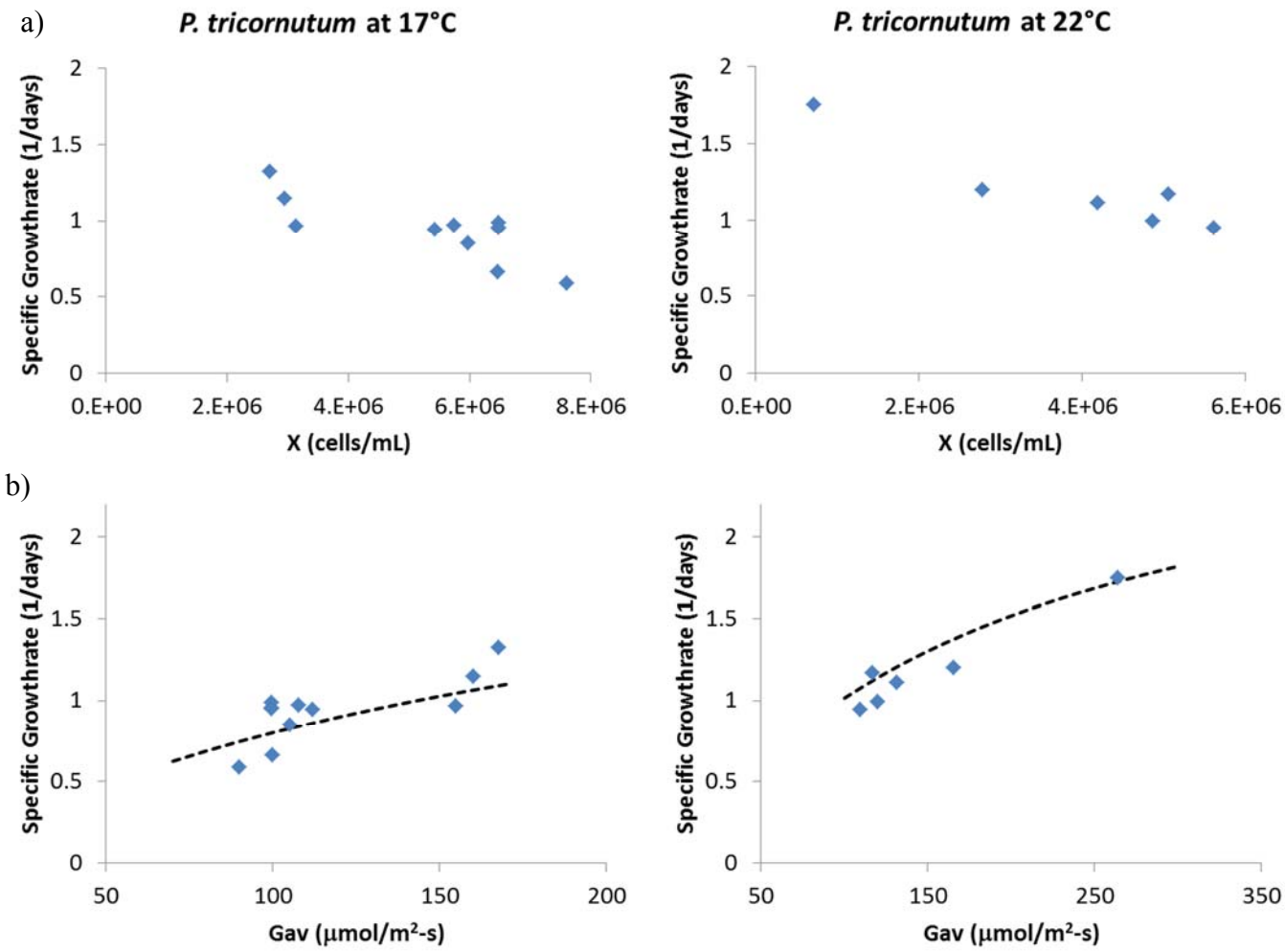

Figure 14: Growth rates of *P. tricornutum* measured at two temperatures (17 and 22°C) over a range of (a) biomass concentrations and (b) average light intensities . Average light intensity was calculated with Equation 28 using measured biomass concentrations and light extinction coefficients.

As expected, both microalgae species had a higher growth rate at a higher average light intensity. The maximum and lowest growth rate observed for *P. tricornutum* were 1.75 day^{-1} at 22°C and 0.58 day^{-1} at 17°C respectively and for *Nannochloris* sp. were 1.39 day^{-1} at 28°C and 0.41 day^{-1} at 17°C.

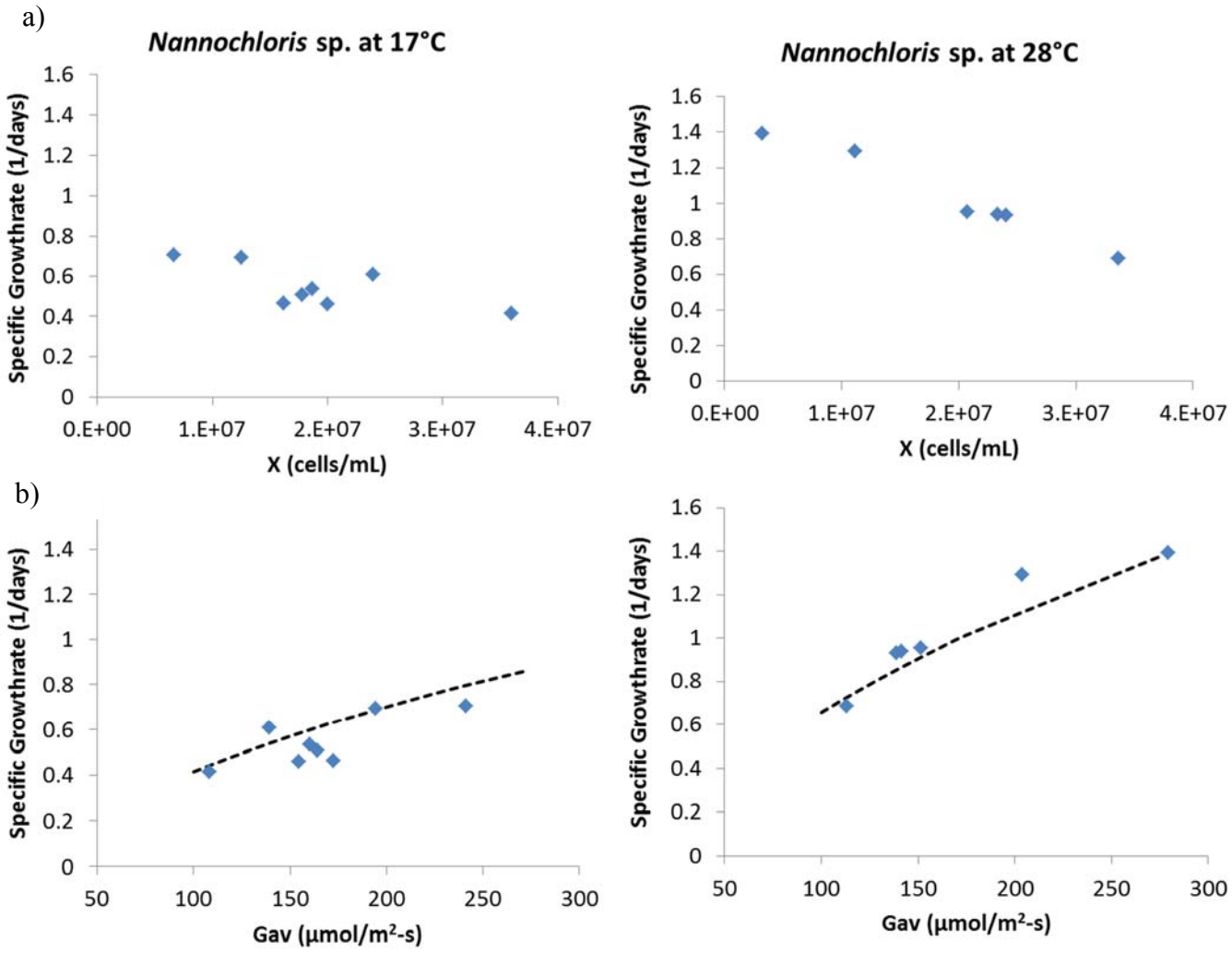

Figure 15: Growth rates of *Nannochloris* sp. measured at two temperatures (17 and 28°C) over a range of (a) biomass concentrations and (b) average light intensities. Average light intensity was calculated with Equation 28 using measured biomass concentrations and light extinction coefficients.

Table 8: Light saturation model parameters obtained for *Nannochloris* sp. and *P. tricornutum*.

Model Parameters	*P. tricornutum*	*95% C.L*	*Nannochloris* sp.	*95% C.L.*
μ_{max} (1/days)	3.1	±2.13	3.7	±4.6
K_g (μmol/m^2-s)	180.6	±209.7	456.5	±770.2
Mean squared error	0.34	NA	0.11	NA

The light half saturation constant (K_G) obtained for *Nannochloris* sp. was larger than the value for *P. tricornutum*. This can be perceived in the data, as a lower slope in the growth rate vs light intensity curve is observed. This could be interpreted to mean that *P. tricornutum* is more efficient at capturing light for growth than *Nannochloris*. The K_G value obtained in this study for *P. tricornutum* (180.67(μmol/m^2-s) is consistent with the values reported by Grima: 145-195 μmol $m^{-2}s^{-1}$ (Grima Molina et al., 1996). They used a similar cylindrical reactor and obtained K_G values by fitting the light saturation model to μ vs Gav data; however they used a different algae species, *Isochrysis galbana*, a Chlorophyll *c* bearing species which is more closely related to *P. tricornutum* than to *Nannochloris*. The value obtained for *Nannochloris sp* is higher than values obtained by Grima in the same study. This may be due to differences between the physiological light affinities of the two species. Also, the 95% confidence limits were high for the light half saturation constants, which is a reflection of the scatter in the data obtained; however, the confidence limits may be reduced if more data is collected across a broader range of light intensities and temperature conditions.

In order to test whether the light calibrated model represents the behavior of *Nannochloris* and *P. tricornutum*, the model (Equation 30) was used to predict (see Figure 16) the growth rates of *Nannochloris* and *P. tricornutum* over a range of temperatures for light intensities of 141 and 120 μmol $m^{-2}s^{-1}$respectively. For comparison, the measured growth rates of *Nannochloris* and *P. tricornutum* at these light

intensities are also presented. The results shown in Figure 16 shows that the calibration obtained for the light portion of the model works well, since both curves fit the observed data (R^2 values were 0.99 and 0.9 for *P. tricornutum* and Nannochloris respectively). Therefore, the model developed in this work successfully represents the behavior of both microalgae species over the range of temperatures and light intensities tested.

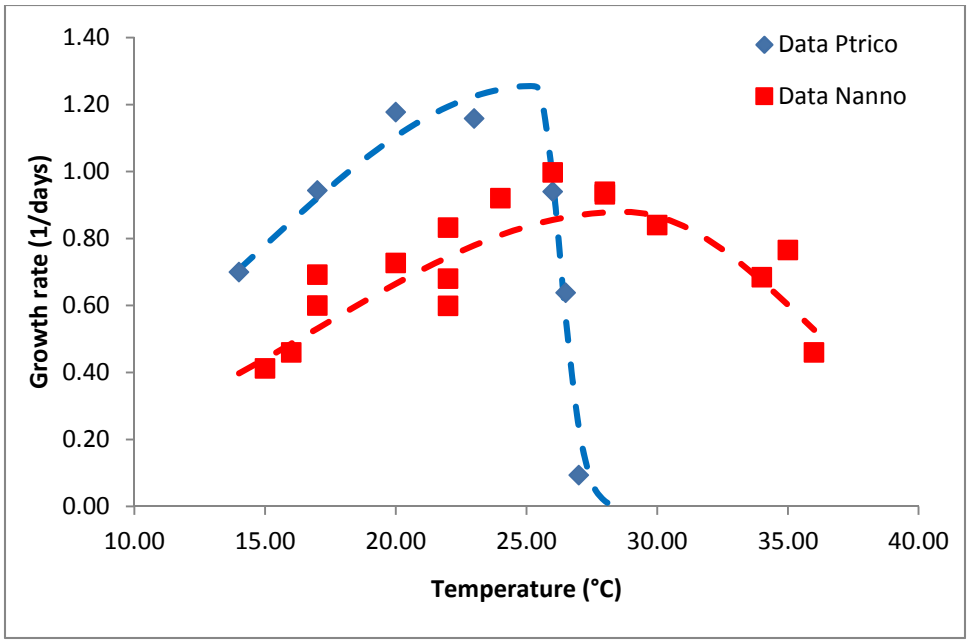

Figure 16: Comparison of data and model predictions for net specific growth rate as a function of temperature and light intensity for *Nannochloris* and *P. tricornutum*.

Also, a sensitivity analysis was performed to determine the effects of average light intensity on the growth rates of both microalgae species over a range of temperatures. As evident in Figure 17, a higher growth rate is observed at higher light intensity for both species. According to the model predictions, a substantial change in growth rate is expected when light intensity changes from 250 to 90 $\mu molm^{-2}s^{-1}$; *P. tricornutum's* growth rate changes from 1.8 to 1 day^{-1} and Nannochloris goes from 1.3 to

0.6 day^{-1} when both are near its optimum temperature of growth. It can also be observed that at temperatures away from their optimum, the absolute change in growth rate related to a change in average light intensity is less than at its optimum, due to the multiplicative nature of the model. This is an expected behavior since at non-optimal temperatures, the photosynthetic reaction rates decreases, and therefore cannot respond equally to a change in light intensity.

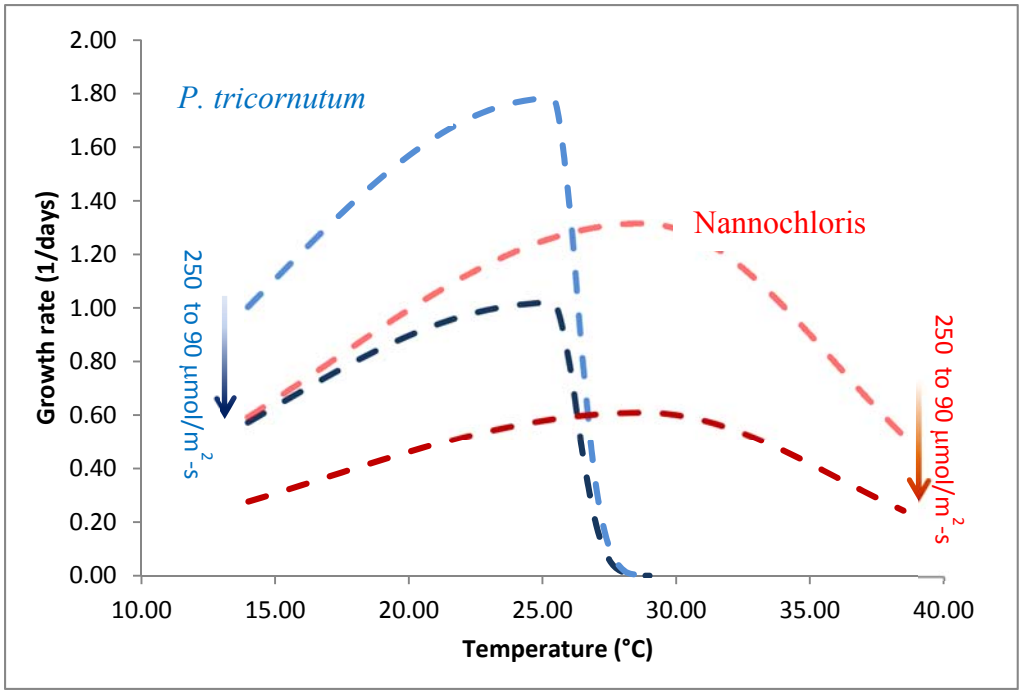

Figure 17: Sensitivity analysis of average light intensity on the growth rate of Nannochloris (red dotted lines) and *P. tricornutum* (blue dotted lines) as a function of temperature. A lighter shade of the lines indicates a lower biomass concentration or higher average light intensity.

CONCLUSIONS

Results of the batch growth experiments indicate that light attenuation due to an increase in cell density during microalgae growth plays an important role in limiting the

growth of microalgae cultures at biomass concentrations relevant to commercial culturing operations.

It was observed that *Nannochloris* and *P. tricornutum* had different growth responses to temperature. The range of growth for *P. tricornutum* and *Nannochloris* extended from 15 to 27°C and 20 to 35°C, respectively. The overlap in their temperature-growth profiles extends the range suitable for growth from approximately 15 ºC to 35 ºC. These two species can potentially be utilized in growth systems located in regions where temperatures oscillate within this range.

Furthermore, the light intensity in the reactor was observed to be a function of biomass concentration as well as a species dependent pseudo extinction coefficient. A mathematical expression was developed to estimate the average light intensity inside the reactor as a function of these two parameters. *Nannochloris* was observed to absorb less light than *P. tricornutum* at the same cell density.

A multiplicative model was developed that describes growth rate of microalgae as a function of temperature and average light intensity. The model consists of two sub-models: one that describes the growth as a function of temperature f(T) and a Monod type, light saturation model, that describes growth as a function of average light intensity $f(G_{av})$. The model chosen to describe the growth as a function of temperature was the empirical model developed by Lehman (1975), since it provided the best fit to the growth curve.

The calibrated model was compared to the behavior of both microalgae cultures over a range of temperatures at constant average light intensity; the resulting predictions compared well with the observed behavior of both microalgae species. The model, also confirms the fact that microalgae grown at high biomass concentrations, tend to grow at a slower rate due to light self-shading effects. This model can help delineate the role that

light limitation plays in mass culture systems subject to temperature fluctuations. It is important to note that the growth model developed in this work uses average light intensity and it can potentially be applied to other reactor geometries as long as the average light intensity is known. However, since the model was constructed and calibrated using data at constant biomass concentration and temperature, it is important to recognize that further work is needed to validate the model in dynamic cultures, where temperature fluctuations exist and biomass concentrations can vary with time.

Chapter 5: Impact of Temperature, Self-Shading and Allelopathy on Co-Culture Microalgae Growth

INTRODUCTION

Photosynthesis is arguably the single most important biochemical process for life on earth. The composition of the atmosphere has been shaped by this process that reduces carbon, produces oxygen and stores chemical energy in the form of biomass. It is thus natural to consider how photosynthetic processes can be utilized to provide a renewable energy source in the form of biofuels. Microalgae, single cell photosynthetic microorganisms, have been a focus of this research since the 1970s, as these organisms have a high photosynthetic efficiency and can be grown on non-arable land (Schenk et al., 2008; Mazzuca Sobczuk and Chisti, 2010). However, the high growth rates observed in controlled laboratory conditions have failed to transfer to open outdoor mass cultivation systems. There are many reasons for decreased productivity including poor control of fluctuating environmental conditions like temperature and light intensity as well as the presence of secondary consumers and predatory organisms that tend to disrupt microalgae growth.

It has long been hypothesized that biodiversity affects the productivity and stability of ecosystems. This hypothesis has been applied to all types of ecosystems and to all trophic levels. There has been particular interest in the role of primary producers in the productivity of ecosystems (biomass production) and several field experiments have demonstrated that the broader the diversity of the primary producers, the more stable the ecosystem (Lehman and Tilman, 2000; Tilman et al., 2001). These experiments have been conducted with plants on grasslands and sea weed species in aquatic ecosystems (Stachowicz et al., 2008). More recently, the hypothesis has been tested with algal systems by artificially creating microalgae communities of varying biodiversity levels

(Stockenreiter et al., 2011; Corcoran and Boeing, 2012; Shurin et al., 2013). The researchers compared the productivity and lipid production in microalgae assemblages with that observed in monoculture systems. Furthermore, they tested the stability of the assemblages by measuring the productivity after the addition of a predator. The authors concluded that in general, biodiversity enhances the resiliency of the cultures in the presence of predators. Additionally, they concluded that the particular combination of species present in the assemblage dictates the productivity of the system, suggesting that choosing a combination of highly productive species is an important factor for optimizing biomass growth of the system as a whole.

One key factor that has been shown to affect the stability and productivity of microalgae cultures is temperature fluctuation (Goldman, 1979 b; Benemann and Tillet, 1987). Temperature variation becomes particularly important for outdoor mass cultivation systems in climates where temperature fluctuates significantly, either during the day or throughout the seasons. Microalgae growth rates, like all chemical reaction rates, are regulated by temperature. Usually, higher temperatures lead to higher growth rates. However, evolution is usually geared towards optimizing traits for a particular environment. Therefore, microalgae that are adapted to grow at low temperatures tend to exhibit lower growth rates at higher temperatures and vice versa. The succession of species dominance with changing environmental conditions, termed ecological trade off (Shurin et al., 2013), is the reason why in natural waters the composition of a microalgae community changes according to the season. In view of the behavior of natural systems and the potential benefits of using a multispecies culture in commercial algae applications, it may be possible to engineer a mixed microalgae culture with more than one species of microalgae, each adapted to grow across a different temperature range. In

this way, increasing biodiversity can help to overcome ecological trade-offs, enhance productivity and stabilize commercial systems.

The development of a stable multispecies culture is not as simple as identifying two or more species that grow within different temperature regimes. Growing multiple microalgae species within the same growth medium may result in inter-species competition. In nature, microalgae are subject to intense competition for nutrients and light. There are different physiological and biochemical adaptations such as surface area to volume ratios or pigment composition that give each species a particular advantage within a particular environment. Some microalgae are capable of releasing chemicals, usually secondary metabolites, into the medium that inhibit the growth of competing microalgae, bacteria or predators (Legrand et al., 2003). This interaction between microalgae and other microorganisms is called allelopathy. These types of interactions are common in nature, and have been documented in the lab for several microalgae species (Gross, 2003; Arzul and Gentien, 2006). The chemicals that cause growth inhibition (allelopathic agents) can vary widely in nature. Researchers have identified peptides, alkaloids, organic acids and fatty acids of varying length, structure, and functional groups composition. The inhibition mechanisms vary and are understood only for a few allelochemicals (Legrand et al., 2003). While allelopathic interactions have been recognized between particular microalgae species, the chemical agents responsible for the interaction have not been chemically isolated or identified. Improving our understanding of allelopathic effects will be crucial for the development of engineered microalgae assemblages for mass culturing operations.

The use of communities for large scale growth operations instead of monocultures is appealing and has the potential of increasing the productivity and stability of cultures. However, in order to apply this promising cultivation method, it is necessary to

understand the interactions between microalgae species and the resulting population dynamics of such systems as a function of the key variables affecting growth.

In this study, two microalgae species, *Nannochloris* sp. (UTEX 1999.) and *Phaedactylum tricornutum* (UTEX 646) were co-cultured under controlled temperature variation conditions in continuous mode. In the previous chapter, the individual growth rates of these two monoculture species were determined as a function of temperature and self-shading. At high concentrations, self-shading was evident for both cultures, and a growth model was developed that described the impact of both temperature and light attenuation as a function of cell density. *Nannochloris* sp. grows between 26 and 28°C whereas *Phaedactylum tricornutum* grows between 18 and 24 °C. Thus, co-cultures of these two species could potentially enhance the stability of an outdoor system subjected to temperature variations. However, light attenuation still needs to be considered in mass cultivation systems where high biomass densities are desired. In multispecies systems, the impact of shading is complicated as the shading properties of microalgae are dependent on cell size and pigmentation. In addition, the impact of allelopathy must be understood and incorporated into models that describe algae growth within natural or engineered bioreactors. Results presented in this chapter address these issues using experimental data to explore the effects of temperature, co-shading, and exudates on the growth rates of a *Nannochloris* and *P. tricornutum* co-culture. A model that incorporates these effects in a co-culture system is also developed.

MATERIALS AND METHODS

Experimental approach

A series of experimental studies were conducted to investigate the effects of shading (light attenuation due to the presence of algae cells), temperature fluctuations,

and allelopathy on algae net specific growth in co-cultures. Allelopathic interactions between *Nannochloris* and *P. tricornutum* were explored in batch reactors (50 ml culture flasks and 200 μL well plates) by culturing *Nannochloris* in spent medium from *P. tricornutum*. The spent medium was amended with macronutrients (N and P) and micronutrients (trace metals and iron). The impact of shading and temperature on the growth of each species was investigated in a continuous flow chemostat and in turbidostat co-culture experiments. Average light intensity was measured for a range of biomass concentrations for different proportions of *Nannochloris* to *P. tricornutum* cells in the continuous flow reactor. The model developed in Chapter 4, was modified to account for the allelopathic interactions observed, and calibrated by minimizing the sum square of error between the model predictions and the data collected in the turbidostat experiments. All of the calibrated constants obtained from the monoculture experiments in Chapter 4 were used without modification in the co-culture, except the light pseudo extinction coefficients that were determined from measurements conducted in co-culture as part of this research. The modified model was then compared to the behavior observed during the chemostat experiment.

Growth Media

All of the experiments were performed using a modified ASP medium (Andersen, 2005) with the following composition (per liter): NaCl, 23.38g; KCl, 0.375g; $CaCl_2$, 0.56g; $NaHCO_3$, 0.168g; $MgCl_2 \cdot 6H_2O$, 4.06g; $MgSO_4 \cdot H_2O$, 4.93g; Tris(hydroxymethyl)aminomethane base, 0.606g; $NaNO_3$, 0.425g; Na_2HPO_4 0.048g; $Na_2SiO_3 \cdot 9H_2O$ 0.057g; Fe-EDTA, 0.842mg; EDTA, 14 mg; $ZnSO_4 \cdot 7H_2O$, 10.064mg; H_3BO_3, 24.732mg; $CoCl_2 \cdot 6H_2O$, 0.071mg; $CuSO_4 \cdot 5H_2O$, 0.075mg; $MnCl_2 \cdot 4H_2O$, 1.979mg; $NaMoO_4 \cdot 2H_2O$, 1.21mg; Vitamin B_{12}, 0.5μg, Vitamin B_1, 100 μg; Biotin,

0.5µg. The medium was prepared with ACS grade reagents, adjusted to pH 7.3 and autoclaved for 45 min at 121°C.

Cell density

A LSRFortessa cytometer (BD Biosciences, San Jose, CA) was used to determine cell densities during the turbidostat experiments. Samples were taken from the culture and diluted by a factor of ten. One mL of the diluted sample was introduced into a falcon tube (BD Falcon polystyrene test tube, 12 x 75-mm, 352052) where 50 µL of 5-5.9µm Accucount Fluorescent Particles (Spherotech Inc., Lake Forest, IL) were added to reach a final concentration of $5x10^4$ particles/mL. A laser with a wavelength of 488nm was used to measure fluorescence of both the microalgae cells and the spheres. Chlorophyll bearing, live cells were counted on the red (670nm Long Pass filter) channel, whereas the fluorescent particles were counted by using the green fluorescence (530nm filter) channel. Cells that fluoresced red were considered living cells since chlorophyll *a* fluorescence only happens when the electron transport chain (ETC) in the thylakoid membrane is active. For each cell that is detected by the photodiode, the fluorescence intensity (at both wavelengths), as well as the light forward and side scattering intensity are plotted on different graphs (see Figure 31 in Appendix B). Two distinct populations, one for *Nannochloris* sp. and one for *P. tricornutum* were visible on the red fluorescence vs forward scattering plot. Each population was counted separately. The standard deviations of the cell density measurements were about ±10% or less. Data was acquired until 200 fluorescent particles were counted and the number of cells/mL for each species was calculated using the following equation that accounts for dilution.

$$\#\frac{cells}{ml} = Cells\ counted\left(\frac{50{,}000}{200}\right)(10) \qquad \text{Equation 31}$$

Average Light Intensity

Light intensity inside the reactor was measured in discrete points using a submersible Spherical Micro Quantum Sensor (US-SQS/L, WALZ, Effeltrich, Germany) across two axes of the reactor cylinder (one parallel and the other perpendicular to the light source) at three different depths for a range of biomass concentrations of *Nannochloris* and *P. tricornutum*. The sensor has a reported measurement error of ±5%. Measurements were performed over a range of biomass concentrations of *Nannochloris* and *P. tricornutum* that yielded: 25%, 50%, and 75% *P. tricornutum* in the co-culture. Seven data points were collected across each axis as shown previously in Chapter 4. Thus, for each depth, three concentric rings, each having four measurements of light intensity were conceived. For each ring, the average of light intensity was calculated from the four measurement points within the ring. To obtain an average light intensity across the area for each depth, a weighted average was obtained by using each of the ring's areas. To calculate the average light intensity within the reactor volume the average light intensity at the three different depths were averaged. The average light intensity at each depth for a given biomass concentration and *Nannochloris* to *P. tricornutum* ratio were very similar (less than 7% difference).

Assessment of Allelopathy

Preliminary experiments

P. tricornutum and *Nannochloris* were grown separately in modified ASP medium in a 500 mL flask, sparged with air for 7 days to a cell density of approximately $5x10^6$ cells/mL for *P. tricornutum* and $4x10^7$ cells/mL for *Nannochloris*. The cultures were centrifuged and the supernatant from each culture was filtered through a 0.2 μm syringe filter to obtain what is referred to here as spent medium. *Nannochloris* was then

grown in triplicate in 50mL flasks sparged with air with the following growth media: a) fresh medium, b) 50% (v/v) fresh medium and 50% *P.triconutum* spent medium, c) 100% *P. tricornutum* spent medium, d) 50% fresh medium and 50% *Nannochloris* spent medium and e) 100% *Nannochloris* spent medium. Nitrogen and phosphorus concentrations in the spent medium, as well as pH were adjusted to the same levels as in the fresh medium at the start of each experiment. The *Nannochloris* was inoculated using 1 mL of the original culture recovered from the spent media described above. The culture was incubated at 22°C for a period of 5 days. Samples were collected every 24 hours and the cell concentration determined by counting the cells under a microscope (Nikon Eclipse 80i, Nikon, Melville, NY) using a hemocytometer (Hausser Bright-Line 3100, Hausser Scientific, PA). Growth rates were calculated from an exponential regression of the growth curves (cell density vs time) obtained for each treatment.

Allelopathy Confirmation Experiments

P. tricornutum was grown as a monoculture in modified ASP medium aerated with ambient air in a 500 mL flask to cell densities between $5x10^6$ and $7.1x10^6$ cells/mL. The cultures were centrifuged and filtered through a 0.2 μm syringe filter. The nitrogen and phosphorus concentrations in the filtered medium, as well as the pH were adjusted to the same levels as in the fresh medium. Fresh and spent medium were mixed at 10 different ratios (from pure fresh to pure spent medium in 10% increments). The spent medium that contained $7.1x10^6$ cells/mL was amended with trace metals (EDTA, 14 mg/L; $ZnSO_4•7H_2O$, 10.064mg/L; H_3BO_3, 24.732mg/L; $CoCl_2•6H_2O$, 0.071mg/L; $CuSO_4•5H_2O$, 0.075mg/L; $MnCl_2•4H_2O$, 1.979mg/L; $NaMoO_4•2H_2O$, 1.21mg/L). The medium that contained $5x10^6$ cells/mL was amended with additional Fe (Fe-EDTA, 0.842mg/L). The medium was distributed in 200 μL aliquots to each well of a clear 96

well plate as described in Figure 18. Four wells per treatment (Fe or trace metal amendment) were not inoculated and left as a blank. Four replicates were used for each ratio of Fresh/Spent medium. *Nannochloris* was inoculated into the well plates using 10 μL of a culture with a cell density of $5x10^6$ cells/mL and was incubated under two fluorescent lights (Philips, Natural Sunshine F15T8). Biomass was estimated by measuring optical density at 688nm every 24 hours in a microtiter plate reader (Bio-Tek Synergy HT, BioTek, Winooski, VT). Growth rate was calculated by performing an exponential regression on the absorbance vs time data. *P. tricornutum* was also grown in its own spent media (the medium that had contained $5x10^6$ cells/mL) in a similar setting as the one used for *Nannochloris*. However, for this assay no additional trace metals nor Fe were provided.

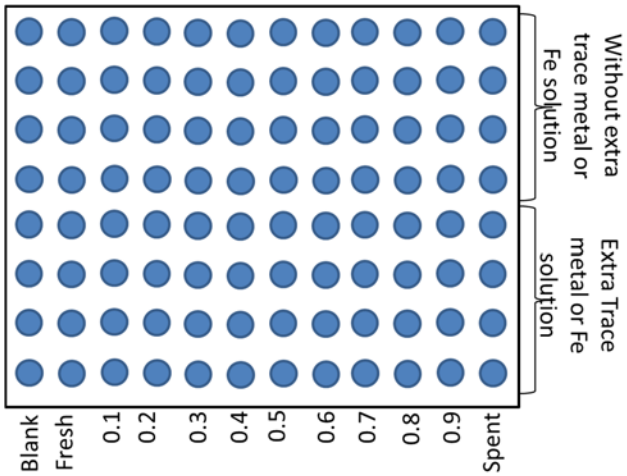

Figure 18: Layout of 96 well plate allelopathy assay.

Turbidostat Experiments with Co-cultures

Mixed cultures (co-cultures) of the two algae species were grown in a turbidostat that was maintained at constant turbidity as described earlier (Figure 6). The reactor was sealed using a glass cap that had inlets for a pH probe (Cole-Parmer Autoclavable pH Probe, Sealed/DJ/Glass), an air sparger tube and sampling ports. Two lamps, each

containing two fluorescent bulbs, 1m in length (Sylvana cool white 4100K, Sylvana, Danvers, MA) were placed on each side of the reactor to illuminate the system. The incident light intensity on the sides closest to the lights was 183.2 $\mu molm^{-2}s^{-1}$ as measured by a Waltz Submersible Spherical Micro Quantum Sensor (US-SQS/L, Effeltrich, Germany). Ambient air bubbled into the medium was pre-humidified by sparging it into a 2L Erlenmeyer flask filled with autoclaved distilled water. Evaporative losses from the culture medium were minimal (less than 1% over a 24 hour period at 33°C). The temperature within the turbidostat culture was controlled using a water bath circulator (Fisher Scientific Isotemp 1013P, Pittsburgh, PA).

The turbidostat reactor was operated exactly as in Chapter 4. The only variant was that two species were inoculated instead of one. At the beginning of the experiment only *Nannochloris* sp. was present in the reactor and the monoculture was grown at a constant turbidity of 50 FTU at 22°C for a period of 24 hours. Then, the reactor was inoculated with *P. tricornutum* and the temperature changed to 16°C. Ninety hours after the inoculation of *P. tricornutum*, the temperature was changed to 22°C. It was maintained at 22°C for an additional 60 hours, then changed to 30°C for 90 hours, and then changed back to 16°C for the remainder of the experiment. Samples were taken through a sample port for cell density determination using flow cytometry.

Co-culture chemostat experiments

The same reactor that was used in the turbidostat experiment was operated in chemostat mode; the only difference in operation was that the dilution rate was maintained at a constant rate of 0.71 day^{-1} in the chemostat experiments and turbidity was allowed to change throughout the duration of the experiment. To initiate the experiment, *Nannochloris* sp. was initially grown at 18°C for a period of 24 hours in the turbidostat at

a constant biomass concentration of approximately $1.5x10^6$ cells/mL. At time zero, the reactor was inoculated with *P. tricornutum* and the system was operated as a chemostat with a constant dilution rate of 0.71 day^{-1}. The temperature was altered from 17-18°C to 27-28°C every 72 hrs, using a 12hr temperature ramp. Periodically, samples were taken through a sample port to determine the cell density of each algae species using flow cytometry.

Mann-Kendall trend test

The Mann-Kendall trend test was performed for the 96 well plate experiments following the method described by Statistical Analysis of Groundwater Monitoring Data at RCRA Facilities (EPA, 2009).

RESULTS AND DISCUSSION

Allelopathic interactions

In order to identify the potential for allelopathic interactions between the two microalgae species, a series of experiments were performed to measure growth rates of the individual microalgae species in filtered spent medium. Results from the triplicate batch reactor experiments conducted in 50mL flasks in which *Nannochloris* was grown in various combinations of fresh media and spent media from *P. tricornutum* and *Nannochloris cultures* are shown in Figure 19.

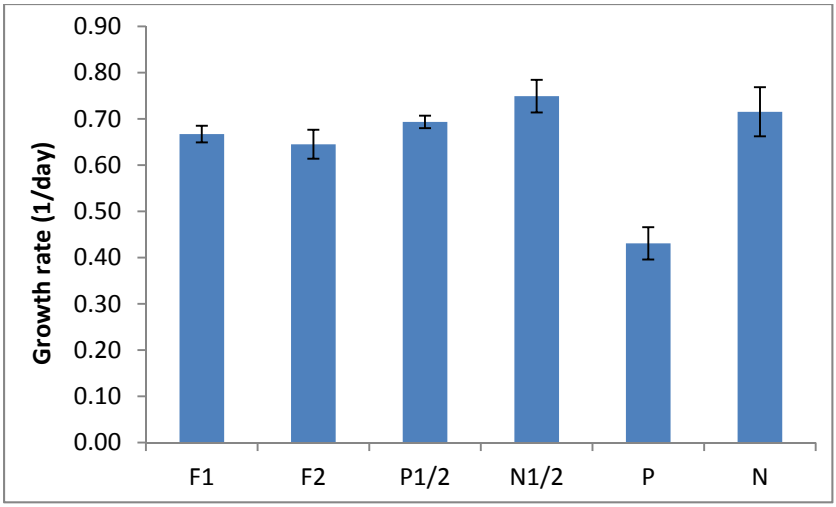

Figure 19: *Nannochloris* growth rates measured in different media: 100% Fresh media, (F1 and F2), 50% fresh medium and 50% spent medium by *P. tricornutum* (P1/2), 50% fresh medium and 50% spent medium by *Nannochloris* (N1/2), 100% spent medium by *P. tricornutum* (P), 100% spent medium by *Nannochloris* (N)

Comparison of the growth rates measured for *Nannochloris* using different media shows that inhibition occurs when grown in 100% *P. tricornutum* spent media. This observation is consistent with other researchers who have reported that the presence of *P. tricornutum* inhibited the growth of certain microalgae species (Legrand et al., 2003). One study specifically reported growth inhibition of *Nannochloris oculata* in the presence of *P. tricornutum* (Mayasich et al., 1987). It is important to note that when *Nannochloris* is grown in its own spent medium (labeled as N in figure above) no self-inhibition is observed. Also, when grown in 50% fresh and 50% spent medium from *P. tricornutum* (P1/2), growth inhibition was also not observed. This may be due to a nonlinear dose-effect response, where a minimum amount of allelochemical needs to be present to cause inhibition.

While these preliminary results provide some evidence that allelopathy exists for growth of *Nannochloris* in the presence of *P. tricornutum*, other causes such as trace

nutrient limitations may also have been responsible for the reduced growth rates observed in the spent media. Another series of experiments were performed to assess whether reduced trace metal (Fe, Zn, Mn, Cu) concentrations were responsible for the observed lower growth rates. For these experiments, Nannochloris was grown in clear 96 well plates under a gradient of fresh to spent medium ratios.

Figure 20 and Figure 21 shows the growth rates measured for Nannochloris in a gradient of fresh to spent medium ratios amended with Fe and trace metals respectively. The experimental results from both assays clearly show an inverse relationship between the amount of spent medium present in the culture and the growth rate of *Nannochloris* regardless of whether trace metals or Fe(II) is added. It should be noted that the final cell density for the experiment shown in Figure 21 ($5x10^6$ cells/mL) and Figure 22 ($7.1x10^6$ cells/mL) are relatively similar. Thus, differences between the two experiments are likely due to potential variations in the by-product concentrations in the spent media samples used in each experiment. Moreover, there does not appear to be any limitation of iron and only a small impact of trace metals at the highest ratios of fresh/spent media. It is therefore reasonable to conclude that the reduction in *Nannochloris* growth rates was due to the presence of allelochemicals in the spent media from *P. tricornutum* growth.

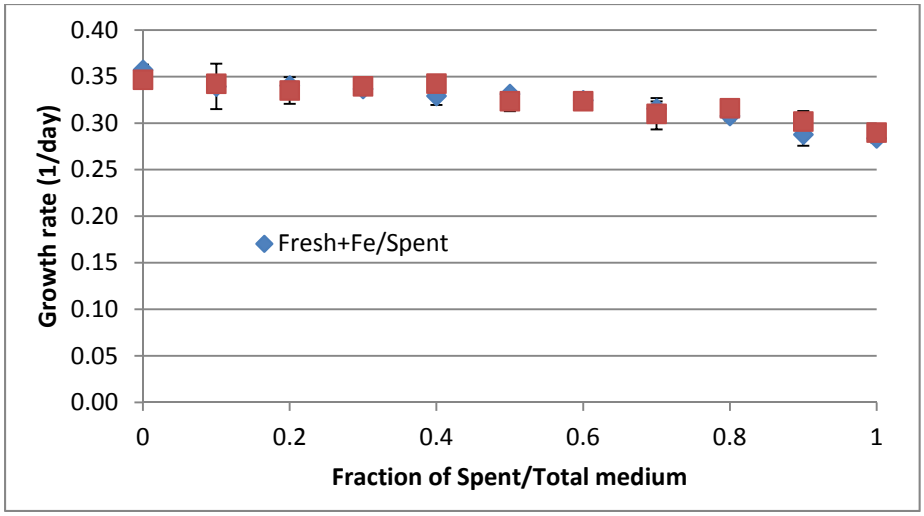

Figure 20: *Nannochloris* grown in a gradient of Fresh to Spent medium. The figure compares growth rates for spent medium with Fe amendment (red squares) and without (blue rhomboids). The spent medium was harvested from a *P. tricornutum* culture with a cell density of $5x10^6$ cells/mL.

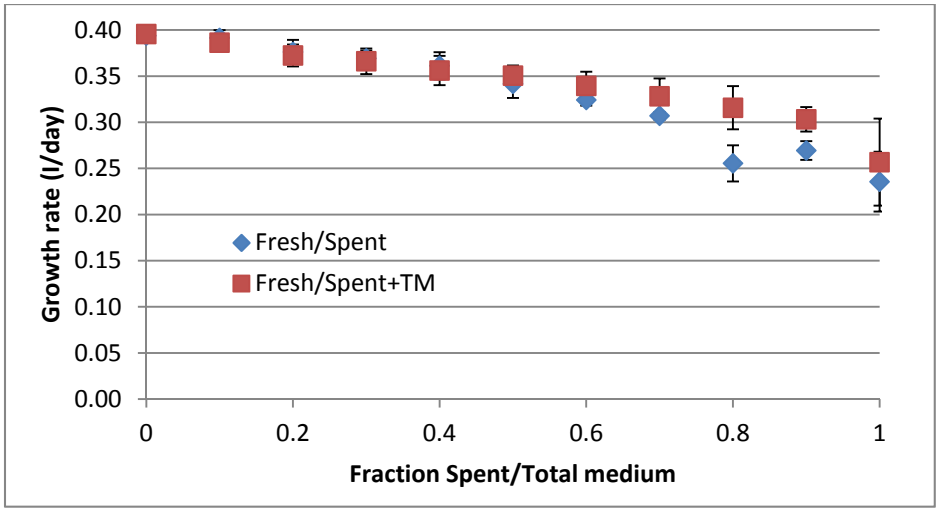

Figure 21: *Nannochloris* grown in a gradient of Fresh to Spent medium. The figure compares growth rates for spent medium with trace metals amendment (red squares) and without (blue rhomboids). The spent medium was harvested from a *P. tricornutum* culture with a cell density of $7.1x10^6$ cells/mL.

Another experiment (Figure 22) was conducted to determine whether self-inhibition affected *P. tricornutum* growth. The biomass concentration of *P. tricornutum*

prior to collection of the supernatant to be used as spent media was $5x10^6$ cells/mL. In this experiment, a slight increase in growth rate is observed with increasing contribution of spent media; however, the R^2 is only 0.64. This slight increase in growth rate was also observed in another study in which *P. tricornutum* was grown in its own spent medium (Vasconcelos and Leal, 2008).

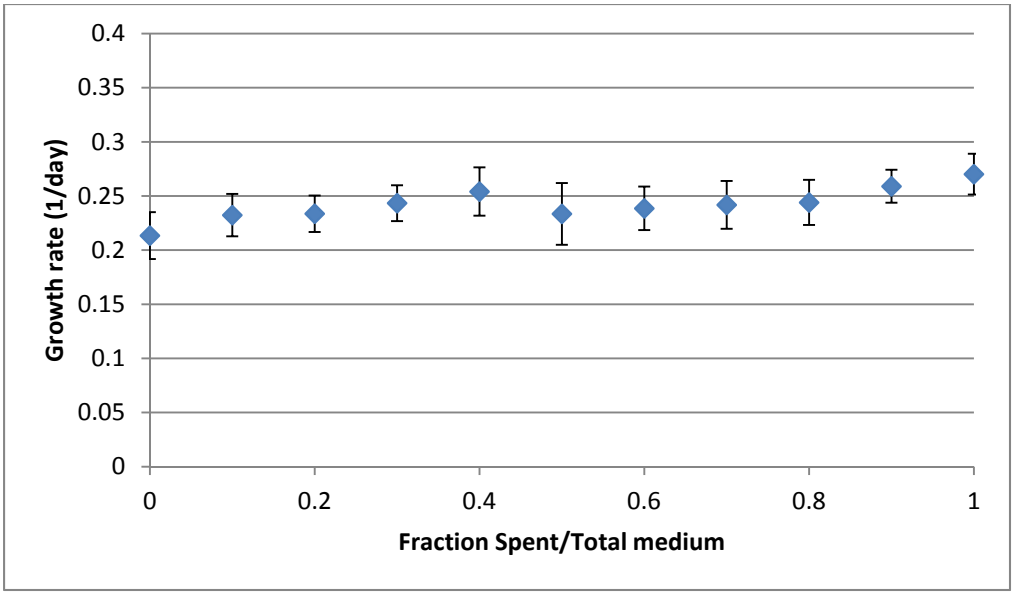

Figure 22: *P. tricornutum* grown in a gradient of fresh to *P. tricornutum* spent medium.

A Mann-Kendall trend test was carried out for all the 96 well assays. The results are tabulated in Table 9. The Mann-Kendal statistic (S) was negative for all the *Nannochloris* assays which implies a declining growth trend as the fraction of *P. tricornutum* spent medium increases. In contrast, for the self-inhibition assay for *P. tricornutum*, the S value was positive. The non-parametric testing yielded p values of less than 0.0001 for *Nannochloris* grown on spent *P. tricornutum* media, and a p value of less than 0.001 for *P. tricornutum* growth on *P. tricornutum* spent media. Therefore, for a typical significance level (α) of 0.05 the null hypothesis of no trend is strongly rejected,

and the impact of allelopathy on Nannochloris is more significant than the impact of spent *P. tricornutum* media on *P. tricornutum* growth.

Table 9: Mann-Kendall trend test results for the 96 well plate assays.

Microalgae species	Media used	Mann-Kendal statistic (S)	Standardized Z statistic	P value
Nannochloris	Fresh/Spent	-51.00	4.23	0.000011
Nannochloris	Fresh+Fe/Spent+Fe	-47.00	3.90	0.000049
Nannochloris	Fresh/Spent	-53.00	4.40	0.000005
Nannochloris	Fresh/Spent+TM	-55.00	4.57	0.000002
P. tricornutum	Fresh/Spent	39.00	3.22	0.000645

Dynamic co-culture model

In Chapter 4, a model for the net specific growth rate that describes monoculture growth of *Nannochloris* and *P. tricornutum* as a function of temperature and light intensity was developed:

$$\mu_i = \mu_{max,i} f_i(T) f_i(G_{av}) \qquad \text{Equation 32}$$

Where:

$$f_i(T) = \begin{cases} e^{\left(-K_{Ti}\left(\frac{T-T_{opt,i}}{T_{sup,i}-T_{opt,i}}\right)^2\right)} \; at\; T > T_{opt,i} \\ e^{\left(-K_{Ti}\left(\frac{T-T_{opt,i}}{T_{inf,i}-T_{opt,i}}\right)^2\right)} \; at\; T < T_{opt,i} \end{cases} \qquad \text{Equation 33}$$

$$f_i(G_{av}) = \frac{G_{av}}{K_{G,i}+G_{av}} \qquad \text{Equation 34}$$

where T is incubation temperature (°C), K_T is an empirical constant, T_{opt} is the optimum temperature for growth, T_{sup} is the temperature above which no growth is observed, T_{inf} is the temperature under which no growth is observed, K_G is the light half saturation constant (μmol m^{-2} s^{-2}). These parameters were determined in Chapter 4 for the two

species studied in this system and are summarized in Table 2 below. The "i" subscript refers to different species.

Table 10: Summary of model parameters obtained for both microalgae species in monoculture.

Model Parameters	*P. tricornutum*	95% C.L	*Nannochloris* sp.	95% C.L
μ_{max} (1/days)	3.07	±2.1	3.72	±4.6
K_g (μmol/m^2-s)	180.6	±209.7	456.5	±770.2
K_T	2.98	±0.97	1.46	±0.81
T_{sup} (°C)	27.50	NA	41.00	
T_{inf} (°C)	0.00	±34.8	8.78	±4.9
T_{opt} (°C)	25.36	±0.87	28.75	±2.9

The model incorporates attenuation of light due to self-shading by estimating the average light intensity $G_{av}(X)$ from the following equation (for a detailed discussion of this equation see Chapter 4):

$$G_{av}(X) = 2\left(\frac{G_{in}\, e^{-2E_sXR}}{E_s^2X^2R^2}\right)\left((E_sXR-1)e^{2E_sXR} + 2e^{E_sXR} - E_sXR - 1\right) \qquad \text{Equation 28}$$

The average light intensity is a function of biomass concentration X, a reactor dependent, empirically determined pseudo extinction coefficient, E_{ext}, and the reactor geometry (R is the radius of the cylindrical reactor used in these studies).

Extension of this model to a dynamic co-culture containing *Nannochloris* and *P. tricornutum* requires:

1) The allelopathic interaction between *P. tricornutum* and *Nannochloris* must be incorporated into the model.
2) The average light intensity as a function of total cell density and the proportion of each of the two species in the co-culture.

Modeling allelopathic interactions

As discussed in the previous section, the presence of *P. tricornutum* inhibits the growth of *Nannochloris* presumably due to allelopathy. However, there was no apparent impact of *Nannochloris* on the growth rate of *P. tricornutum.* Previous research conducted by Solé et al. (2005) validated a model that described the allelopathic interaction between two microalgae species grown in batch culture. The model is adapted from a common approach to analyze microbial competition which is based on the logistic equation and takes the form:

$$\frac{dX}{dt} = x(a - bx - cy - \gamma xy) \qquad \text{Equation 35}$$

in which the *cy* term accounts for competition and *γxy* term accounts for allelopathy (Maynard Smith, 1974). In this research, only a single species is affected by the presence of by-products from the other species (i.e., allelopathy) and competition is not considered as excess nutrients were provided. Incorporation of the allelopathy term into the mass balance equation for the reactor yields:

$$\frac{dX_1}{dt} = -DX_1 + (\mu_1 X_1 - \gamma {X_1}^2 X_2) \qquad \text{Equation 36}$$

$$\frac{dX_2}{dt} = \mu_2 X_2 - DX_2 \qquad \text{Equation 37}$$

where: X_1 is the biomass concentration of microalgae species 1 and X_2 is the biomass concentrations of microalgae species 2 growing together (cells/mL). μ_1 and μ_2 are the specific growth rates of species 1 and 2 as a function of light and temperature (1/day), D is the dilution rate of the system (1/days), and t is time (day). In this case, the subscript 1 refers to *Nannochloris*, as it is the species that is affected by the presence of *P. tricornutum's* (subscript 2) by-products.

Incorporating the effect of light intensity for a multispecies culture

Results from Chapter 4 (presented in Figure 21) demonstrated that the impact of self-shading could be incorporated into the net specific growth rate for each microalgae species via a biomass concentration dependent average light intensity (G_{av}).

$$G_{av}(X) = 2\left(\frac{G_{in}\, e^{-2E_{s,a}XR}}{E_{s,a}^2 X^2 R^2}\right)\left(\left(E_{s,a}XR - 1\right)e^{2E_{s,a}XR} + 2e^{E_{s,a}XR} - E_{s,a}XR - 1\right) \qquad \text{Equation 38}$$

Application of this approach to a multispecies system required estimation of an apparent pseudo extinction coefficient ($E_{s,a}$) for different proportions of each species. The average light intensity determined in the reactor as a function of overall cell density for a range of different mixtures of *Nannochloris* and *P. tricornutum* is presented in Figure 23.

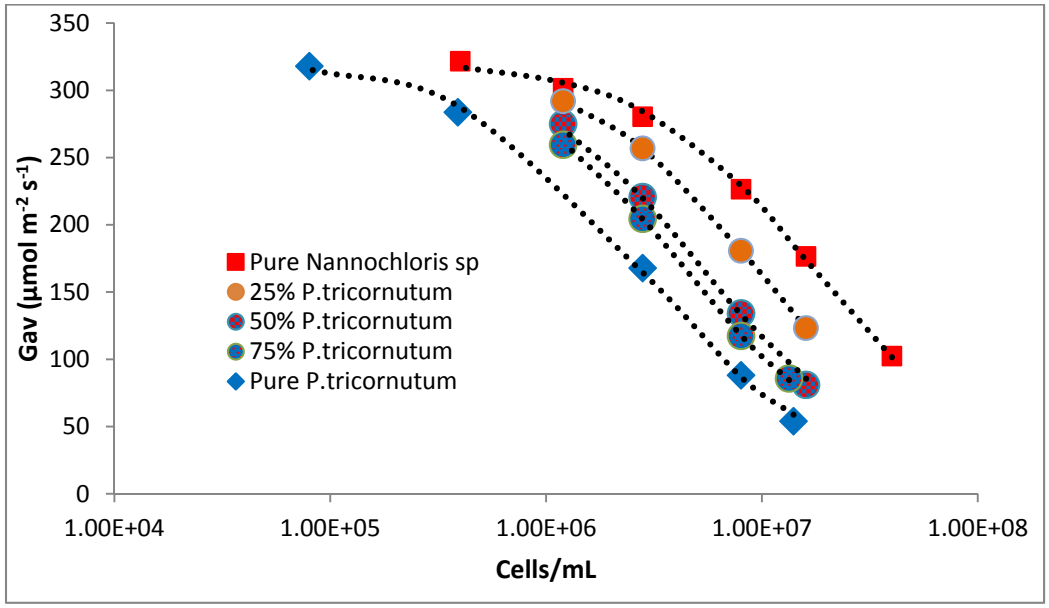

Figure 23: Measured average light intensity in the reactor for a range of biomass concentration and different mixtures of *P. tricornutum* and *Nannochloris.*

As demonstrated in Chapter 4, the *P. tricornutum* cell suspension absorbs more light than the *Nannochloris* cell suspension at the same cell density. Thus it is not surprising that the data obtained for the co-cultures lie between the two curves generated in pure cultures.

An estimation of $E_{s,a}$ was obtained for each ratio of *P. tricornutum* to total cell density by minimizing the sum of the square errors between the model and the data in Figure 23. The apparent pseudo extinction coefficient was the only fitting parameter. The apparent pseudo extinction coefficients obtained for each curve depicted in Figure 23 are plotted versus the fraction of *P. tricornutum* cells in the suspension in Figure 24. Linear regression of the data yields the relationship:

$$E_{s,a}(f_{P.t}) = 3.34\, f_{P.t} + 0.47 \qquad \text{Equation 39}$$

where $E_{s,a}(f_{P.t})$ is the apparent pseudo extinction coefficient ($x10^{11}cm^2$/cells) and $f_{P.t}$ is the fraction of *P. tricornutum* cells/Total cells in the suspension.

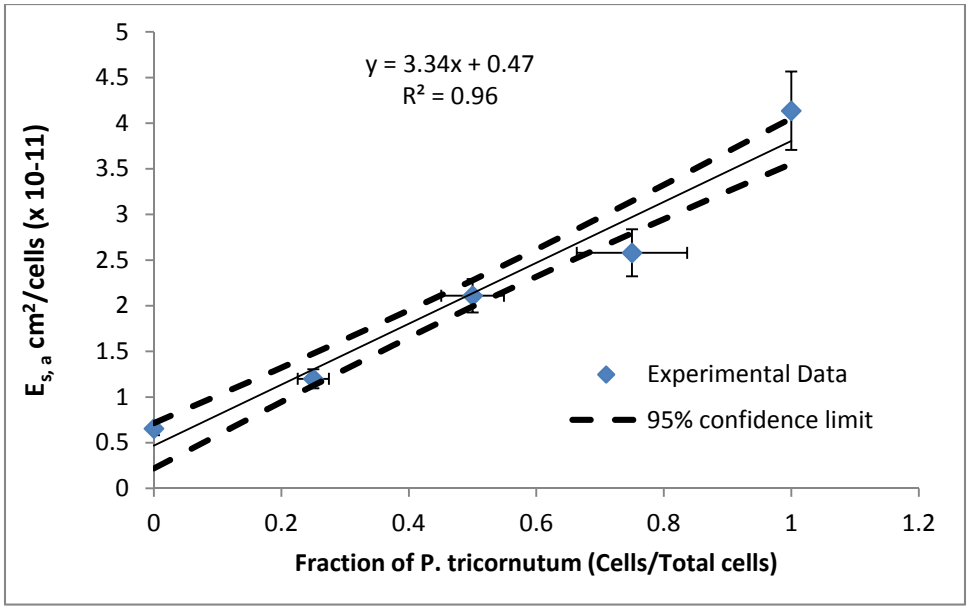

Figure 24: Pseudo extinction coefficients obtained through nonlinear regression for five combinations of *P. tricornutum* and *Nannochloris*. Error bars were determined using error propagation based on the uncertainty in the cell density determination and 95% confidence limits on the regression line are shown.

Equation 39, together with Equation 38 (G_{av} (X)), allows estimation of the average light intensity within the reactor as a function of the total biomass concentration and the fraction of *P. tricornutum* present in the culture. Thus, the effect of shading of one species by the other can be incorporated into the net specific growth rate through:

$$f_i(G_{av}) = \frac{G_{av}}{K_{G,i} + G_{av}}$$

And

$$\mu_i = \mu_{max,i} f_i(T) f_i(G_{av})$$

where the value of $K_{G,i}$ does not change between monocultures and co-cultures.

Calibration of the Allelopathic constant for *Nannochloris*

To calibrate the allelopathy constant, γ, under co-culture conditions, continuous, turbidostat reactor data was collected in an experiment operated under fluctuating temperatures. The experiment was initiated by growing *Nannochloris* in monoculture at 16°C (See Figure 25A). At time zero, *P. tricornutum* was inoculated into the reactor. Within the first 90 hours, *P. tricornutum* grew rapidly and displaced the *Nannochloris*. When the temperature was increased to 22°C, the trend continued; *P. tricornutum* continued to displace *Nannochloris*. This was expected since *P. tricornutum* grows faster than *Nannochloris* between 16 and 24 °C. After 150 hrs of operation, the *Nannochloris* cell density had dropped almost two orders of magnitude. The temperature was then increased to 30°C, which is near the optimum growth temperature for *Nannochloris*. The *Nannochloris* population responded to favorable temperature conditions as the growth rate increased dramatically. In contrast, *P. tricornutum's* population started to decline rapidly, at an even faster rate than dictated by the dilution rate. This implies that the *P. tricornutum* decay rate exceeded the growth rate during this phase of operation; the overall net growth rate was negative. It is also important to note that the maximum temperature reached in the turbidostat reactor was 30°C, which falls outside the range of the temperature model presented in Equation 24 (T_{sup} for *P. tricornutum* is 27.5°C). Net specific growth rates measured in *P. tricornutum* monoculture batch reactors for temperatures in excess of T_{sup} were -0.23, -0.20, and -0.22 day^{-1} at 34, 37.5 and 41°C, respectively (See Table 13 in Appendix).

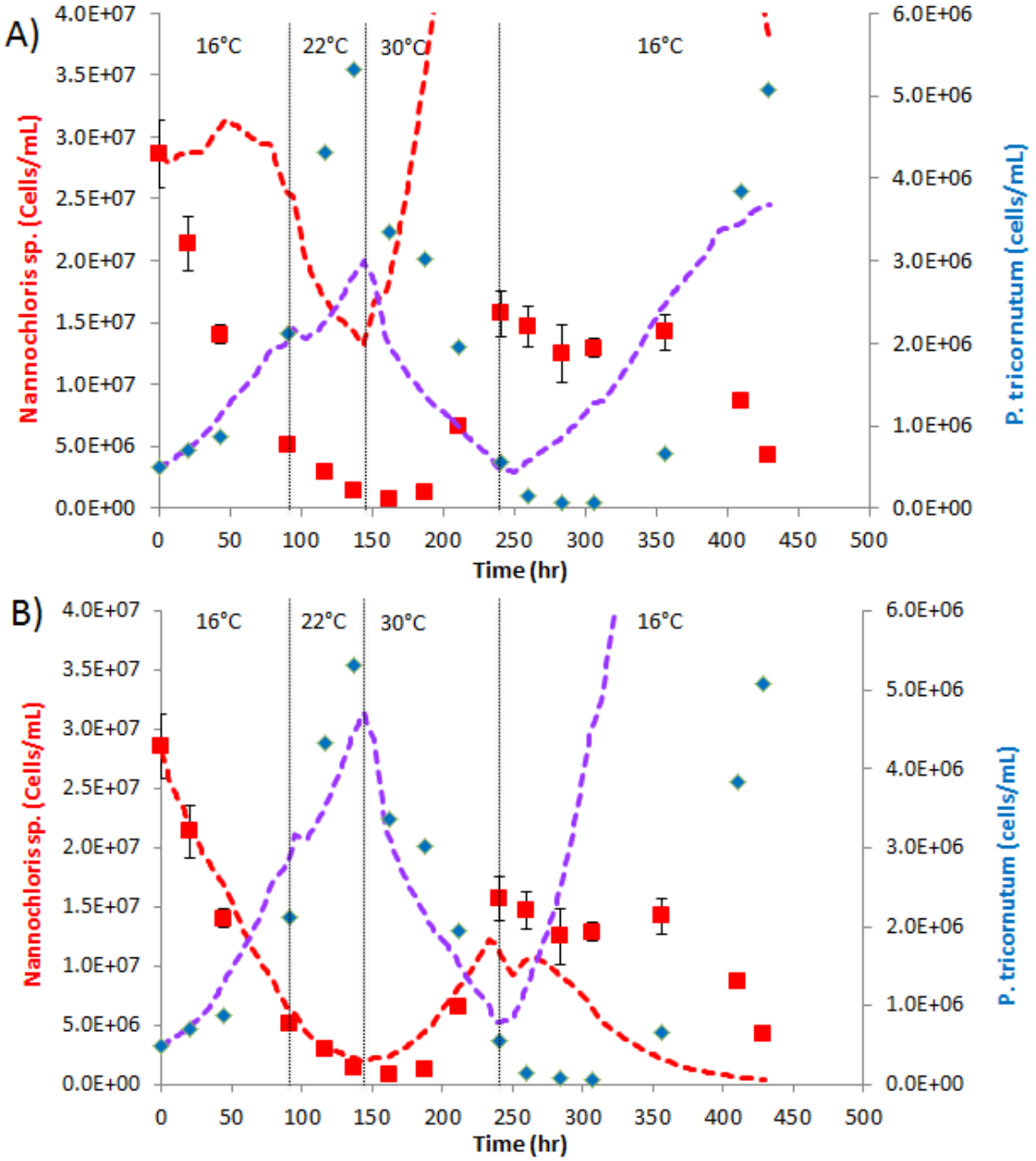

Figure 25: *Nannochloris* and *P. tricornutum* grown in a turbidostat with temperatures fluctuating between 16 and 30°C. Dotted lines represent the model simulation without lag time. A) Without an allelopathic term included, and B) with an allelopathic term. Black lines are used to identify the times when the reactor temperature was set to a new value. Red and blue data points refer to *Nannochloris* and *P.tricornutum*, respectively.

Figure 25A and 25B also present model simulations for both algae species with and without the incorporation of the allelopathic term in equation 34 for *Nannochloris* sp. The importance of allelopathy is demonstrated by the differences in the model results shown in these figures. The model without the incorporation of allelopathy fails to describe the cell density profiles for either species (Figure 25A). Nannochloris cell densities are overestimated throughout the experiment. As a result, *P. tricornutum* cell densities are underestimated because co-shading by *Nannochloris* has a significant impact on *P. tricornutum* growth. Incorporation of allelopathy yields significant improvements in the model simulation.

The only inputs for the model were dilution rate (D), initial biomass concentration for both species and temperatures. In both graphs, the model utilized an average decay rate of -0.22 day^{-1} for *P. tricornutum* at 30°C based on the results of the monoculture growth rate experiments. However, it can be observed that after the temperature change from 30 to 16°C at 240 hours, the model fails to predict the behavior of both microalgae populations. An apparent lag time of 48 hours was observed before *P. tricornutum* responded to the change to favorable temperature conditions. Lag times in response to a change to more favorable environmental conditions after a "shock" is relatively common in biological systems (Rao and Engelberg, 1965; Araki, 1991); however, it is species dependent. For temperature fluctuations, Rutter and Nedwell (1994) described the temperature perturbation in terms of a temperature challenge index ($\Delta T/dt$), and they showed that the speed of response to an environmental change is related to the temperature challenge index. These results imply that the lag time observed in the turbidostat experiment for the algae co-culture (48 hours for a change in temperature of 14°C over a 1 hour period in this case) is dependent on the duration and magnitude of the

temperature change. The researchers also showed the importance of incorporating the lag time into modeling efforts that describe the outcomes of competition in variable environments.

To improve the model fit, a lag time of 48 hrs was incorporated into the response of *P. tricornutum* growth rates to the 14°C step change in temperature. Figure 26 shows the model calibrated with the allelopathic term together with the 48 hour lag time.

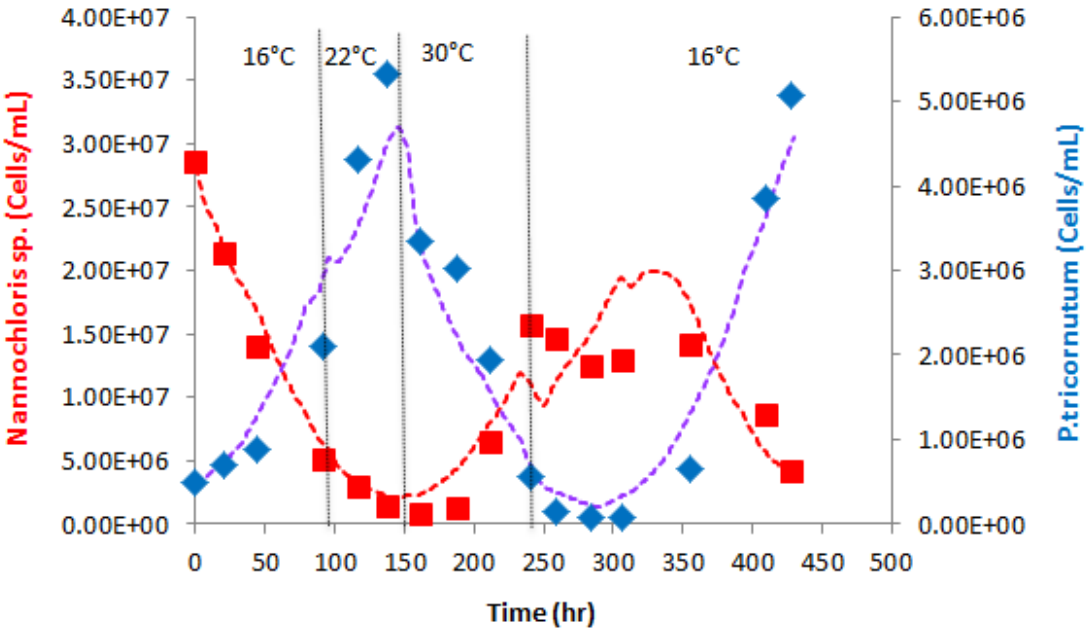

Figure 26: *Nannochloris* and *P. tricornutum* grown in a turbidostat with temperatures fluctuating between 16 and 30°C. Dotted lines represent the model simulation with the allelopathic term and a lag time included. Black lines are used to identify the times when the reactor temperature was set to a new value. Red and blue data points refer to *Nannochloris* and *P.tricornutum*, respectively.

The allelopathy constant (γ) described in equation 34 was determined by minimizing the sum of the squares of the error between the model (which also incorporates the 48hr lag time) and the turbidostat data. The value of the allelopathy

constant was $2.2x10^{-14}$ $ml^2day^{-1}cells^{-2}$ with a 95% confidence interval of ± 0.71 $x10^{-14}$ $ml^2day^{-1}cells^{-2}$. The confidence interval was calculated following the method used by Wahman, (2006). A summary of all other model parameters used in the simulations are shown in Table 11.

Table 11: Parameters used in model simulations of dynamic growth in Turbidostat and Chemostat Experiments

Model Parameters	*P. tricornutum*	95% C.L	*Nannochloris* sp.	95% C.L
μ_{max} (1/days)	3.07	±2.1	3.72	±4.6
K_g (μmol/m^2-s)	180.6	±209.7	456.5	±770.2
K_T	2.98	±0.97	1.46	±0.81
T_{sup} (°C)*	27.50	NA	41.00	NA
T_{inf} (°C)	0.00	±34.8	8.78	±4.9
T_{opt} (°C)	25.36	±0.87	28.75	±2.9
γ ($ml^2day^{-1}cells^{-2}$)**	NA	NA	$2.2x10^{-14}$	$\pm 0.71x10^{-14}$

*T_{sup} were not fit to the data. It was directly estimated by the growth experiments.
**All values except γ were determined from monoculture experiments (see Chapter 4)

The model fit in Figure 26 represents the behavior of both species especially for the first 200 hours of the experiment. However, differences between the model simulation and the *Nannochloris* data are apparent between 250 and 350 hrs. The inability of the model to match the data in this range may be related to the decrease in the dilution rate between 150 to 200 hrs and the accumulation of dead *P. tricornutum* cells which contribute to turbidity. Since *P. tricornutum* creates more turbidity per cell than *Nannochloris*, when *P. tricornutum* stops growing at high temperature and *Nannochloris* is growing, the dilution rate decelerates considerably (See Figure 29). At the same time, the decay of *P. tricornutum* cells at 30°C and minimal dilution required to maintain constant turbidity, lead to accumulation of dead *P. tricornutum* cells which causes additional co-shading effects that are not taken into account by the model. The model

only accounts for living, fluorescent cells (the cells counted by the flow cytometer). As a result, the model overestimates the *Nannochloris* growth rate over this time period.

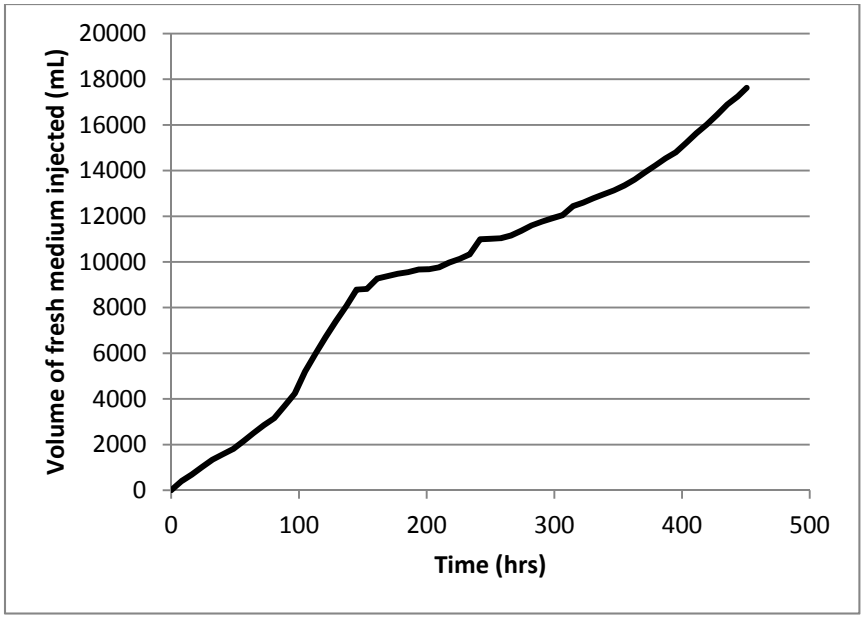

Figure 27: Fresh medium injected during the turbidostat co-culture experiment. The slope of the line represents the dilution rate at a given point in time during the experiment.

Model validation in a chemostat co-culture

To avoid varying dilution rates and the possible accumulation of dead cells in the system, a chemostat experiment was performed. Temperature changes were made at a constant frequency of 3 days, with a 12hr ramp and within a range of 17 to 28°C. Within this temperature range, the net specific growth rate for *P. tricornutum* remained positive throughout the experiment. The data shown in Figure 28 exhibits the same general behavior for both species as observed in the turbidostat experiment; at low temperature *P. tricornutum* displaces *Nannochloris* whereas at higher temperatures *Nannochloris* displace *P. tricornutum*. It is clear that at these temperature fluctuation conditions,

Nannochloris sp will dominate the system in the long term. The dotted lines represent model simulations for inputs of dilution rate, initial biomass concentrations and temperature. A lag time in the response of *P. tricornutum* to temperature changes was also included; however, in this case, the lag time was reduced to 36 hrs, 40% lower than

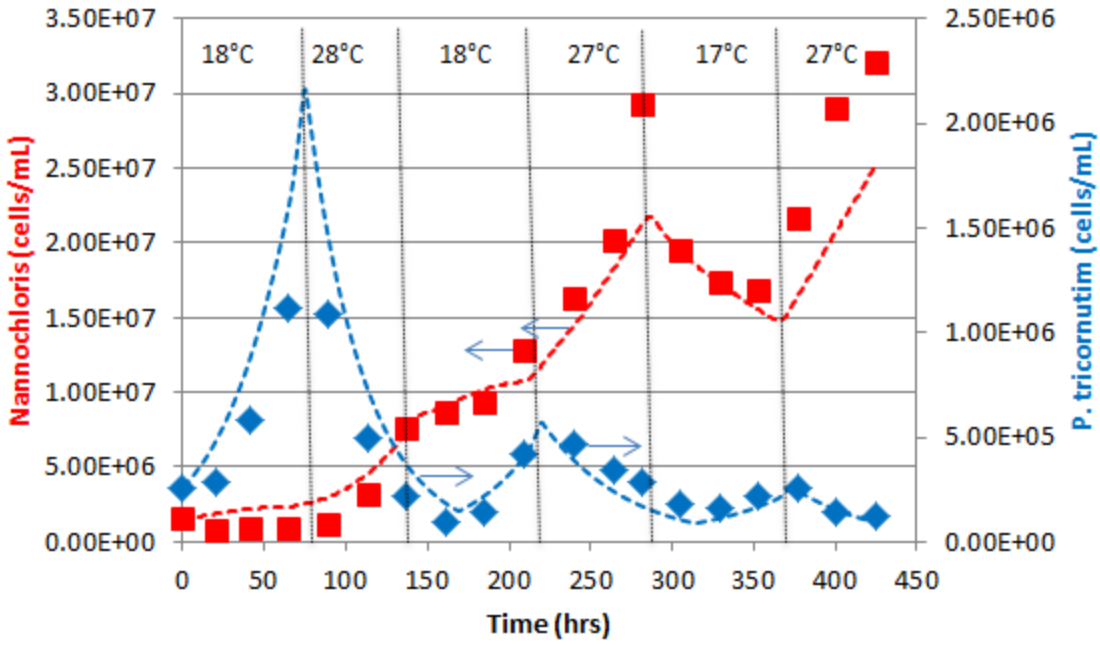

Figure 28: *Nannochloris* and *P. tricornutum* growth in a chemostat under cyclical temperature variation (temperatures were alternated between 18±1 and 28°±1C every three days. Black dotted lines are used to identify the times when the reactor temperature was set to a new value.

in the turbidostat experiment, since the ΔT in this experiment is approximately 40% lower. All other model parameters were as previously determined and are presented in Table 11. It can be seen that the model follows the expected trends based on the temperature optimums of each microalgae species. *P. tricornutum*'s population increases when growing at low temperature and decreases when growing at high temperature. However, due to its long lag time relative to the frequency of temperature fluctuations, *P.*

tricornutum cannot recover its original cell numbers before the next temperature change. *Nannochloris*, on the other hand has no significant lag time and can grow reasonably well within the temperature ranges tested.

The model provides a reasonable fit to the data especially for *P. tricornutum.* For *Nannochloris*, the model fits the data well for the first 300 hours of the experiment. However, the model tends to underpredict the peak *Nannochloris* cell concentration at 27°C which is near the optimal temperature for *Nannochloris* growth. This result suggests that the model overpredicts the allelopathic effect in the chemostat and that the response of *Nannochloris'*s growth rate to the presence of low cell densities of *P. tricornutum* is different than at higher densities.

CONCLUSIONS

In this chapter, a model that describes the population dynamics of both microalgae species grown in co-culture as a function of average light, temperature and allelopathy interaction was calibrated and validated by using continuous cultures.

The growth model developed in Chapter 4 was the basis for the model developed in this chapter. However two parameters had to be incorporated in order to describe the co-culture system: 1) the apparent pseudo extinction coefficient, which is a function of the relative amounts of *P. tricornutum* and *Nannochloris* sp. present in the culture and 2) an allelopathic interaction term.

The apparent extinction coefficients were estimated by measuring the average light intensities at different biomass concentrations and ratios of both species. A formulation to calculate the apparent pseudo extinction coefficient was based on these measurements.

During the batch culture experiments it was possible to observe that *P. tricornutum* exhibits an inhibitory effect on the growth of *Nannochloris*, possibly caused by the excretion of secondary metabolites into the growth medium. In order to incorporate these effects on the model, a turbidostat experiment was employed to calibrate the allelopathic term. Finally, a chemostat experiment was used to validate the model developed in this work. It was observed that the model predicted reasonably well the behavior of both microalgae populations under temperature fluctuations.

This work, can serve as a framework to calibrate and develop models capable of describing the behavior of individual microalgae species in co-cultures subject to temperature fluctuations and cell densities relevant to mass culturing operations.

Chapter 6: Conclusions

The objective of this study was to examine and model the factors affecting microalgae production at concentrations and environmental conditions expected in mass culturing operations. These effects were examined using two representative microalgae species *Nannochloris sp* (UTEX LB1999 and UTEX 1999.) and *Phaeodactylum tricornutum* (UTEX 646) that varied with respect to optimal temperature range, size and pigmentation. Experiments were conducted to isolate the effects of temperature, DIC concentration and light penetration in monoculture and to examine the effects of temperature, light and allelopathy in co-cultures of these species. Batch and turbidostat data were used to calibrate a microalgae productivity model, and a final chemostat experiment was used to validate the model.

In Chapter 3, a series of experiments were carried out to isolate the effects of temperature and DIC concentration on the specific growth rate of *Nannochloris* sp. These effects were examined at conditions that simulate enriched-CO_2 culture operations. The main findings of this phase of the research were:

- Increasing temperatures resulted in higher growth rates of *Nannochloris*, at a given DIC concentration, a finding that has been identified in numerous studies and was confirmed in this research.
- An optimal DIC concentration of approximately 3 mM was identified for *Nannochloris* sp. that was independent of temperature from 25 to 35°C. This result has been masked in studies that have failed to isolate the effects of temperature and DIC and suggests that at elevated temperatures, it would be necessary to increase the gas-phase CO_2 partial pressure to maintain the DIC concentration at a desired set point.

In Chapter 4, monoculture experiments were performed at ambient pCO_2 levels to elucidate the impact of self-shading effects and temperature on the growth rate of two microalgae species (*Nannochloris* sp. UTEX 1999. and *P. tricornutum* UTEX 646). The data was used to develop a model that describes microalgae growth rates as a function of temperature and average light intensity in the reactor. The key findings are as follows:

- Based on the batch reactor growth curves, self-shading effects play an important role in limiting the growth of microalgae cultures at biomass concentrations relevant to commercial culturing operations.
- The effects of temperature on the growth rates of each microalgae species in monoculture conditions were well described by a model developed by Lehman (1975).
- The two microalgae species used in this study had different growth responses to temperature. The range of growth for the *P. tricornutum* and *Nannochloris* extended from 15 to 27°C and 20 to 35°C, respectively. The overlap in their growth profiles extends the temperature range suitable for growth from approximately 15 ºC to 35 ºC. These two species can potentially be used in culture systems located in geographical regions where temperatures fluctuate within this range.
- The average light intensity in the reactor was observed to be a function of biomass concentration as well as a species dependent pseudo extinction coefficient. A mathematical expression was developed to estimate the average light intensity inside the reactor as a function of these two parameters. *Nannochloris* was observed to absorb less light than *P. tricornutum* at the same cell density.

- A multiplicative model that describes growth rate as a function of average light intensity was developed and calibrated using the growth rates measured over a range of temperatures and average light intensities.

In Chapter 5, a dynamic model was developed that describes the behavior of the two microalgae cultures grown together in the same medium as a function of temperature and average light. The most important outcomes of this phase of research are described below:

- Based on batch culture experiments, *P. tricornutum* was found to have an allelopathic effect on the growth of *Nannochloris*, possibly caused by the excretion of secondary metabolites into the growth medium.
- The average light intensity inside the reactor was found to be a function of the relative proportions of *Nannochloris* and *P. tricornutum* in the medium and the biomass concentration. The relationship between the proportions of each algae species present and light intensity was used to determine an apparent extinction coefficient.
- The growth model developed in Chapter 4 was modified to incorporate the apparent extinction coefficient and an allelopathic term. The calibrated model was able to describe the population dynamics of both microalgae species as a function of temperature, average light intensity and allelopathy.
- The model successfully predicted the population dynamics of *Nannochloris* and *P. tricornutum* grown in a continuous reactor subject to temperature fluctuations. The only inputs to the model were the initial biomass concentrations and two key operating parameters: dilution rate and temperature. However, the model tended to underestimate *Nannochloris* cell densities at the end of the experiment, which

suggests that the response of *Nannochloris* to the presence of *P. tricornutum* needs further investigation.

The model developed in this work can serve as a basis to explore the possible productivities of mono and co-cultures that are subject to temperature fluctuations. This work proves that the population dynamics of different microalgae species in the same culture can be modeled and predictions of their behavior can be made under different environmental conditions. The factors that must be considered in such a multispecies system include not only temperature, but also the light co-shading effects and potential allelopathic interactions between the microalgae species present.

While the results of this research have highlighted the importance of temperature, DIC, light and allelopathy, additional research into a variety of mixed microalgae systems would be useful to better understand their performance under more complex conditions. For instance, it is possible that different microalgae species will have different growth responses to increases in DIC concentration, and therefore the addition of CO_2 into mixed microalgae cultures will potentially produce changes in the composition of the community. Therefore, understanding how DIC concentrations affects microalgae communities in mass culturing operations would be an important next step in the design of multispecies production systems.

Furthermore, based on the confidence limits obtained for the light half saturation constant (K_G) for both species, further experiments to measure growth rates at different light intensities over a range of temperatures are needed to refine the values obtained for these model parameters.

Also, further work is needed to better understand the interactions within different microalgae species if co-cultures are to be used extensively for mass producing microalgae. For example, in depth understanding of the allelopathic interactions observed

between certain microalgae species is key to engineer co-culture systems. The best approach would be to understand the chemical basis of the interaction, the rate at which the allelochemicals are produced and how they affect the receptor species.

Appendix A

CHAPTER 3

Table 12: Summary of experiments: Temperature, alkalinity, pH, calculated DIC and specific growth rate measured for each condition.

Temperature (°C)	Experiment number	Alkalinity (meq)	pH	DIC (mM)	μ (1/day)
15	5	4.4	8.4	1.4	0.31
	5	4.6	6.9	4.8	0.48
	5	4.7	6.5	5.8	0.50
	6	5.2	7.0	5.3	0.58
	7	4.9	8.2	2.5	0.47
	8	5.2	7.9	3.7	0.51
25 (Nitrogen limited)	1	3.1	7.9	0.9	0.25
	2	4.7	6.8	4.8	0.35
	2	4.2	8.1	1.3	0.29
25	3	5.2	8.4	1.3	0.35
	2	4.2	8.1	1.3	0.38
	3	5.2	6.8	5.3	0.79
	3	5.2	6.6	5.8	0.66
	6	5.2	6.6	5.8	0.67
	7	4.8	7.9	2.5	0.85
	8	5.2	7.7	3.4	0.95
	8	4.9	8.4	1.1	0.33
35	4	5.0	8.1	1.2	0.44
	4	5.0	6.6	5.2	0.97
	4	5.1	6.4	5.9	0.84
	7	5.1	8.0	1.6	0.67
	9	5.2	7.6	2.9	1.16
	9	5.3	7.3	3.9	1.04

Table 13: *Nannochloris* growth rate measured in batch at different temperatures.

Nannochloris sp.		
Exp ID	**T (°C)**	**μ (1/day)**
NTemp1 Batch	12	0.00
	17	0.07
	22	0.23
	33	0.23
	37	0.16
	41	0.00

Table 14: *Phaeodactylum tricornutum* growth rate measured in batch at different temperatures.

Phaeodactylum tricornutum		
Exp ID	**T (°C)**	**μ (1/day)**
PTemp1 Batch	14	0.23
	19	0.30
	23.5	0.31
	26.5	0.28
	34	-0.23
	37.5	-0.20
	41	-0.22

Table 15: *Nannochloris* growth rate measured in continuous culture at different temperatures.

Nannochloris sp.		
Exp ID	**T (°C)**	**μ (1/day)**
NTemp1	17	0.69
	20	0.73
	24	0.92
	26	1.00
	22	0.83
	16	0.46
NTemp2	28	0.93
	28	0.94
	30	0.84
	34	0.68
	36	0.46
N35	22	0.60
	35	0.77
	15	0.41
N15FTU	17	0.60
	22	0.68

Table 16: *Phaeodactylum tricornutum* growth rate measured in continuous culture at different temperatures.

Phaeodactylum tricornutum		
Exp ID	**T (°C)**	**μ (1/day)**
PTemp1	17	0.94
	14	0.70
	20	1.18
	23	1.16
	26	0.94
	26.5	0.64
	27	0.09
	28	0.00

Table 17: *Phaeodactylum tricornutum* grown at 17°C in continuous culture at different average light intensities (Gav)

***Phaeodactylum tricornutum* grown at 17°C**			
Exp ID	**X (cells/mL)**	**μ (1/day)**	**Gav (μmol m^{-2} s^{-1})**
P15FTU(1)	7.60E+06	0.58	89.89
	5.97E+06	0.85	105.15
	2.95E+06	1.15	160.21
	5.75E+06	0.97	107.76
P15DIC2	6.47E+06	0.66	99.86
PEXP15-35	6.48E+06	0.95	99.76
P15Nitro	6.48E+06	0.99	99.76
	6.48E+06	0.95	99.76
	2.71E+06	1.33	167.57
	3.14E+06	0.96	155.00
PTemp1	5.42E+06	0.94	111.84

Table 18: *Phaeodactylum tricornutum* grown at 22°C in continuous culture at different average light intensities (Gav)

***Phaeodactylum tricornutum* grown at 17°C**			
Exp ID	**X (cells/mL)**	**μ (1/day)**	**Gav (μmol m^{-2} s^{-1})**
P22FTU1	5.61E+06	0.95	109.47
	4.19E+06	1.11	131.27
	5.06E+06	1.17	116.83
PTemp1	4.87E+06	0.99	119.70
P22FTU3	2.78E+06	1.20	165.30
	7.13E+05	1.75	263.95

Table 19: *Nannochloris* sp. grown at 17°C in continuous culture at different average light intensities (Gav)

Nannochloris sp. **grown at 17°C**			
Exp ID	**X (cells/mL0**	**μ (1/day)**	**Gav (μmol m^{-2} s^{-1})**
F15FTU	2.40E+07	0.61	139.18
	1.78E+07	0.51	164.36
N35	3.60E+07	0.41	108.37
NTemp1	1.25E+07	0.69	194.33
	2.00E+07	0.46	154.44
N17FTU2	6.66E+06	0.70	241.34
	1.62E+07	0.46	172.41
N28FTU1	1.87E+07	0.53	160.20

Table 20: *Nannochloris* sp. grown at 28°C in continuous culture at (Gav)

Nannochloris sp. **grown at 28°C**			
Exp ID	**X (cells/mL)**	**μ (1/day)**	**Gav (μmol m^{-2} s^{-1})**
NTemp1	2.41E+07	0.93	138.95
NTemp2	2.33E+07	0.94	141.40
N28FTU1	3.19E+06	1.39	279.40
	1.11E+07	1.29	203.78
	2.07E+07	0.95	151.30
	3.36E+07	0.69	113.16

Table 21: Summary of measured average light intensities for *Nannochloris* and *P. tricornutum* at various cell densities

P. tricornutum		*Nannochloris*	
X (cells/mL)	Gav (μmol $m^{-2}s^{-1}$)	X (cells/mL)	Gav (μmol $m^{-2}s^{-1}$)
1.40E+07	54.01	4.00E+07	102.45
8.00E+06	88.15	1.60E+07	176.55
2.80E+06	167.80	8.00E+06	226.49
3.90E+05	283.75	2.80E+06	280.33
8.00E+04	317.94	1.20E+06	301.51
0.00E+00	323.36	0	323.36

Table 22: Growth rates obtained for *Nannochloris* grown in different media (Fresh, half fresh and half spent by *P. tricornutum* and *Nannochloris*, spent medium by *Nannochloris* and *P. tricornutum*)

Condition	**μ (1/day)**	**SD**
Fresh Medium 1 (Fresh1)	0.67	0.02
Fresh Medium 2 (Fresh2)	0.65	0.03
Half fresh medium and half spent medium by *P. tricornutum* (NinP1/2)	0.69	0.01
Half fresh medium and half spent medium by *Nannochloris* (NinN1/2)	0.75	0.04
Spent medium by *P. tricornutum* (NinP)	0.43	0.04
Spent Medium by *Nannochloris* (NinN)	0.72	0.05

Table 23: Growth rates obtained for *Nannochloris* grown in a 96 well plate under a gradient of fresh to spent medium by *P. tricornutum* (Fresh/spent) amended with extra Fe (Fresh/spent+Fe).

NinP	Fresh/Spent		Fresh/Spent+Fe	
Fraction Spent/Fresh	μ (1/day)	Standard Deviation	μ (1/day)	Standard Deviation
0	0.32	0.01	0.33	0.01
0.1	0.34	0.01	0.34	0.01
0.2	0.32	0.00	0.34	0.01
0.3	0.32	0.00	0.33	0.01
0.4	0.31	0.01	0.33	0.00
0.5	0.31	0.01	0.32	0.01
0.6	0.30	0.02	0.33	0.01
0.7	0.30	0.02	0.30	0.00
0.8	0.30	0.01	0.30	0.00
0.9	0.28	0.01	0.28	0.03
1	0.28	0.01	0.29	0.00

Table 24: Growth rates obtained for *Nannochloris* grown in a 96 well plate (in quadruplicates) under a gradient of fresh to spent medium by *P. tricornutum* (Fresh/spent) amended with extra trace metals (Fresh/spent+TM).

NinP	Fresh/Used		Fresh/Used+TM	
Fraction Spent/Fresh	μ (1/day)	Standard Deviation	μ (1/day)	Standard Deviation
0	0.39	0.00	0.40	0.01
0.1	0.39	0.01	0.39	0.01
0.2	0.38	0.01	0.37	0.01
0.3	0.37	0.01	0.37	0.01
0.4	0.36	0.01	0.36	0.02
0.5	0.34	0.02	0.35	0.01
0.6	0.32	0.01	0.34	0.02
0.7	0.31	0.00	0.33	0.02
0.8	0.26	0.02	0.32	0.02
0.9	0.27	0.01	0.30	0.01
1	0.24	0.03	0.26	0.05

Table 25: Growth rates obtained for *P. tricornutum* grown in a 96 well plate (in quadruplicates) under a gradient of fresh to spent medium by *P. tricornutum*

PinP	Spent/Fresh	
Fraction Spent/Fresh	μ (1/day)	Standard Deviation
1	0.27	0.02
0.9	0.26	0.02
0.8	0.24	0.02
0.7	0.24	0.02
0.6	0.24	0.02
0.5	0.23	0.03
0.4	0.25	0.02
0.3	0.24	0.02
0.2	0.23	0.02
0.1	0.23	0.02
0	0.21	0.02

Table 26: Summary of measured average light intensity for different combinations of *Nannochloris* and *P. tricornutum* at various cell densities

100% *P. tricornutum*		75% *P. tricornutum* 25% *Nannochloris*		50% *P. tricornutum* 50% *Nannochloris*		25% *P. tricornutum* 75% *Nannochloris*		100% *Nannochloris*	
X (cells/mL)	Gav (μmol $m^{-2}s^{-1}$)	X (cells/mL)	Gav (μmol $m^{-2}s^{-1}$)	X (cells/mL)	Gav (μmol $m^{-2}s^{-1}$)	X (cells/mL)	Gav (μmol $m^{-2}s^{-1}$)	X (cells/mL)	Gav (μmol $m^{-2}s^{-1}$)
1.40E+07	54.01	1.33E+07	85.79	1.60E+07	81.05	1.60E+07	124.11	4.00E+07	102.45
8.00E+06	88.15	8.00E+06	117.46	8.00E+06	134.17	8.00E+06	182.08	1.60E+07	176.55
2.80E+06	167.80	2.80E+06	204.43	2.80E+06	220.62	2.80E+06	256.23	8.00E+06	226.49
3.90E+05	283.75	1.20E+06	259.58	1.20E+06	275.02	0.00E+00	323.36	2.80E+06	280.33
8.00E+04	317.94	0.00E+00	323.36	0.00E+00	323.36			1.20E+06	301.51
0.00E+00	323.36							0	323.36

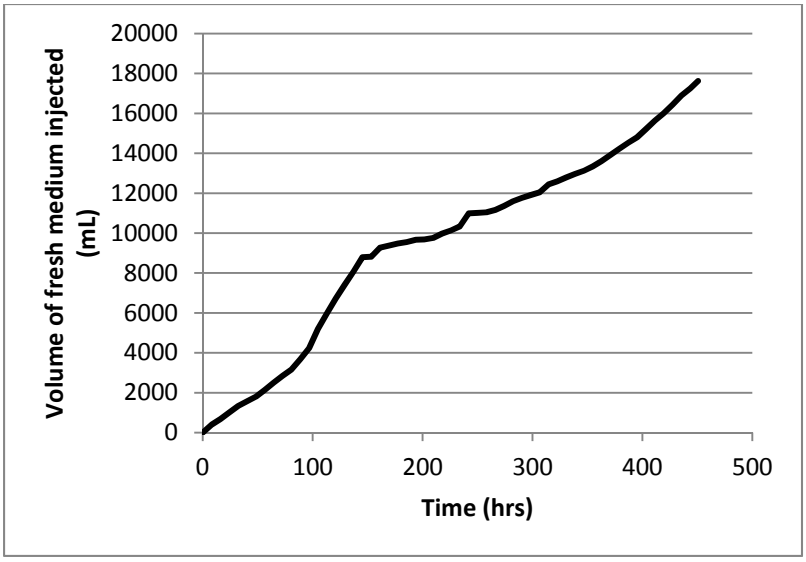

Figure 29: Fresh medium injected during turbidostat co-culture experiment. The slope of the line represents the dilution rate at a given point in time during the experiment. The slope as a function of time was used as an input for the dynamic model.

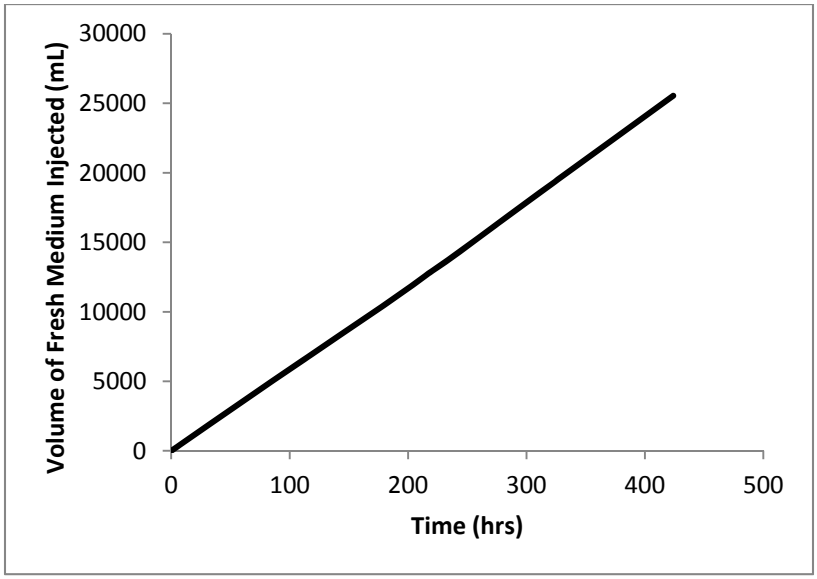

Figure 30: Fresh medium injected during chemostat experiment. The slope of the line represents the dilution rate at a given point in time during the experiment. The slope as a function of time was used as an input for the dynamic model.

Appendix B

EXTENDED METHOD FOR FLOW CYTOMETRY

Flow cytometry can be used to determine cell densities of microalgae cultures. It can also be used to quantify cell densities of different microalgae species within the same growth medium, as long as the different populations are distinctive in either of the following characteristics: Size, shape, pigments, or are capable of being stained with a fluorescent dye that stains differently depending on the characteristics of your populations. For example, Sytox Green dye can be used to stain cells that have a disrupted membrane, which usually indicates that the cells are no longer viable. In the case of microalgae, red fluorescence can be used to distinguish microalgae cells from the rest of the particles in the culture. Also, it is possible to distinguish between different microalgae species as long as they differ in cell size or red fluorescence intensity (different amounts and types of pigments in chloroplasts). For this work, a method to count cells in mono- and co-culture of *Nannochloris* and *P. tricornutum* using flow cytometry was developed:

First, if the sample to be measured was suspected to be higher than 4×10^6 cells/mL (in the case of *P. tricornutum*) the sample was diluted to one tenth of the concentration with fresh ASP medium (filtered with a 2μm syringe filter). This was done to make sure that the flow cytometry response remained in the linear range (see Figure 32). In the case of *Nannochloris* (Figure 33) there was no evidence of non-linearity up to 4×10^7, but if the cell concentration was suspected to be higher than that, was equally diluted to make sure that the concentrations were within the calibration curve.

Second, the sample was introduced in a falcon tube (BD Falcon polystyrene test tube, 12 x 75-mm, 352052) and 50μl of Accucount Fluorescent Particles (Spherotech Inc., Lake Forest, IL) were added to the sample to a final concentration of $5x10^4$ spheres

per mL. The tube was inserted to the sample port of the Fortessa (LSR Fortessa, BD Biosciences, San Jose, CA). Data was acquired until 200 spheres were counted. The flow velocity was set so that the instrument counted the 200 spheres in a span of about 1 minute. The number of cells were calculated using the following equation:

$$\frac{cells}{ml} = Cells\ counted\left(\frac{50{,}000}{200}\right) (10)$$

The data acquirement protocol was developed previously and saved in the instrument's computer in the FACSDiva software (version 6.1.3). It consisted of acquiring data for forward and side scattering, as well as on the red and green fluorescence channel. The filter used for red fluorescence was changed from the 605nm filter to the 670nm with a Long Pass filter, which needed to be physically changed every time. The acquirement setup can clearly be seen in Figure 31. The top three graphs from left to right show: 1) side vs forward scatter, 2) side scatter vs red fluorescence and 3) forward scatter vs red fluorescence. The second row of graphs from left to right show histograms for: i) forward scattering, ii) side scattering and iii) red fluorescence. Graph A) represents the red vs green fluorescence and B) a histogram of green fluorescence. On graph 2) and 3) it can be seen how both populations separate into two distinct groups, where *Nannochloris* is the population on the left (P2) and *P. tricornutum* is the population on the right (P6). The tables are the summary of the events that were acquired in that time. The spheres are counted as P1 in Graph A).

In order to make sure that the results obtained from the flow cytometer were reasonably accurate, a comparison was made between the flow cytometer results and a hemocytometer. Figures 34 and 35 show the comparison between the flow cytometer (FC) and the hemocytometer (HC) cell counts for *Nannochloris* and *P. tricornutum* respectively.

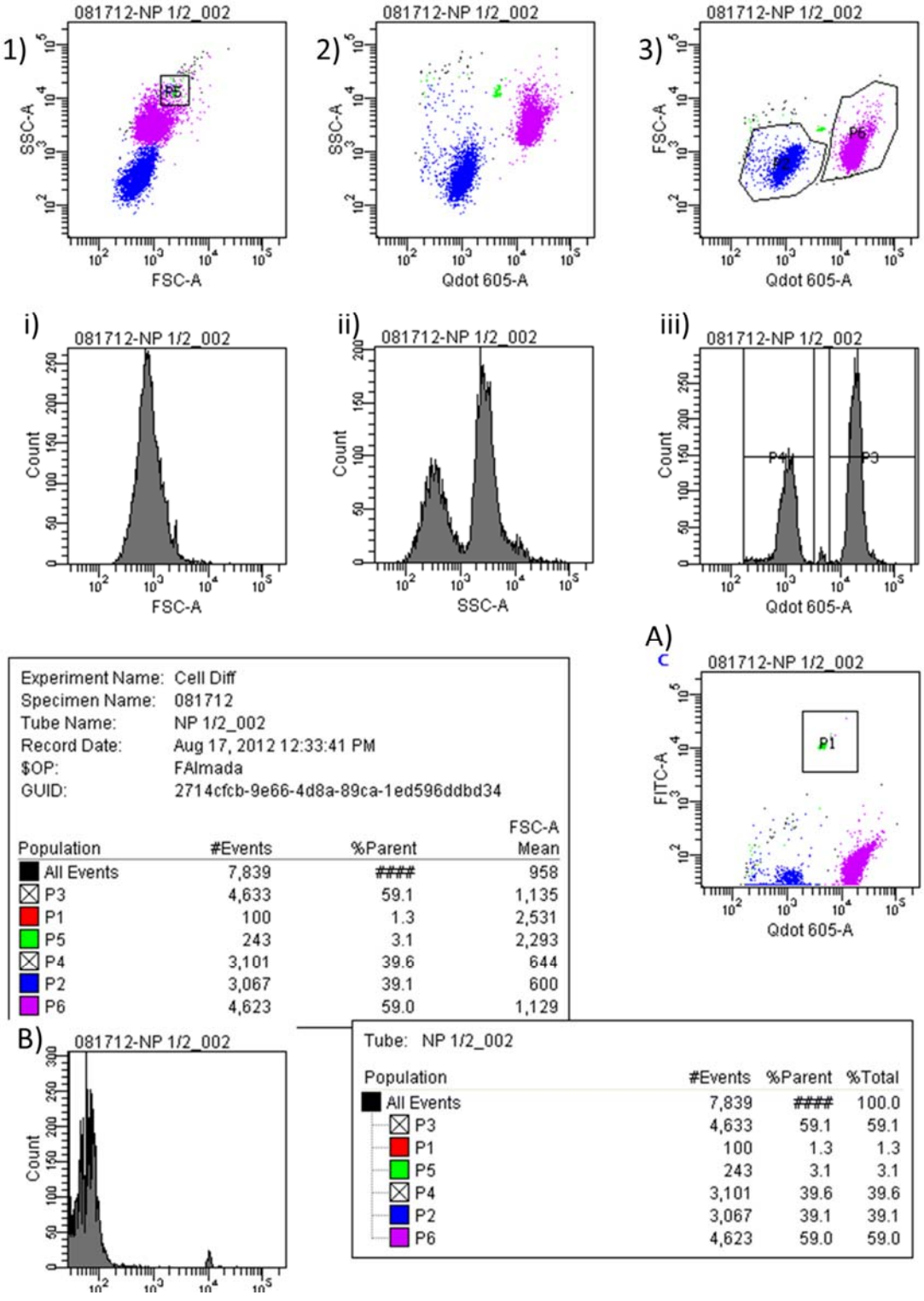

Figure 31: Example of flow cytometer data.

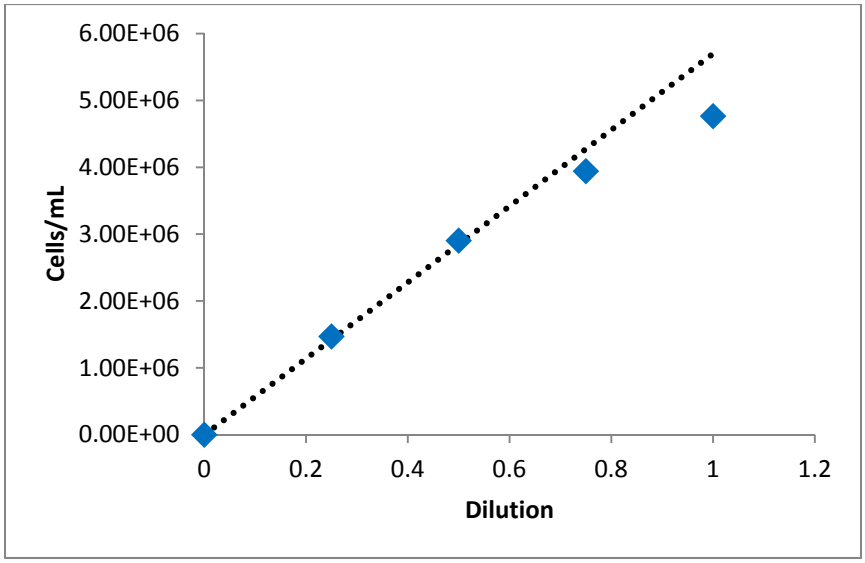

Figure 32: *P. tricornutum* cells/mL vs dilution determined by flow cytometry

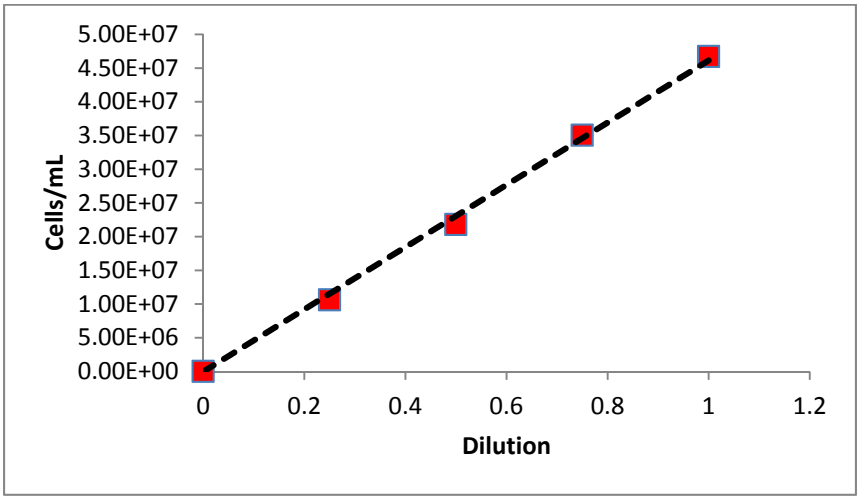

Figure 33: *Nannochloris* cell/mL vs dilution determined by the flow cytometry

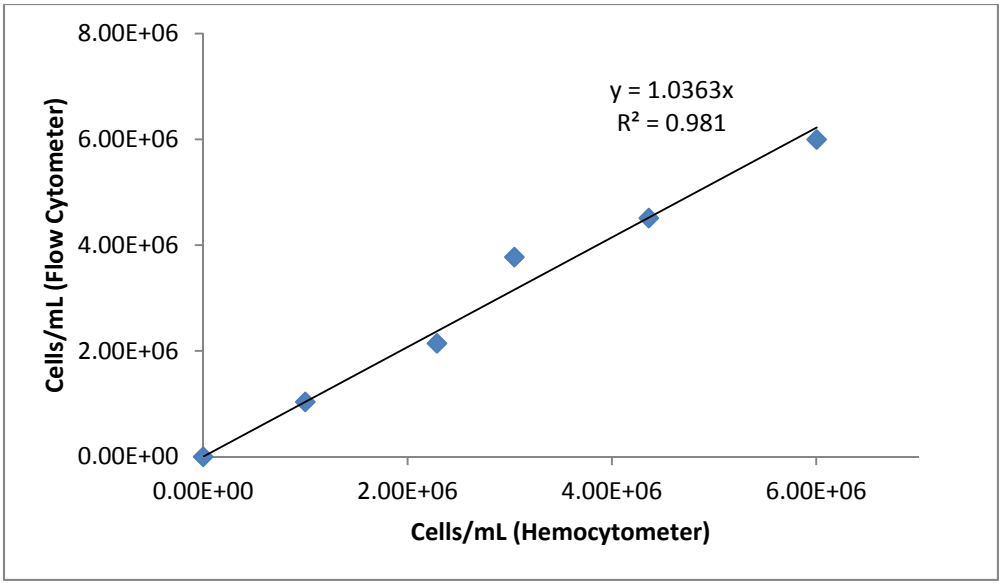

Figure 34: Comparison of *P. tricornutum* cells counted in flow cytometer and hemocytometer.

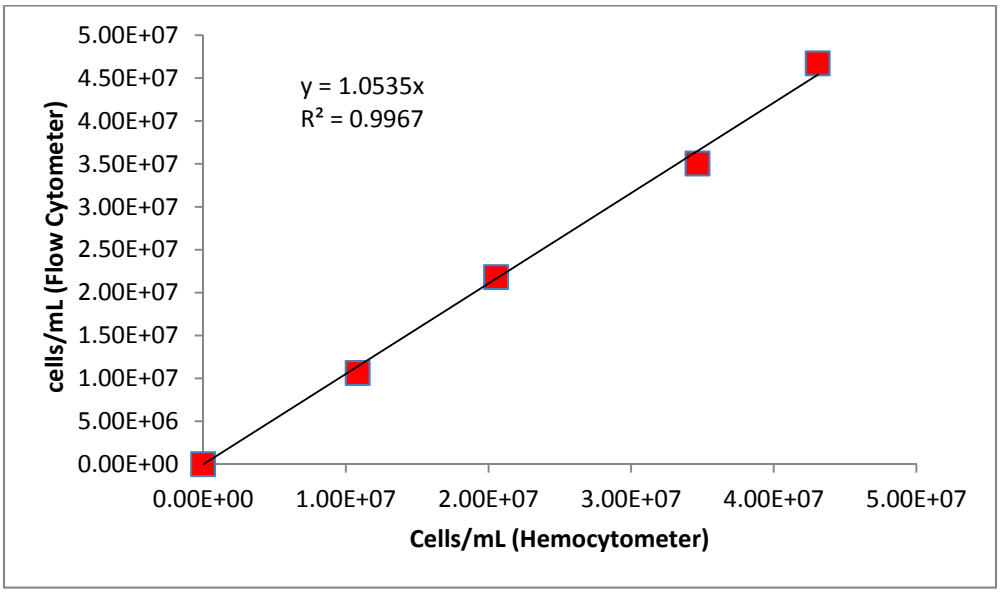

Figure 35: Comparison of *Nannochloris* cells counted in flow cytometer and hemocytometer.

LIGHT MEASUREMENTS

To measure the average light intensity inside the reactor as a function of biomass density and combination of *P. tricornutum* and *Nannochloris*, both species were grown in separate 2L bottles, sparged with air until they reached a biomass concentration of $4x10^7$ and $2x10^7$ cells/mL respectively. The cultures were used to make different blends of both microalgae, as seen in Table 26.

Table 27: Total cell concentrations of mixtures of *Nannochloris* and *P. tricornutum* for light penetration measurements.

Mixture	Total cells/mL
100% *P. tricornutum*	1.40E+07
75% *P. tricornutum* and 25% *Nannochloris*	1.33E+07
50% *P. tricornutum* and 50% *Nannochloris*	1.60E+07
25% *P. tricornutum* and 75% *Nannochloris*	1.60E+07
100% *Nannochloris*	4.00E+07

After the measurements were performed at each point in the reactor (7 points in both axis at 3 heights) for a given combination, the microalgae suspension was diluted to about half of the original concentration with water containing NaCl, $MgCl_2$ and $MgSO_4$ at the same concentration as ASP medium. Light inside the reactor was measured again in the same fashion and the suspension was diluted at approximately half the concentration. This was performed between 3 and 4 times, depending on the combination, so that light intensity curves as a function of total cell concentration were created for 5 different *Nannochloris* and *P. tricornutum* combinations. Examples of the light penetration profiles across the perpendicular and parallel axis (relative to the light source) of the reactor are depicted in Figure 36 and Figure 37.

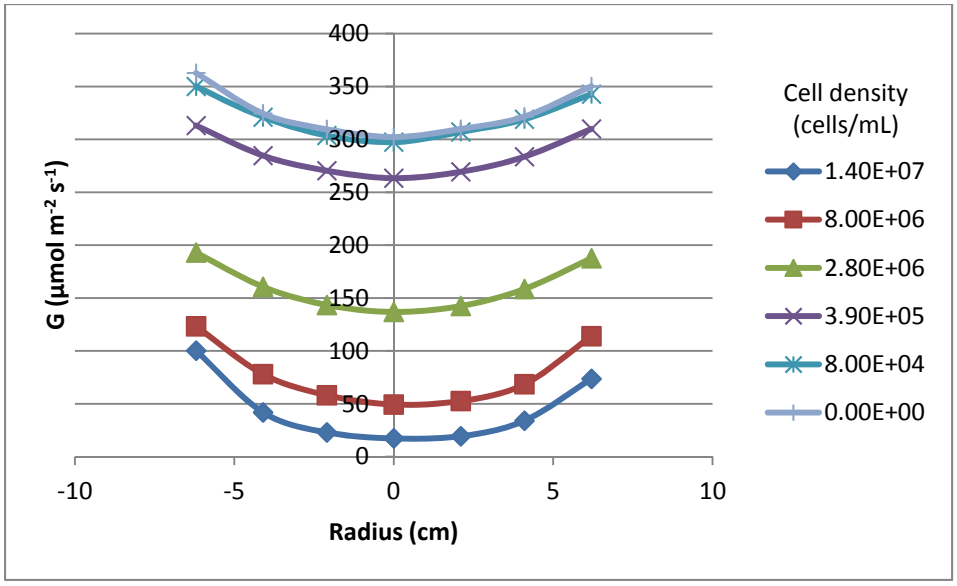

Figure 36: Light penetration profiles perpendicular to the light source at mid depth of a *P. tricornutum* suspension at various cell densities (cells/mL).

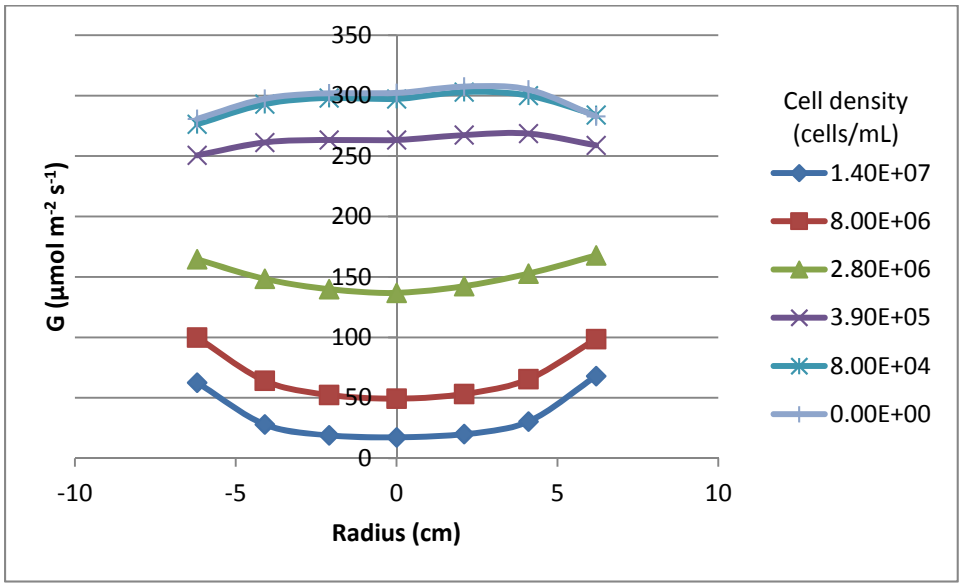

Figure 37: Light penetration profiles parallel to the light source at mid depth of a *P. tricornutum* suspension at various cell densities (cells/mL)

NUTRIENT LIMITATION EXPERIMENTS

In order to prove that at the conditions tested no nutrient limitation existed, two experiments were carried out at constant light intensity with *P.tricornutum* at varying concentrations of nitrate and phosphorus. The results are shown below:

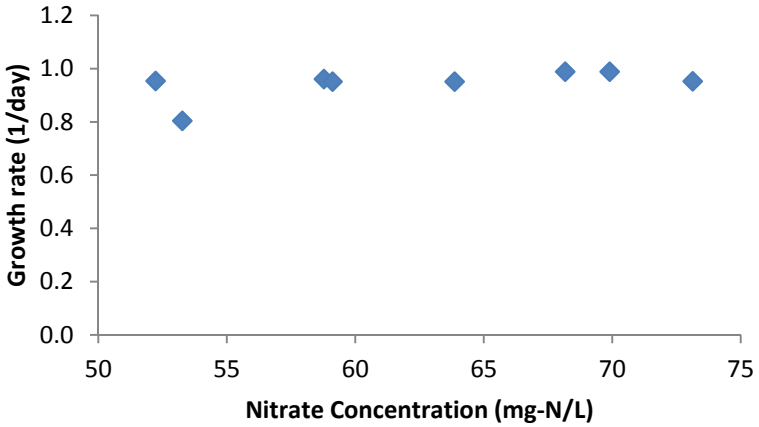

Figure 38: *P. tricornutum* grown in turbidostat at varying nitrate concentrations and constant biomass concentration ($6.5x10^6$ cells/mL).

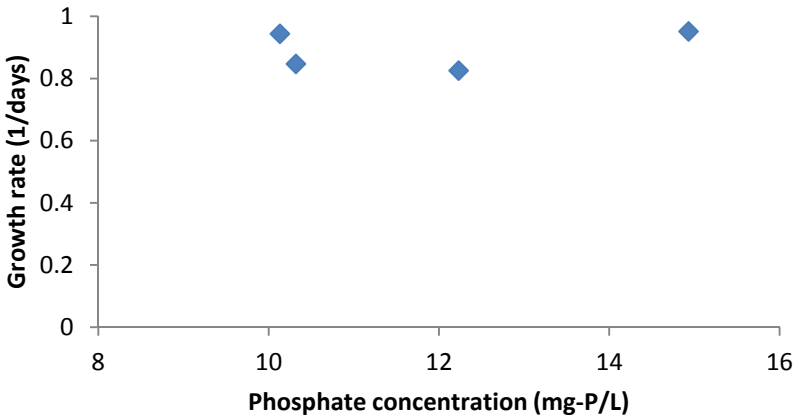

Figure 39: *P. tricornutum* grown in turbidostat at varying phosphate concentrations and constant biomass concentration ($4.9x10^6$ cells/mL).

It is clear that between the concentrations of N and P tested, growth was not a function of nutrient concentrations. Also, according to several authors, the typical half saturation constants of microalgae for nitrate and phosphate are in the range of 0.1mg/L (Halterman and Toetz, 1972; Auer and Canale, 1982). In this work, the initial nitrate and phosphate concentration were 70mg/L and 12.4 mg/L, respectively (more than 100 fold over the Ks values).

DYNAMIC MODEL METHOD

Euler's method was used to numerically solve the dynamic model employed in Chapter 5. The model consisted in the following mass balance on the cells for both microalgae species:

$$\frac{dX_N}{dt} = \mu_N X_N - D_t X_P - \gamma {X_N}^2 X_P$$

$$\frac{dX_P}{dt} = \mu_P X_P - D_t X_P$$

$$\mu_i(T, G_{av}) = \mu_{max,i} f_i(T_t) f_i(G_{av})$$

where X_N, and X_P are the biomass concentrations for *Nannochloris* and *P. tricornutum* respectively (cells/mL), D is the dilution rate (1/day), μ_i is the specific growth rates for each species (1/day), γ is the allelopathic term ($mL^2 cells^{-2} day^{-1}$). $f_i(T)$ and $f_i(G_{av})$ are the models developed in Chapter 4 that describe growth as a function of temperature and average light intensity respectively.

The model needs Temperature (T) and dilution rate (D) as inputs, which are a function of time, as well as the initial biomass concentrations ($X_{N,0}$ and $X_{P,0}$). Discrete data points of T and D at each time from the experimental conditions were used to solve the model:

$$T_t = f(t) \; and \; D_t = f(t)$$

At the initial conditions, it is possible to calculate the specific growth rate expected at t=0 for both microalgae species ("i"):

$$\mu_{i,0}(T_{t=0}, G_{av,t=0}) = \mu_{max,i} f_i(T_{t=0}) f_i(G_{av,t=0})$$

$G_{av,t=0}$ is calculated with the initial biomass concentrations of both microalgae species using Equation 38. The biomass concentration at the next point in time was calculated by using the initial growth rate $\mu_{i,0}(T_{t=0}, G_{av,t=0})$, the initial biomass concentrations, the dilution rate at t=0 ($D_{t=0}$), and Δt. A time step of 0.0417 days was chosen to perform the method (Δt=0.0417). Here is the example for Nannochloris:

$$\Delta X_N = (\mu_{i,0}(T_{t=0}, G_{av,t=0}) X_{N,0} - D_{t=0} X_{P,0} - \gamma {X_{N,0}}^2 X_{P,0}) \Delta t$$

$$X_{N,t=0.0417} = X_{N,t=0} + \Delta X_N$$

The same method was used to calculate the biomass concentration of *P. tricornutum* at the next Δt. The method was carried out in Excel and the biomass obtained for each time step was plotted to compare the model with the data.

Chapter 3

The following figure describes the general features of the turbidostat reactor used in the experiments performed in Chapter 3:

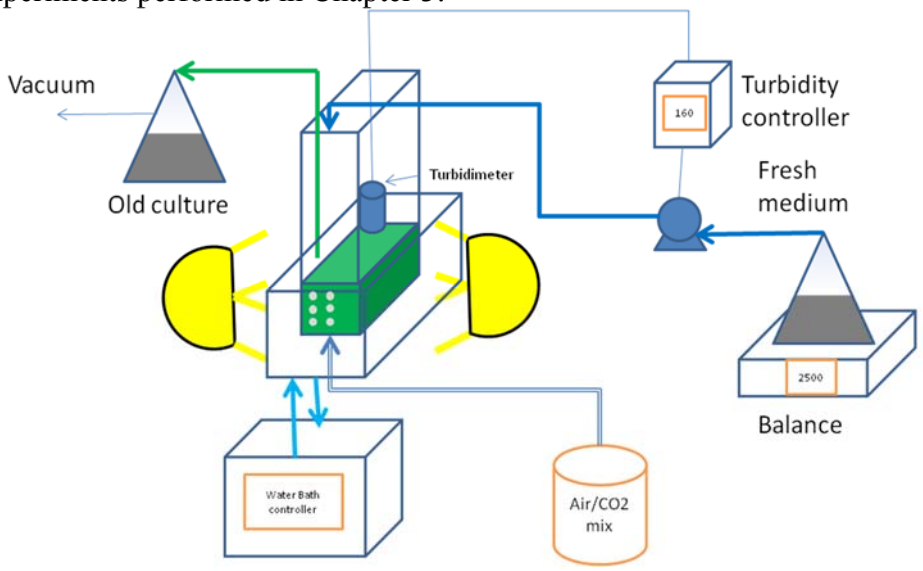

Figure 40: Turbidostat reactor setup for experiments performed in Chapter 3

Fresh medium was injected to keep the turbidity at set point of 150FTU. The amount of medium injected was recorded every few hours manually by reading the weight on a balance. The weight vs time data was used to calculate the dilution rate of the system.

Chapter 4 and 5

The following figure describes the general features of the turbidostat reactor used in the experiments performed in Chapters 4 and 5:

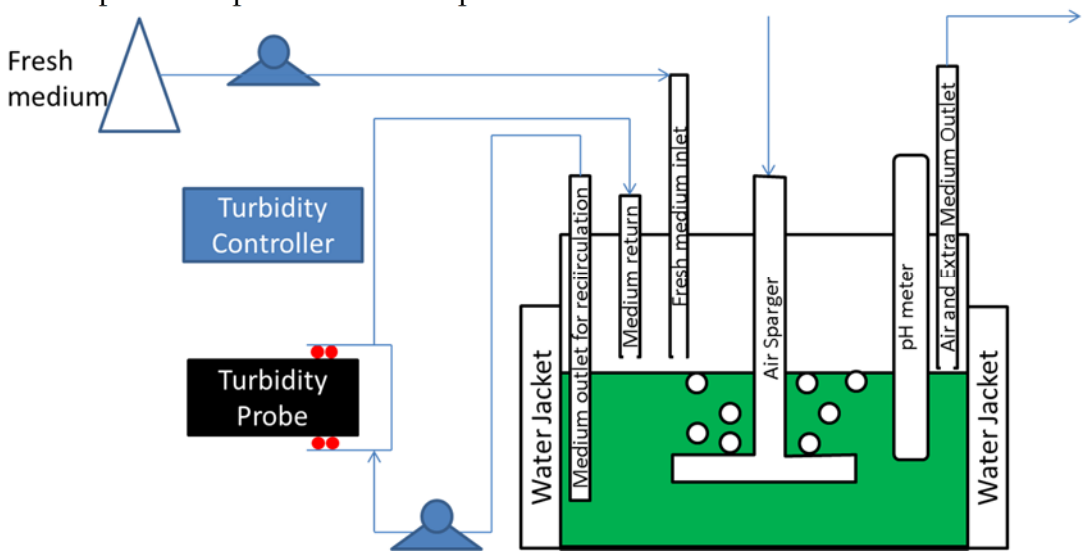

Figure 41: Turbidostat reactor setup for experiments performed in Chapters 4 and 5

Fresh medium was injected to keep the turbidity at a certain set point. The amount of medium injected was recorded every 60s by the use of a balance connected to a computer. The data was recorded in a text file which was later transferred to an excel file. Only data points for every 3 hours were used to calculate dilution rates. An example of volume of medium injected vs time is shown in Figure 42.

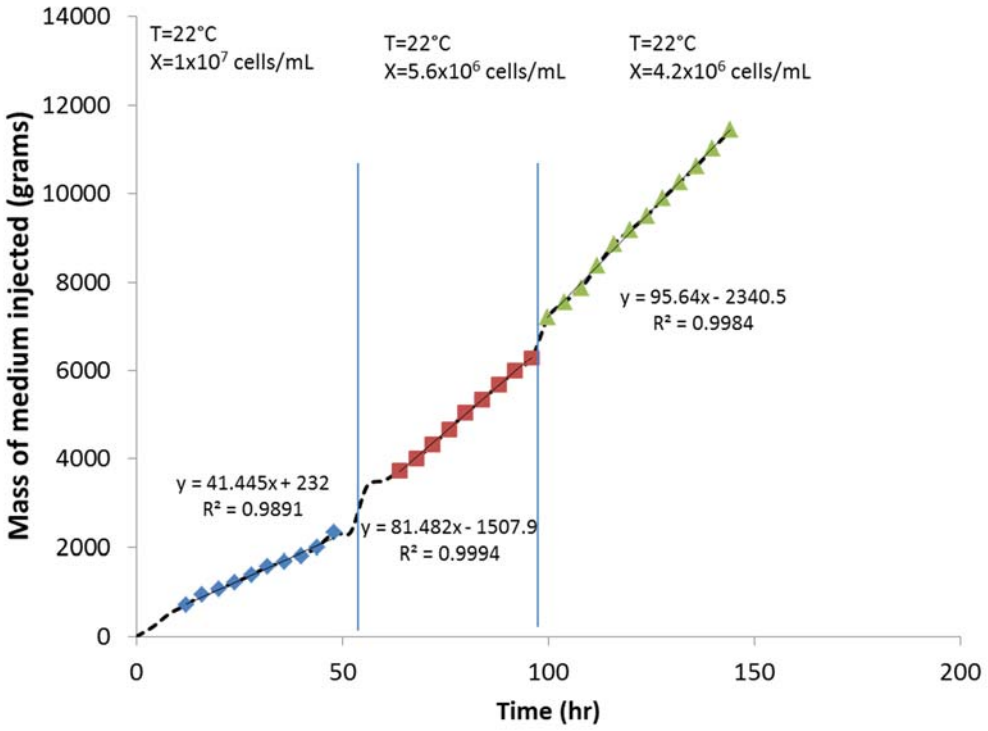

Figure 42: Example of data gathered for mass of medium injected through time at 22°C and three biomass concentrations: $1x10^7$, $5.6x10^6$ and $4.2x10^6$

References

Adir, N.; Zer, H.; Shochat, S.; Ohad, I. Photoinhibition - a Historical Perspective. *Photosynth. Res.* **2003**, *76*, 343–370.

Andersen, R. A. *Algal Culturing Techniques*; Elsevier Science, 2005; p. 588.

APHA. *Standard Methods for the Examination of Water and Wastewater*; Clesceri, L. S.; Greenberg, A. E.; Eaton, A. D., Eds.; 20th ed.; American Public Health Association, American Water Works Association and Water Environment Federation: Washington, DC, 1998.

Araki, T. The Effect of Temperature Shifts on Protein Synthesis by the Psychrophilic Bacterium Vibrio Sp. Strain ANT-300. *J. Gen. Microbiol.* **1991**, *137*, 817–826.

Arzul, G.; Gentien, P. Allelopathic Interactions Among Marine Microalgae. In *Algal Cultures Analogues of Blooms and Applications*; Rao, S., Ed.; Science Publishers: Enfield, New Hampshire, USA, 2006; p. 971.

Auer, M. T.; Canale, R. P. Ecological Studies and Mathematical Modeling of Cladophora in Lake Huron: 2. Phosphorus Uptake Kinetics. *J. Great Lakes Res.* **1982**, *8*, 84–92.

Benemann, J. R.; Tillet, D. M. *Effects of Fluctuating Environments on the Selection of High Yielding Microalgae. Final Report to the Solar Energy Research Institute.*; Atlanta, Georgia, USA, 1987; p. 121.

Benemann, J. R.; Weissmann, J. C.; Koopmann, B. L.; Oswald, W. J. Energy Production by Microbial Photosynthesis. *Nature* **1977**, *268*, 19–23.

Berberoglu, H.; Barra, N.; Pilon, L.; Jay, J. Growth, CO2 Consumption and H2 Production of Anabaena Variabilis ATCC 29413-U under Different Irradiances and CO2 Concentrations. *J. Appl. Microbiol.* **2008**, *104*, 105–121.

Bitaubé Pérez, E.; Caro Pina, I.; Pérez Rodríguez, L. Kinetic Model for Growth of Phaeodactylum Tricornutum in Intensive Culture Photobioreactor. *Biochem. Eng. J.* **2008**, *40*, 520–525.

Bouterfas, R.; Belkoura, M.; Dauta, A. Light and Temperature Effects on the Growth Rate of Three Freshwater Algae Isolated from a Eutrophic Lake. **2002**, 207–217.

Butler, J. N. *Carbon Dioxide Equilibria and Their Applications*; Addison-Wesley Publishing Company, 1982; p. 259.

Caperon, J.; Smith, D. F. Photosynthetic Rates of Marine Algae as a Function of Inorganic Carbon Concentration. *Limnol. Oceanogr.* **1978**, *23*, 704–708.

Carvalho, A. P.; Meireles, L. A.; Malcata, F. X. Microalgal Reactors: A Review of Enclosed System Designs and Performances. *Biotechnol. Prog.* **2006**, *22*, 1490–1506.

Chan, a. T.; Andersen, R. J.; Blanc, M. J.; Harrison, P. J. Algal Plating as a Tool for Investigating Allelopathy among Marine Microalgae. *Mar. Biol.* **1980**, *59*, 7–13.

Chen, C.; Durbin, E. Effects of pH on the Growth and Carbon Uptake of Marine Phytoplankton. *Mar. Ecol. Prog. Ser.* **1994**, *109*, 83–94.

Chinnasamy, S.; Ramakrishnan, B.; Bhatnagar, A.; Das, K. C. Biomass Production Potential of a Wastewater Alga Chlorella Vulgaris ARC 1 under Elevated Levels of CO2 and Temperature. *Int. J. Mol. Sci.* **2009**, *10*, 518–532.

Chisti, Y. Biodiesel from Microalgae Beats Bioethanol. *Trends Biotechnol.* **2008**, *26*, 126–131.

Chiu, S.-Y.; Kao, C.-Y.; Tsai, M.-T.; Ong, S.-C.; Chen, C.-H.; Lin, C.-S. Lipid Accumulation and CO2 Utilization of Nannochloropsis Oculata in Response to CO2 Aeration. *Bioresour. Technol.* **2009**, *100*, 833–838.

Cho, S. H.; Ji, S. C.; Hur, S. B.; Bae, J.; Park, I. S.; Song, Y. C. Optimum Temperature and Salinity Conditions for Growth of Green Algae Chlorella Ellipsoidea and Nannochloris Oculata. *Fish. Sci.* **2007**, *73*, 1050–1056.

Clarens, A. F.; Resurreccion, E. P.; White, M. a; Colosi, L. M. Environmental Life Cycle Comparison of Algae to Other Bioenergy Feedstocks. *Environ. Sci. Technol.* **2010**, *44*, 1813–1819.

Clark, D. R.; Merrett, M. J.; Flynn, K. J. Utilization of Dissolved Inorganic Carbon (DIC) and the Response of the Marine Flagellate Isochrysis Galbana to Carbon or Nitrogen Stress. *New Phytol.* **1999**, *144*, 463–470.

Colman, B.; Huertas, I. E.; Bhatti, S.; Dason, J. S. The Diversity of Inorganic Carbon Acquisition Mechanisms in Eukaryotic Microalgae. *Funct. Plant Biol.* **2002**, *29*, 261–270.

Corcoran, A. a; Boeing, W. J. Biodiversity Increases the Productivity and Stability of Phytoplankton Communities. *PLoS One* **2012**, *7*, e49397.

Costa, J. A. V.; de Morais, M. G. The Role of Biochemical Engineering in the Production of Biofuels from Microalgae. *Bioresour. Technol.* **2010**, *102*, 2–9.

Dauta, A.; Devaux, J.; Piquemal, F.; Boumnich, L. Growth Rate of Four Freshwater Algae in Relation to Light and Temperature. *Hydrobiologia* **1990**, *207*, 221–226.

Davis, R.; Aden, A.; Pienkos, P. T. Techno-Economic Analysis of Autotrophic Microalgae for Fuel Production. *Appl. Energy* **2011**.

Day, J. D.; Benson, E. E.; Fleck, R. A. In Vitro Culture and Conservation of Microalgae : Applications for Aquaculture , Biotechnology and Environmental Research. *Vitr. Cell. Dev. Biol. Plant.* **2010**, *35*, 127–136.

Dickson, A. G. Thermodynamics of the Dissociation of Boric Acid in Synthetic Seawater from 273.15 to 318.15 K. *Deep Sea Res.* **1990**, *37*, 755–766.

Dickson, A. G.; Riley, J. P. The Estimation of Acid Dissociation Constants in Sea-Water Media from Potentiometric Titrations with Strong Base. *Mar. Chem.* **1979**, *7*, 101–109.

Dismukes, G. C.; Carrieri, D.; Bennette, N.; Ananyev, G. M.; Posewitz, M. C. Aquatic Phototrophs: Efficient Alternatives to Land-Based Crops for Biofuels. *Curr. Opin. Biotechnol.* **2008**, *19*, 235–240.

EPA. STATISTICAL ANALYSIS OF GROUNDWATER MONITORING DATA AT RCRA FACILITIES UNIFIED GUIDANCE, 2009, 17–31.

Eppley, R. W. Temperature and Phytoplankton Growth in the Sea. *Fish. Bull.* **1972**, *70*, 1063–1085.

Eriksen, N. T. The Technology of Microalgal Culturing. *Biotechnol. Lett.* **2008**, *30*, 1525–1536.

Falkowski, P. G.; Dubinsky, Z.; Wyman, K. Growth-Irradiance Relationships in Phytoplankton. *Limnol. Oceanogr.* **1985**, *30*, 311–321.

Falkowski, P. Ocean Science: The Power of Plankton. *Nature* **2012**, *483*, S17–20.

Fishman, D.; Majundar, R.; Morello, J.; Pate, R.; Yang, J. *National Algal Biofuels Technology Roadmap*; 2010; p. 124.

Fu, F.-X.; Warner, M. E.; Zhang, Y.; Feng, Y.; Hutchins, D. a. Effects of Increased Temperature and CO2 on Photosynthesis, Growth, and Elemental Ratios in Marine Synechococcus and Prochlorococcus (Cyanobacteria). *J. Phycol.* **2007**, *43*, 485–496.

Geider, R. J.; Osborn, B. A. Light Absorption, Photosynthesis and Growth of Nannochloris Atomus in Nutrient-Saturated Cultures. **1986**, *360*, 351–360.

Giordano, M.; Beardall, J.; Raven, J. A. CO2 Concentrating Mechanisms in Algae: Mechanisms, Environmental Modulation, and Evolution. *Annu. Rev. Plant Biol.* **2005**, *56*, 99–131.

Goldman, J. C. A Kinetic Approach to the Effect of Temperature on Algal Growth. *Limnol. Oceanogr.* **1974**, *19*, 756–766.

Goldman, J. C. Outdoor Algal Mass cultures—I. Applications. *Water Res.* **1979 a**, *13*, 1–19.

Goldman, J. C. Outdoor Algal Mass cultures—II. Photosynthetic Yield Limitations. *Water Res.* **1979 b**, *13*, 119–136.

Goldman, J. C.; Ryther, J. H. Temperature-Influenced Species Competition in Mass Cultures of Marine Phytoplankton. *Biotechnol. Bioeng.* **1976**, *18*, 1125–1144.

Goldman, J. C.; Mann, R. Temperature-Influenced Variations in Speciation and Chemical Composition of Marine Phytoplankton in Outdoor Mass Cultures. *J. Exp. Mar. Bio. Ecol.* **1980**, *46*, 29–39.

Goldman, J. C.; Oswald, W. J.; Jenkins, D. The Kinetics of Inorganic Carbon Limited Algal Growth. *Water Pollut. Control Fed.* **1974**, *46*, 554–574.

Graham, L. E.; Graham, J. M.; Wilcox, L. L. *Algae*; Second.; Pearson: San Francisco, 2009; p. 616.

Grima Molina, E.; Garcia Camacho, F.; Sanchez Perez, J. A.; Fernandez Sevilla, J. M.; Acien Fernandez, F. G.; Contreras Gomez, A. A Mathematical Model of Microalgal Growth in Light-Limited Chemostat Culture. *J. Chem. Technol. Biotechnol.* **1994**, *61*, 167–173.

Grima Molina, E.; Fernandez Sevilla, J. M.; Sanchez Perez, J. A.; Garcia Camacho, F. A Study on Simultaneous Photolimitaion and Photoinhibition in Dense Microalgal Cultures Taking into Account Incident and Averaged Irradiances. *J. Biotechnol.* **1996**, *45*, 59–69.

Gross, E. M. Allelopathy of Aquatic Autotrophs. *CRC. Crit. Rev. Plant Sci.* **2003**, *22*, 313–339.

Halterman, S. G.; Toetz, D. W. Kinetics of Nitrate Uptake by Freshwater Algae. **1972**.

Hanagata, N.; Takeuchi, T.; Fukuju, Y.; Barnes, D. J.; Karube, I. Tolerance of Microalgae to High CO2 and High Temperature. *Phytochemistry* **1992**, *31*, 3345–3348.

Hase, R.; Oikawa, H.; Sasao, C.; Morita, M.; Watanabe, Y. Photosynthetic Production of Microalgal Biomass in a Raceway System under Greenhouse Conditions in Sendai City. *J. Biosci. Bioeng.* **2000**, *89*, 157–163.

Hoffmann, J. P. Wastewater Treatment With Suspended and Nonsuspended Algae. *J. Phycol.* **1998**, *34*, 757–763.

Huertas, E.; Lubián, L. M. Comparative Study of Dissolved Inorganic Carbon Utilization and Photosynthetic Responses in Nannochloris (Chlorophyceae) and Nannochloropsis (Eustigmatophyceae) Species. *Can. J. Bot.* **1998**, *76*, 1104–1108.

Huertas, E.; Montero, O.; Lubián, L. M. Effects of Dissolved Inorganic Carbon Availability on Growth, Nutrient Uptake and Chlorophyll Fluorescence of Two Species of Marine Microalgae. *Aquac. Eng.* **2000**, *22*, 181–197.

Huisman, J.; Matthijs, H. C. P.; Visser, P. M.; Balke, H.; Sigon, C. a M.; Passarge, J.; Weissing, F. J.; Mur, L. R. Principles of the Light-Limited Chemostat: Theory and Ecological Applications. *Antonie Van Leeuwenhoek* **2002**, *81*, 117–133.

International Allelopathy Society. International Allelopathy Society http://www.international-allelopathy-society.org/.

Jacob-Lopes, E.; Lacerda, L. M. C. F.; Franco, T. T. Biomass Production and Carbon Dioxide Fixation by Aphanothece Microscopica Nägeli in a Bubble Column Photobioreactor. *Biochem. Eng. J.* **2008**, *40*, 27–34.

James, S. C.; Boriah, V. Modeling Algae Growth in an Open-Channel Raceway. *J. Comput. Biol.* **2010**, *17*, 895–906.

James, S. C.; Janardhanam, V.; Hanson, D. T. Simulating pH Effects in an Algal-Growth Hydrodynamics Model 1. *J. Phycol.* **2013**, *49*, 608–615.

Kovárová, K.; Zehnder, a J.; Egli, T. Temperature-Dependent Growth Kinetics of Escherichia Coli ML 30 in Glucose-Limited Continuous Culture. *J. Bacteriol.* **1996**, *178*, 4530–4539.

Lardon, L.; Hélias, A.; Sialve, B.; Steyer, J.-P.; Bernard, O. Life-Cycle Assessment of Biodiesel Production from Microalgae. *Environ. Sci. Technol.* **2009**, *43*, 6475–6481.

Law, A. T.; Button, D. K. Multiple-Carbon-Source-Limited Growth Kinetics of a Marine Coryneform Bacterium Cu / Tui Heat. *Microbiology* **1977**, *129*, 115–123.

Legrand, C.; Rengefors, K.; Fistarol, G. O.; Graneli, E. Allelopathy in Phytoplankton - Biochemical , Ecological and Evolutionary Aspects. *Phycologia* **2003**, *42*, 406–419.

Lehman, C. L.; Tilman, D. Biodiversity, Stability, and Productivity in Competitive Communities. *Am. Nat.* **2000**, *156*, 534–552.

Lehman, J. T. The Assumptions of Phytoplankton and Rationales of a Computer Population Dynamic ? Model. **1975**, *20*.

Lepetit, B.; Sturm, S.; Rogato, A.; Gruber, A.; Sachse, M.; Falciatore, A.; Kroth, P. G.; Lavaud, J. High Light Acclimation in the Secondary Plastids Containing Diatom Phaeodactylum Tricornutum Is Triggered by the Redox State of the Plastoquinone Pool. *Plant Physiol.* **2013**, *161*, 853–865.

Li, Y.; Horsman, M.; Wu, N.; Lan, C. Q.; Dubois-Calero, N. Biofuels from Microalgae. *Biotechnol. Prog.* **2008**, *24*, 815–820.

Macías, F. a.; Galindo, J. L. G.; García-Díaz, M. D.; Galindo, J. C. G. Allelopathic Agents from Aquatic Ecosystems: Potential Biopesticides Models. *Phytochem. Rev.* **2007**, *7*, 155–178.

Masuda, T.; Tanaka, A.; Melis, A. Chlorophyll Antenna Size Adjustments by Irradiance in Dunaliella Salina Involve Coordinate Regulation of Chlorophyll a Oxygenase (CAO) and Lhcb Gene Expression. *Plant Mol. Biol.* **2003**, *51*, 757–771.

Mayasich, J. M.; Karlander, E. P.; Terlizzi, D. E. Growth Responses of Nannochlor & Oculata Droop and Phaeodactylum Tricornutum Bohlin to the Herbicide Atrazine as Influenced by Light Intensity and Temperature in Unialgal and Bialgal Assemblage. **1987**, *10*, 187–197.

Mayo, A. W. Effects of Temperature and pH on the Kinetic Growth of Unialgal Chlorella Vulgaris Cultures Containing Bacteria. *Water Environ. Res.* **1997**, *69*, 64–72.

Mazzuca Sobczuk, T.; Chisti, Y. Potential Fuel Oils from the Microalga Choricystis Minor. *J. Chem. Technol. Biotechnol.* **2010**, *85*, 100–108.

Millero, F. J. The pH of Estuarine Waters. *Limnol. Oceanogr.* **1986**, *31*, 839–847.

Millero, F. J.; Graham, T. B.; Huang, F.; Bustos-Serrano, H.; Pierrot, D. Dissociation Constants of Carbonic Acid in Seawater as a Function of Salinity and Temperature. *Mar. Chem.* **2006**, *100*, 80–94.

Miyachi, S.; Iwasaki, I.; Shiraiwa, Y. Historical Perspective on Microalgal and Cyanobacterial Acclimation to Low- and Extremely High-CO(2) Conditions. *Photosynth. Res.* **2003**, *77*, 139–153.

Munoz, J.; Merrett, M. J. Inorganic-Carbon Transport in Some Marine Eukaryotic Microalgae. *Planta* **1989**, *178*, 450–455.

Nakagawara, E.; Sakuraba, Y.; Yamasato, A.; Tanaka, R.; Tanaka, A. Clp Protease Controls Chlorophyll B Synthesis by Regulating the Level of Chlorophyllide a Oxygenase. *Plant J.* **2007**, *49*, 800–809.

Nakamura, T.; L., S. C.; Olaizola, M.; Bridges, T.; Flores, S.; Sombardier, L.; Masutani, S. M. *Recovery and Sequestration of CO2 from Stationary Combustion Systems by Photosynthesis of Microalgae Final Report*; National Energy Technology Laboratory: Pittsburgh, PA, 2005; p. 200.

Noüe, J. de la; Laliberté, G.; Proulx, D. Algae and Waste Water. *J. Appl. Phycol.* **1992**, *4*, 247–254.

Novak, J.; Brune, D. Inorganic Carbon Limited Growth Kinetics of Some Freshwater Algae. *Water Res.* **1985**, *19*, 215–225.

Olguın, E. J. Phycoremediation : Key Issues for Cost-Effective Nutrient Removal Processes. *Biotechnol. Adv.* **2003**, *22*, 81 – 91.

Oswald, W. J. My Sixty Years in Applied Algology. *J. Appl. Phycol.* **2003**, *15*, 99–106.

Oswald, W. J.; Gotaas, H. B.; Golueke, C. G.; Kellen, W. R.; Gloyna, E. F. Algae in Waste Treatment. *Sewage Ind. Waste.* **1957**, *29*, 437–457.

Ota, M.; Kato, Y.; Watanabe, H.; Watanabe, M.; Sato, Y.; Smith, R. L.; Inomata, H. Effect of Inorganic Carbon on Photoautotrophic Growth of Microalga Chlorococcum Littorale. *Biotechnol. Prog.* **2009**, *25*, 492–498.

Papazi, A.; Makridis, P.; Divanach, P.; Kotzabasis, K. Bioenergetic Changes in the Microalgal Photosynthetic Apparatus by Extremely High CO2 Concentrations Induce an Intense Biomass Production. *Physiol. Plant.* **2008**, *132*, 338–349.

Pate, R.; Klise, G.; Wu, B. Resource Demand Implications for US Algae Biofuels Production Scale-Up. *Appl. Energy* **2011**, *88*, 3377–3388.

Pennings, S. C.; Pablo, S. R.; Paul, V. J. Chemical Defenses of the Tropical, Benthic Marine Cyanobacterium Hormothamnion Enteromorphoides: Diverse Consumers and Synergisms. *Limnol. Oceanogr.* **1997**, *42*, 911–917.

Pulz, O.; Gross, W. Valuable Products from Biotechnology of Microalgae. *Appl. Microbiol. Biotechnol.* **2004**, *65*, 635–648.

Rao, P. N.; Engelberg, J. HeLa Cells : Effects of Temperature on the Life Cycle HeLa Cells : Effects of Temperature on the Life Cycle. *Science (80-.).* **1965**, *148*, 1092–1094.

Raven, J. A.; Geider, R. J. Adaptation, Acclimation and Regulation in Algal Photosynthesis. In *Advances in Photosythesis and Respirationn Volume 14: Photosythesis in Algae*; 2003; pp. 386–409.

Reynolds, C. S. Phyoplankton. In *Ecology of Phytoplankton*; Cambridge University Press: Cambridge, UK, 2006 a; pp. 1–37.

Reynolds, C. *Ecology of Phytoplankton*; Cambridge University Press: New York, 2006 b; p. 436.

Rhee, G.-Y. Effects of N : P Atomic Ratios and Nitrate Limitation on Algal Growth , Cell Composition , and Nitrate Uptake. *Limnol. Oceanogr.* **1978**, *23*, 10–25.

Richardson, B.; Orcutt, D. M.; Schwertner, H. A.; Martinez, C. L.; Wickline, H. E. Effects of Nitrogen Limitation on the Growth and Composition of Unicellular Algae in Continuous Culture. *Appl. Microbiol.* **1969**, *18*, 245–250.

Satoh, a; Kurano, N.; Miyachi, S. Inhibition of Photosynthesis by Intracellular Carbonic Anhydrase in Microalgae under Excess Concentrations of CO(2). *Photosynth. Res.* **2001**, *68*, 215–224.

Schenk, P. M.; Thomas-Hall, S. R.; Stephens, E.; Marx, U. C.; Mussgnug, J. H.; Posten, C.; Kruse, O.; Hankamer, B. Second Generation Biofuels: High-Efficiency Microalgae for Biodiesel Production. *BioEnergy Res.* **2008**, *1*, 20–43.

Scott, S. a; Davey, M. P.; Dennis, J. S.; Horst, I.; Howe, C. J.; Lea-Smith, D. J.; Smith, A. G. Biodiesel from Algae: Challenges and Prospects. *Curr. Opin. Biotechnol.* **2010**, *21*, 277–286.

Sheehan, J. *A Look Back at the U . S . Department of Energy ' S Aquatic Species Program : Biodiesel from Algae*; Golden, Colorado, USA, 1998; p. 294.

Shurin, J. B.; Abbott, R. L.; Deal, M. S.; Kwan, G. T.; Litchman, E.; McBride, R. C.; Mandal, S.; Smith, V. H. Industrial-Strength Ecology: Trade-Offs and Opportunities in Algal Biofuel Production. *Ecol. Lett.* **2013**, *16*, 1393–1404.

Smith, V. H.; Sturm, B. S. M.; Denoyelles, F. J.; Billings, S. a. The Ecology of Algal Biodiesel Production. *Trends Ecol. Evol. (Personal Ed.* **2010**, *25*, 301–309.

Sorokin, C.; Krauss, R. W. The Effects of Light Intensity on the Growth Rates of Green Algae. *Plant Physiol.* **1958**, *33*, 109–113.

Srivastava, a; Jüttner, F.; Strasser, R. J. Action of the Allelochemical, Fischerellin A, on Photosystem II. *Biochim. Biophys. Acta* **1998**, *1364*, 326–336.

Stachowicz, J. J.; Graham, M.; Bracken, M. E. S.; Szoboszlai, A. I. Diversity Enhances Cover and Stability of Seaweed Assemblages: The Role of Heterogeneity and Time. *Ecology* **2008**, *89*, 3008–3019.

Steele, J. H. Environmental Control of Photosynthesis in the Sea. *Limnol. Oceanogr.* **1962**, *7*, 137–150.

Stephens, E.; Ross, I. L.; Mussgnug, J. H.; Wagner, L. D.; Borowitzka, M. a; Posten, C.; Kruse, O.; Hankamer, B. Future Prospects of Microalgal Biofuel Production Systems. *Trends Plant Sci.* **2010**, *15*, 554–564.

Stephenson, A. L.; Kazamia, E.; Dennis, J. S.; Howe, C. J.; Scott, S. a.; Smith, A. G. Life-Cycle Assessment of Potential Algal Biodiesel Production in the United Kingdom: A Comparison of Raceways and Air-Lift Tubular Bioreactors. *Energy & Fuels* **2010**, *24*, 4062–4077.

Stockenreiter, M.; Graber, A.-K.; Haupt, F.; Stibor, H. The Effect of Species Diversity on Lipid Production by Micro-Algal Communities. *J. Appl. Phycol.* **2011**, *24*, 45–54.

Takagi, M.; Watanabe, K.; Yamaberi, K.; Yoshida, T. Limited Feeding of Potassium Nitrate for Intracellular Lipid and Triglyceride Accumulation of Nannochloris Sp. UTEX LB1999. *Appl. Microbiol. Biotechnol.* **2000**, *54*, 112–117.

Talbot, P.; Bault, J. T. H. I.; Dauta, A.; L, J. D. E. L. A. N. A COMPARATIVE STUDY AND MATHEMATICAL MODELING OF TEMPERATURE , LIGHT AND GROWTH OF THREE MICROALGAE POTENTIALLY USEFUL FOR WASTEWATER TREATMENT. **1991**, *25*, 465–472.

Tanaka, A.; Ito, H.; Tanaka, R.; Tanaka, N. K.; Yoshida, K.; Okada, K. Chlorophyll a Oxygenase (CAO) Is Involved in Chlorophyll B Formation from Chlorophyll a. *Plant Biol.* **1998**, *95*, 12719–12723.

Terry, K. L.; Hirata, J.; Laws, E. A. Phaeodactylum Tricornutum. *J. Exp. Mar. Bio. Ecol.* **1985**, *86*, 85–100.

Thompson, P. Effect of Temperature and Irradiance on Marine Microalgal Growth and Physiology. In *Algal Cultures Analogues of Blooms and Applications*; Rao, S., Ed.; Science Publishers, 2006; pp. 571–638.

Tilman, D. Causes, Consequences and Ethics of Biodiversity. *Nature* **2000**, *405*, 208–211.

Tilman, D.; Reich, P. B.; Knops, J.; Wedin, D.; Mielke, T.; Lehman, C. Diversity and Productivity in a Long-Term Grassland Experiment. *Science* **2001**, *294*, 843–845.

Tilman, D.; Reich, P. B.; Knops, J. M. H. Biodiversity and Ecosystem Stability in a Decade-Long Grassland Experiment. *Nature* **2006**, *441*, 629–632.

Vasconcelos, M. T. S. D.; Leal, M. F. C. Exudates of Different Marine Algae Promote Growth and Mediate Trace Metal Binding in Phaeodactylum Tricornutum. *Mar. Environ. Res.* **2008**, *66*, 499–507.

Wahman, D. G. COMETABOLISM OF TRIHALOMETHANES BY NITRIFYING BIOFILTERS UNDER DRINKING WATER TREATMENT PLANT CONDITIONS, The University of Texas at Austin, 2006, p. 367.

Weiss, R. F. Carbon Dioxide in Water and Seawater: The Solubility of a Non-Ideal Gas. *Mar. Chem.* **1974**, *2*, 203–215.

Wigmosta, M. S.; Coleman, A. M.; Skaggs, R. J.; Huesemann, M. H.; Lane, L. J. National Microalgae Biofuel Production Potential and Resource Demand. *Water Resour. Res.* **2011**, *47*, 1–13.

Yamaberi, K.; Takagi, M.; Yoshida, T. Nitrogen Depletion for Intracellular Triglyceride Accumulation to Enhance Liquefaction Yield of Marine Microalgal Cells into a Fuel Oil. *J Mar Biotechnol* **1998**, *6*, 44–48.

Yue, L.; Chen, W. Isolation and Determination of Cultural Characteristics of a New Highly CO2 Tolerant Fresh Water Microalgae. *Energy Convers. Manag.* **2005**, *46*, 1868–1876.

Growth and Replication of Phytoplankton. In *Ecology of Phytoplankton*; Reynolds, C. S., Ed.; Cambridge University Press: Cambridge, UK, 2006 c; pp. 178–238.

Vita

Fernando Almada was born in Culiacán, Sinaloa, Mexico. He graduated from Universidad Iberoamericana in May 2006 as a Chemical Engineer and worked for two years in the National Institute of Ecology in Mexico City on issues related to hazardous waste disposal and ecotoxicological risks. In May 2010, he obtained an M.S. in Environmental and Water Resources Engineering at The University of Texas at Austin. His work has been focused on water treatment and optimization of microalgae production for bioenergy purposes. After obtaining his degree he opted to continue his education in the doctoral program in Civil Engineering.

Permanent email address: falmadac@gmail.com

This dissertation was typed by the author.